OPTIMAL DESIGN OF ELECTROMAGNETIC DEVICE

A Thesis Submitted
In Partial Fulfilment of the Requirements
for the Degree of
DOCTOR OF PHILOSOPHY

By
K. S. RAMA RAO

to the

DEPARTMENT OF ELECTRICAL ENGINEERING
INDIAN INSTITUTE OF TECHNOLOGY KANPUR
JULY, 1978

EE-1978-D-RAO-OPT

To

my wife and children

CERTIFICATE

It is certified that this work, 'Optimal Design of Electromagnetic Devices' by Mr. K.S. Rama Rao, has been carried out under my supervision and that this work has not been submitted elsewhere for a degree.

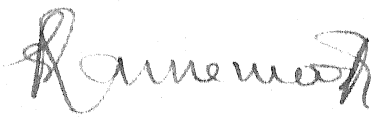

(M. Ramamoorty)
Professor
Department of Electrical Engineering
Indian Institute of Technology
Kanpur

July, 1978

ACKNOWLEDGEMENTS

It is with great pleasure that I express my profound gratitude to Dr. M. Ramamoorty who suggested the problems and provided me with excellent guidance and inspiration all along. I am grateful to him for sparing his valuable time and energy on several occasions even after he took up an assignment at Baroda.

I am grateful to Dr. K.R. Padiyar, for the many useful discussions and for the kind help extended by him. I sincerely thank Dr. V.V. Sastry whose many valuable suggestions have improved the quality of this thesis.

I am thankful to Dr. K. Kurma Rao and Dr. T.A. Prasada Rao for their valuable association. I am much indebted to Mr. Thomas Chacko for reading the manuscript through and suggesting stylistic improvements.

I have a strong feeling of appreciation for M/S N.N. Kishore, K. Surayya, M.V.S. Rao, E.S. Reddy, K.S. Sarma, M. Arunachalam, S.V. Tambe, K.K. Ray and Dr. P.J. Rao from whose association, I have greatly benefitted. I also acknowledge the help extended by Mr. A.V.A. Swamy and Mr. K.S. Ramakrishna in the proof reading of this thesis.

I am greatly indebted to the authorities of the Jawaharlalnehru Technological University for sponsoring me under the Q.I.P. My thanks are also to the staff of

Computer Centre, I.I.T. Kanpur and to Smt. Rukmini Devi for her patient and skilful typing.

I appreciate my wife Parvati and my sons Suresh and Ravindra for their forbearance throughout this venture.

K.S. RAMA RAO

LIST OF TABLES

OPTIMIZATION

F	objective function
FA	augmented objective function
g, G	constraints
n	number of independent variables
r	penalty factor
X	vector of independent variables
x_i	i-th component of X

POWER TRANSFORMERS

a	area of c.s. of conductor, mm^2
a_s	area of c.s. of end coil conductor, mm^2
AO, BO	dimensions of bare conductor, mm
AO_c, BO_c	dimensions of insulated conductor, mm
A_i	net core section, m^2
b	width of winding, m
b_{ph}	clearance between different phase windings, m
b_s	width of spacer, m
B_y	flux density in yoke, Tesla
C	initial cost, Rs.
C_1, C_2	loss capitalization factors, Rs/kW
CC, CI	cost of copper windings and stamptings, Rs/kg
CL	maximum demand charge, Rs/kW

CE	cost of electrical energy, Rs/kW
d	diameter of core circle, m
D12	mean diameter between windings, m
DM	(maximum demand/CMR of transformer)
DR	(r.m.s. demand/maximum demand)^2
DZS	equivalent drop in d.c. voltage due to source impedance, V
f	frequency, Hz
FF(x_1)	core loss function at x_1, kW/kg
G_c, G_l, G_y	weight of copper, limbs and yoke, kg
h_c, h_w	height of copper and winding, m
HI(x_1)	magnetizing power function for joints at x_1, VA/m^2
i	percentage annual rate of interest
I	current in the winding per phase, A
I_c	circuit current, kA
I_d	d.c. load current, A
I_o	percentage no-load current
I_{oa}, I_{or}	percentage active and reactive components of no-load current
J	current density in the winding, A/mm^2
k_1, k_2, ...	constants used in expressions
$K_{e,\ pul}$	eddy loss ratio with pulsating current
L_{mt}	length of mean turn, m
m	number of parallel conductors
MC, MT	perimeter of coil and tank, m

n_c	number of coils in parallel in l.v. winding
n_s	number of spacers
n_A, n_R	number of axial and radial straps
N	life of the transformer, years
NR	number of external heat exchangers
P_{c1}, P_{c2}	copper loss in h.v. and l.v. windings, kW
P_e	eddy current loss in conductors, kW
P_i, P_s	iron loss and stray loss, kW
PF	power factor of the load
q_o, q_w	specific thermal load of oil and winding, W/m^2
R	resistance of winding per phase, ohm
R_A	average arc resistance per phase, ohm
R_{sc}, X_{sc}, Z_{sc}	percentage short-circuit resistance, reactance and impedance
RF	capital recovery factor
S	rating of the transformer, kVA
S_1	kVA per phase
T, T_s	turns per phase of normal and strengthened insulation coil
T_c	turns per coil
TKH, TKL, TKW	height, length and width of tank, m
u	overlap angle
V	voltage per phase, V
V_c	circuit voltage, V

V_d	d.c. load voltage, V
X	reactance per phase, ohm
Z_c	total circuit impedance per phase, ohm
Z_s	secondary circuit impedance per phase, ohm
θ_o	permissible average oil temperature above ambient, °C
θ_{oa}, θ_{wa}	temperature rise above ambient of top oil and winding, °C
θ_w	temperature difference between winding surface and oil, °C
θ_{wo}	maximum temperature difference between any winding surface and oil, °C
μ_o	magnetic space constant, $4\pi \times 10^{-7}$ H/m
ρ	specific resistance of copper, 0.021 ohm-m/mm^2
η	percentage efficiency of the transformer

DC MOTORS

a	area of c.s. of conductor, mm^2
a_p	number of armature parallel circuits
A_d	area of axial ducts, m^2
AO, BO	conductor dimensions, mm
AT	ampere-turns per pole
b	width of winding, m
b'	pole-arc, m
b_{pc}	periphery of armature coil sides per layer, m

B_{gm}, B_{ipg}	maximum flux density in gap and inter-pole gap, Tesla
CC, CI	cost of copper windings and stampings, Rs/kW
C_{cex}, C_{cin}, C_{cd}	cooling coefficients for armature
C_{cc}	cooling coefficient for commutator
d	diameter, m
d_{sh}	diameter of shaft, m
E_b	armature counter c.m.f., V
E_{dc}	average value of d.c. voltage, V
E_{do}	maximum value of average d.c. voltage, V
E_f	field winding voltage, V
f	frequency, Hz
G_c, G_i	weight of copper windings and stampings, kg
h_{ip}	height of interpole, m
h_{py}	height between pole-face and yoke, m
H_s	shaft centre height, mm
I_{dc}, I_{min}, I_{peak}, I_{rms}	average, minimum, peak, r.m.s. values of d.c. current, A
K_g, K_{ipg}	gap coefficients
K_{yk}	proportion constant between two adjacent sides of yoke
K_o, K_d	Carter's coefficients for opening and duct
l_{fr}	free length of armature coil, m
l_o	length of outhang, m
L	length, m

L_{ag}, L_{bg}, L_{abg}	inductance of armature, compensating and mutual between armature and compensating windings, H
L_{al}, L_{bl}, L_{cl}	inductance due to armature slot, pole-face slot and interpole leakage, H
L_{an}	inductance in armature end turns, H
L_f	inductance of field circuit, H
L_g	inductance due to pole flux under main poles, H
L_i	effective length of armature core, m
L_{ipg}	inductance due to interpole flux, H
L_m	length of mean turn or conductor, m
L_{sn}	inductance in stator end connection, H
+ L_t	total armature circuit inductance, H
n_{br}, n_d	number of brushes and ducts
N	speed of the motor, r.p.m.
N_b	number of conductors in pole-face slots
N_{cs}	number of commutator segments
N_{ps}	number of pole-face slots
P	number of Poles or with subcript represent losses in watts
P_{bc}	brush contact loss, W
P_{fw}	friction and windage loss, W
R	resistance of winding, ohm
R_t	total resistance of armature circuit, ohm
t_{br}	thickness of brush, mm
T	number of turns per pole
+ m	number for parallel conductors

T_c	turns per coil
T_a	armature turns
u_a	peripheral speed of armature, m/sec
v_c	velocity of commutator, m/sec
V_{max}	maximum value of a.c. line voltage, V
w	width, m
w_{sh}	width of shoe, m
w_{tm}	mean width of armature tooth, m
w_{tcm}	width of pole-face tooth at 1/3 height, m
y	pitch of slots or commutator segments, m
Y	pole-pitch, m
Z	number of armature conductors
ϕ	flux per pole, Wb
λ	permeance of slot and overhang portion of armature
β	distance moved by armature during commutation, m

Subscripts:

a,br,c,cr,d,f,g, ip,p,t,y	represent armature, brush, commutator, core, duct, field, gap, interpole, pole, teeth and yoke respectively.
	cm represents compensating winding.

INDUCTION MOTOR

a	area of c.s. of conductor, mm^2
A	surface area, m^2
AC, BC	conductor dimensions, mm

B_g, B_t	flux density in air gap and teeth, Tesla
CB, CC, CI	costs of brass, copper and stampings, Rs/kW
d_2, d_{er}	diameter of rotor and end ring, m
d_o	outside diameter of stator, m
d_{sh}	diameter of shaft, m
E_{dc}	d.c. link voltage, V
E_s	counter e.m.f. of stator per phase, V
f_{op}	operating frequency, Hz
g	slots per pole
g'	slots per pole per phase
G_b, G_i, G_w	weight of brass rings, stampings and copper windings, kg
h_{er}	height of end ring section, mm
I	current per phase, A
I_b, I_{er}	current per phase in rotor bar and end ring, A
I_l	locked rotor current per phase, A
I_o	no-load current per phase, A
I_{oa}, I_{or}	active and reactive components of no-load current per phase, A
K_f	constant, volts/Hz
K_r, K_x	skin-effect factors for resistance and leakage reactance
K_w	winding factor
L_2	length of rotor core, m
L_e	length of stator overhang, m

L_{is}	effective length of stator core, m
L_o	length of outhang, m
m	order of harmonic
$M_{av}, M_{fl}, M_{st}, M_{po}$	average, full-load, starting and pull-out torques, Nm
M_{pul}	p.u. torque pulsation
M_{pmx}, M_{pmn}	peak and minimum values of torque pulsation, Nm
M_{6c}, M_{6s}	cosine and sine components of sixth harmonic torque pulsation
M_{12c}, M_{12s}	cosine and sine components of twelfth harmonic torque pulsation
M_{sp}	specified average torque, Nm
n_d	number of radial ducts in stator
N	speed of the motor, r.p.m.
N_{cd}, N_{cw}	number of stator conductors depth-wise and width-wise
p	number of pairs of poles
P	number of poles
P_1, P_2	total losses in stator and rotor, W
P_c	copper loss, W
P_{fw}	friction and windage loss, W
PF	power factor
R, X, Z	resistance, reactance and impedance per phase, ohm
R_o, X_m, Z_m	magnetizing resistance, reactance and impedance per phase, ohm
R_{be}	resistance per phase of rotor winding outside the slots, ohm

R_c	resistance per phase of slot portion of winding, ohm
s_{fl}, s_m	p.u. slip at full-load and m-th harmonic
S	number of slots
T_{ph}	turns per phase of stator
U_a	peripheral speed, m/sec
V_s	applied voltage per phase, V
w_d, w_t	width of duct and teeth, m
w_{er}	width of end ring, mm
X_{sl}, X_{ol}, X_{zl}	reactance per phase of stator slot, overhang and zig-zag leakage, ohm
X_{s2}, X_{o2}, X_{z2}	reactance per phase of rotor slot, overhang and zig-zag leakage, ohm
y	slot-pitch, m
Y	pole-pitch, m
Z_T	total impedance per phase, ohm
ϕ_m	mutual flux, Wb
θ	power factor angle
ω	angular frequency
ψ'_{rm}	angle between flux and rotor harmonic m.m.f.

with s as first or second subscript represent for stator, with r as first or second subscript represent for rotor, with m as second or third subscript represent for m-th harmonic component.

Superscript 'prime' indicates rotor values referred to stator.

Computer-aided design of electrical machines using digital computers has been in vogue for the past two decades. The computer is being used as an aid for design analysis and design synthesis making use of iterative techniques. The availability of powerful and efficient general algorithms of mathematical programming has stimulated renewed interest in the design of electromagnetic devices. An engineer is frequently faced with the problem of optimizing a design to obtain minimum material cost, volume or weight of a given configuration of equipment satisfying many exacting constraints. Optimization has become a key concept in modern engineering practice. The optimization process fits very naturally into the computer-aided design procedure and leads to significantly improved designs with considerably less effort on the part of the designer.

The optimal design problem of any electromagnetic device can be posed as a mathematical programming problem in which the cost or the weight, or any such criterion forms the objective function and the specifications and/or some of the performance characteristics form the constraints. The mathematical model involved in the analysis and design of most electromagnetic devices is nonlinear in nature and hence Nonlinear Programming (NLP) procedures are of interest in this thesis. Another way of approaching nonlinear optimization problems is by linear approximation which is also

considered in this thesis.

Mathematical programming techniques have been applied to the design of electrical equipment since 1960. The design optimization of transformers for minimum cost is approached as a problem in geometric programming by Duffin and Zener. The cost function of induction motor is formulated and minimized as an unconstrained minimization problem by Appelbaum and Erlicki. Ramaratnam and Desai have approached the design optimization of polyphase induction motors as a problem in NLP using Sequential Unconstrained Minimization Technique (SUMT). The problem of designing large induction motors at minimum cost is approached using NLP by Menzies and Neal. Ramamoorty and Rao have established the suitability of Powell's unconstrained optimization technique to the design of polyphase reluctance motors.

The major aim of the present thesis is to extend the available optimization techniques to obtain optimized design, at minimum material cost, of electromagnetic devices such as power transformers, d.c. motors and induction motors. Optimal design of conventional power transformers is approached by NLP and linear approximation methods separately. Two special purpose power transformers viz, furnace and rectifier transformers for supplying direct arc furnace and d.c. loads respectively, are considered and design problems are formulated

by NLP approach. The problem of designing d.c. separately excited and series motors, when supplied through three-phase thyristor converters, is approached by NLP technique. Finally the optimal design problem of a variable speed squirrel-cage induction motor supplied with nonsinusoidal voltage is formulated as an NLP problem.

In this thesis, every NLP problem is converted into a sequence of unconstrained optimization problems using exterior penalty function approach; and Powell's unconstrained optimization technique is employed to obtain minimum cost of the equipment concerned.

The power transformer is one of the most important links in a power system. The optimal design problem of a 5 MVA power transformer is solved as an NLP problem with some of the specifications of the equipment as constraints. The same problem is then solved by Linear Programming (LP) approach by linearizing the nonlinear objective function and nonlinear constraints around an operating point by first order Taylor's series approximation. Here the well-known revised simplex method of LP is used to obtain optimized design. Sensitivity analysis or post-optimality is carried out to study the effect of discrete changes in different parameters of the problem on the optimal solution. For a given operating point, the effect of relaxing the maximum limit on constraints

like flux density of core and temperature rise of windings, keeping the other constraints same on the overall objective function is investigated.

With the increase in production capabilities of direct arc furnaces for making steels, the ratings of the associated transformers have increased substantially and hence the need for optimal design of these transformers. The application of nonlinear optimization procedure to the design of a 64.5 MVA furnace transformer supplying a 150 ton arc furnace is considered. Arc power, secondary circuit impedance and arc resistance are taken into account while arriving at the transformer rating. The NLP problem is solved, satisfying important constraints like temperature rise, efficiency of the transformer etc.

The optimal design of rectifier power transformers is imperative with the growth of static converting equipment supplying high current loads. A 4 MVA rectifier power transformer supplying d.c. load through a six-pulse converter (three-phase diode bridge) is then considered. For a specified connection of the transformer, the secondary current waveform is derived, considering the source impedance. Eddy current losses in windings, temperature rise of the equipment and mechanical stresses in windings are obtained on the basis of actual current waveform. The optimal design problem

is then solved as an NLP problem satisfying important constraints like efficiency of the transformer, d.c. voltage regulation etc.

A large percentage of d.c. motors manufactured today are supplied from thyristor converters and optimal design of these motors to suit the rectifier supply is one of the demands made by the manufacturers and users. DC motors, when supplied with thyristor converters, require special consideration in the design procedure. Important constraints like commutating ability of the machine, ratio of torque to armature moment of inertia, pulse duty factor of armature current, efficiency of the machine etc., are imposed on the design problem to meet some of the requirements of industry. Design analysis program includes calculation of armature circuit inductance, additional losses due to flux pulsations in the armature and magnetic circuit, additional losses in windings due to harmonic currents and additional losses due to harmonic components in armature conductors undergoing commutation due to the trapezoidal shape of current. Laminated field structure with octagonal frame, compensating winding in the pole-face slots and interpole winding are considered in line with current practice. The design optimization using NLP technique of 150 h.p. d.c. separately excited and series motors are solved independently.

The number of applications of three-phase squirrel-cage induction motors with static frequency converter power supplies is increasing because of their simplicity, ruggedness and economy. Optimal design of these motors, when supplied with variable frequency nonsinusoidal voltages, require important considerations regarding a limit on additional losses and torque pulsations. For this design problem important constraints like power factor, magnetizing current, locked rotor current, breakdown torque, per unit torque pulsation etc., are considered. In the performance evaluation program, torque pulsations and additional losses are calculated over a frequency range. The design optimization problem of a 5 h.p., three-phase, squirrel-cage induction motor is formulated as an NLP problem over a frequency range and solved, satisfying the desired constraints.

The major purpose of the thesis is to obtain optimal design of electromagnetic devices mentioned above, minimizing the cost by mathematical programming techniques for a given steady state mathematical model of the equipment with specified design variables and a large number of constraints. The models used are those available in the literature. No attempt is made in the thesis to verify the accuracy of these models as this is considered to be beyond the objectives of this thesis. Similarly, on the programming side, the

available optimization techniques are considered and the most suitable one is adopted for obtaining the optimal design of these equipments. The verification of the optimal design by actual fabrication is beyond the scope and it is hoped that the manufacturers of the respective equipments will in future be guided by the methods proposed in this thesis.

CHAPTER 1

I N T R O D U C T I O N

1.1 GENERAL

The design of electromagnetic devices can be viewed as a three stage iterative process: (1) the selection or modification of a configuration of an equipment and the identification of the design variables in this configuration, (2) the assignment of numerical values to these design variables, (3) evaluation of the resulting design and the decision as to which of the steps (1) or (2), if either, must be repeated [1]. Today computers have to be used to perform calculations and memorize large amounts of information for developing and applying design data of electromagnetic devices, despite the need for extensive preliminary studies. The computers offer the benefits of optimization, precision and exact calculation. The availability of powerful and efficient general algorithms of mathematical programming has stimulated renewed interest in the design of electromagnetic devices at minimum material cost, volume or weight, satisfying many exacting constraints. Optimization has become a key tool in modern engineering design practice either as an outcome of escalation of material costs or of increased competition.

The steady state behaviour of an electrical equipment can be quantitatively represented with reasonable accuracy by mathematical models comprising of equations and inequalities.

The number of specified design variables normally exceeds the number of equations (and active inequalities) and finding a unique solution is not easy. To achieve a solution to a design problem with unique operating conditions viz., the constraints, together with a definite objective such as minimum weight, minimum cost or minimum volume, optimization must be employed. An objective function is formulated to serve as the criterion in determining an admissible set of operating conditions. Normally the specifications, performance characteristics, national and international standards of the equipment, etc., are taken as constraints. The objective and constraint functions are expressed in terms of the specified design variables. In addition suitable values are necessary for coefficients in the mathematical model, such as per unit costs of materials, physical parameters etc. The main purpose of this thesis is to outline the concepts related to optimal design of electromagnetic devices viz., power transformers, d.c. machines and induction motors and explain the procedures with specific examples.

The thesis is divided into three major parts. Part I deals with the design of a conventional power transformer and two special purpose power transformers viz., furnace and rectifier transformers. The design problems of d.c. separately excited and series motors supplied through thyristor

convertors, constitute part II. The third part deals with the design of a variable speed squirrel-cage induction motor when fed from a static frequency inverter.

Since the mathematical model describing the above electromagnetic devices is inherently nonlinear in nature, NLP techniques are adopted for arriving at optimal designs.

1.2 STATE OF THE ART

Mathematical programming techniques have been applied to the design of electrical equipment since 1960. The design optimization of transformers at minimum cost is taken up as a problem in geometric programming by Duffin and Zener [2,3]. The cost function of an induction motor is formulated and minimized as an unconstrained minimization problem by Appelbaum and Erlicki [4]. Anderson [5] described a general procedure to the design optimization of power transformers and hydro-electric generators, using a descent method. Ramaratnam and Desai [6,7] have approached the design optimization of polyphase induction motors as a problem in NLP using interior penalty function method of Fiacco and McCormick [8,9]. The problem of designing large induction motors at minimum cost is approached using NLP by Menzies and Neal [10]. Ramamoorty and Rao [11] have established the suitability of exterior penalty function method, with Powell's

unconstrained minimization technique to the design optimization of polyphase reluctance motors. Sridhar Rao et al. [12] have compared the NLP techniques for transformer design, replacing the constrained problem with a single constraint [13]. Exact penalty function approach is claimed to be the best one for design optimization of transformers by the same authors.

1.3 OBJECTIVE AND SCOPE OF THE PRESENT WORK

Most of the present literature is concerned with the optimal design of conventional electrical machines with conventional power supplies. In the present work, emphasis is given in the first part of the thesis to the optimal design of power transformers and special purpose power transformers. In the later parts of the thesis, the optimal design of d.c. and a.c. motors with nonsinusoidal power supplies derived from static converters is considered. Accordingly the objectives of the thesis can be setforth as:

1. to formulate a nonlinear optimization procedure for the optimal design of power transformers,
2. to study the applicability of linear programming technique to the design of power transformers and to the sensitivity analysis on the optimal solution,
3. to develop optimal design procedures for two special purpose power transformers for supplying furnace and rectifier d.c. loads,

4. to present systematic design procedures for the optimal design of d.c. separately excited and series motors, supplied through thyristor converters,
5. to develop a design procedure for a variable speed squirrel-cage induction motor when fed from a non-sinusoidal voltage source.

The design optimization of a conventional power transformer is attempted by both NLP and LP techniques. The major difference in the construction and design procedures of two special purpose transformers and that of a conventional power transformer is brought out. In the case of furnace transformer, importance is given in the design procedure to the l.v. winding configuration as very large currents at very low voltages are supplied to the furnace. The nonsinusoidal nature of current in a rectifier power transformer supplying a d.c. load is recognised. The effect of this current on the operation of the transformer is taken care of in the design procedure. The secondary winding of this transformer is designed to supply large currents at very low voltages to the d.c. load.

The effect of rectified power supply on the operation of d.c. separately excited and series motors when supplied through three-phase fully controlled thyristor converters is considered in the design procedures. Also the present day manufacturing practice is incorporated while formulating

the design problems. The nonlinearity of the magnetic circuit of the series motor is considered in the design procedure.

In contrast to a conventional induction motor, the variable speed squirrel-cage induction motor when fed from a static frequency inverter presents a different problem. Torque pulsations and additional losses are important factors in the design procedure.

The mathematical model of the equipment considered is formulated with a cost function and desired constraints. An attempt is made in this thesis to establish the suitability of Zangwill's exterior penalty function formulation [14] along with Powell's minimization technique [15] to the design optimization of the above mentioned electromagnetic devices.

1.4 ORGANIZATION OF THESIS

The thesis is organized in ten chapters.

Mathematical programming methods as applied to the design problems of this thesis are discussed in Chapter 2.

The optimal design problem of a 5 MVA, 66 kV/11 kV, delta-star connected, three-phase conventional power transformer is posed as a constrained minimization problem with some of the specifications as constraints in Chapter 3.

This constrained minimization problem is converted into a sequence of unconstrained optimization problems using exterior penalty function formulation and solved by Powell's method to obtain minimum cost.

The design problem of a 5 MVA, 66 kV/11 kV, delta-star connected, three-phase power transformer, considered as an NLP problem in Chapter 3, is solved for the first time by LP approach in Chapter 4 by linearizing the nonlinear objective function and nonlinear constraint equations around an operating point by first order Taylor's series approximation. Revised simplex method of LP [16,17] is used to obtain the optimized design of the power transformer. Sensitivity analysis is carried out to study the effect of relaxing the maximum limit on constraints like flux density of core and temperature rise of windings, keeping the other constraints same on the overall cost function of the transformer.

In Chapter 5, the design procedure of a 64.5 MVA, 33 kV/384-712 volts, star-delta connected, three-phase, core type furnace transformer supplying a 150 ton direct arc furnace is developed. While deriving the rating of the transformer arc power, secondary circuit impedance and arc resistance are taken into consideration. The design optimization problem is solved as an NLP problem, minimizing the cost and satisfying important constraints like temperature rise, short-

circuit impedance, no-load current, efficiency of the transformer etc. Exterior penalty function method, along with Powell's unconstrained minimization technique is used to obtain the optimized design.

Chapter 6 is devoted to the design of another special purpose transformer viz., the rectifier power transformer supplying a d.c. load through a three-phase semiconductor diode bridge. A 4 MVA, 33kV/296 volts, star-delta connected three-phase, core type transformer is considered as an example for optimal design. The secondary current waveform is derived for star-delta connection of the transformer and the effect of the source impedance is considered. In the design analysis program, the eddy current losses in the windings, temperature rise of the equipment and mechanical stresses in windings are considered on the basis of actual current waveform. The optimal design problem is then solved as an NLP problem, minimizing the cost of the transformer and satisfying important constraints like temperature rise, no-load current, short-circuit impedance, efficiency, d.c. voltage regulation etc. The same technique as indicated in Chapter 5 is adopted to obtain the optimized design.

Optimal design of a 150 h.p., 550 volts, 4-pole, 1500 r.p.m., separately excited d.c. motor supplied through a three-phase thyristor convertor is the main theme of Chapter 7.

A d.c. motor fed from a thyristor converter is subjected to a pulsating voltage. The ripple current due to pulsating voltage causes additional losses in electric and magnetic circuits, introduces additional commutation problem etc. Laminated field structure with octagonal frame, compensating winding in the pole-face slots and interpole winding are considered in line with the current design practice. The design problem is formulated as an NLP problem with important constraints like commutating ability of the machine, ratio of torque to armature moment of intertia, pulse duty factor of armature current, efficiency of the motor etc. The active material cost of the d.c. motor is minimized, satisfying the desired constraints by exterior penalty function method with Powell's unconstrained minimization technique. The effects of source impedance and of the firing angle of the converter are studied on the optimal solution.

Chapter 8 deals with the optimal design of a 150 h.p., 550 volts, 4-pole, 1500 r.p.m., d.c. series motor supplied through a three-phase thyristor converter. In addition to the considerations of Chapter 7 on d.c. seperately excited motor, nonlinearity of the magnetic circuit is considered by a suitable approximation of the magnetization curve in the design problem. The design problem is solved as an NLP problem by the same technique as indicated in Chapter 7, minimizing

the active material cost of the motor. At the optimal solution, torque pulsation as well as the associated speed variation of the motor is determined.

Chapter 9 deals with the optimal design of another important electromagnetic device in the present day industry, viz., the three-phase squirrel-cage induction motor supplied with variable frequency, six-stepped nonsinusoidal voltages. A 5 h.p., 400 volts, 4-pole, three-phase, delta connected squirrel-cage motor is taken as an example for the optimal design. In the formulation of the design problem, additional losses and torque pulsations of the motor are considered over a frequency range. The design problem is posed as a constrained optimization problem with important constraints like per unit torque pulsation, power factor, magnetizing current, efficiency of the motor etc. The NLP problem is solved by exterior penalty function approach with Powell's unconstrained optimization technique, minimizing the active material cost of the motor over a frequency range.

The conclusions drawn from this thesis are presented in Chapter 10.

CHAPTER 2

FORMULATION OF THE OPTIMIZATION PROBLEMS AND SOLUTION TECHNIQUES

2.1 OPTIMIZATION PROBLEM

The design optimization problem of any electromagnetic device can be stated as a mathematical programming problem in the following way.

Find X where X is a n-dimensional vector consisting of x_j, $j = 1,2, \ldots , n$ such that F(X) is minimum, subject to given constraints $g_j(X)$ $\{ \leq = \geq \}$ 0, $j = 1,2, \ldots , m$ with $X \geq 0$.

The function F(X) is called the objective function and its choice is governed by the nature of the problem. F(X) and $g_j(X)$, $j = 1,2, \ldots , m$ denote single valued, real functions of n real variables. Each parameter might be constrained explicitly by upper and/or lower bounds as follows:

$$x_{li} < x_i < x_{ui} \quad , \quad i = 1,2, \ldots , n$$

Any vector X which satisfies the constraints is called a feasible solution.

As indicated in Section 1.1, NLP techniques are of interest for the design optimization of electromagnetic devices under consideration. The algorithms for general NLP are of the following two categories [18].

i. Transformation to an unconstrained problem.

ii. Linear approximation.

The essential idea of the transformation approach to NLP is to transform the constrained nonlinear problem into a sequence of unconstrained problems by adding one or more functions of the active constraints to the objective function and deleting the constraints as such. The penalty forces the solution to be confined to the feasible (or near feasible) region, the search for the minimum lies in the nonfeasible region. This approach is sometimes referred to as the indirect method. These transformation methods have proved most popular and successful for constrained minimization problems.

Linear approximation methods replace some or all nonlinear functions in the problem by their first order Taylor's series approximations obtained around the point of interest, $X^{(k)}$. By the repeated linearization of the nonlinear functions at each intermediate solution, a sequence $X^{(0)}$, $X^{(1)}$, ..., $X^{(k)}$ is generated which, under restricted conditions, can be proved to converge to the optimal solution X^* of the problem and which, under most reasonable model formulations, will converge to at least a local optimum.

2.2 NLP PROBLEM FORMULATION AND SOLUTION TECHNIQUE

The problem formulation is as follows

Find the design variables $X = (x_1, x_2, \ldots, x_n)$, (2.1)

such that $F(X)$ is minimum, (2.2)

subject to $g_j(X) \leq 0, \quad j = 1, 2, \ldots, m$, (2.3)

where X, $F(X)$ and $g_j(X)$ have the usual meanings.

Among search techniques of NLP, direct search methods are superior to gradient search methods as the gradients are to be evaluated numerically [19] for many engineering problems. Out of the powerful search methods, sequential unconstrained minimization technique of Fiacco and McCormick [20] and Powell's method of conjugate directions [15] are more prominent. The first method requires a feasible design to start with, which involves more computational time. For some of the practical problems, obtaining a feasible design itself is difficult when the design has to satisfy exacting constraints Powell's method, on the otherhand, is most efficient on the basis of function evaluations and has rapid convergence near the optimum.

The constrained design problem as given in equations (2.1) to (2.3) is transformed into a sequence of unconstrained optimization problems by Zangwill's exterior penalty function formulation [14]. The initial vector of variables, which

satisfies all the constraints, is not required in this formulation. A brief description of Zangwill's exterior penalty function formulation and Powell's method is presented in the next two sub-sections.

2.2.1 Exterior Penalty Function Formulation [14,19]

The augmented objective function, FA is formulated in this method with penalty parameter, r_k as

$$FA(X,r_k) = F(X) + r_k \sum_{j=1}^{m} < g_j(X) >^q , \quad r_k > 0 \qquad (2.4)$$

where $< g_j(X) >$ is defined as $\max[g_j(X), 0]$.

With a suitable value of r_1 and for any starting vector X_1, $FA(X,r_1)$ is minimized, using any of the unconstrained minimization techniques. The resulting point is X_2. This process is denoted as one unconstrained minimization cycle. At this point X_2, a new FA function is formed with $r_2 = k_0 r_1$, $k_0 > 1$ such that

$$FA(X,r_2) = F(X) + r_2 \sum_{j=1}^{m} < g_j(X) >^q \qquad (2.5)$$

With X_2 as the initial point, $FA(X,r_2)$ is minimized at X_3 and the process is continued.

It can be proved that as $r_k \to \infty$

$$\text{Min} \quad FA(X,r_k) = \text{Min} \quad F(X) \qquad (2.6)$$

$k \to \infty$

If FA is convex i.e. F and g_j's are convex, then the minimum obtained is the global minimum. Popular value of q is 2.

2.2.2 Powell's Method [15,19]

This method is an extension of the basic pattern search method, using conjugate directions. Quadratic convergence is an important property of this method. Since most of the functions near their minimum can be approximated very closely by a quadratic, Powell's method is claimed to be the most efficient among the direct search methods. Powell's modified procedure, which overcomes the tendency of his basic method to choose linearly dependent search directions, is as follows [21]:

1. With a starting point $X_0^{(0)}$ and initial search directions, $M_i^{(0)}$, i = 1,2,..., n parallel to the original co-ordinate axes, a sequence of single variable searches are made in the n initial directions, using quadratic approximation.

2. The last point, $X_n^{(k)}$; the point of greatest function improvement between the searches, $X_m^{(k)}$; the expanded point,

   $$X_t^{(k)} = 2 X_n^{(k)} - X_0^{(k)} \qquad (2.7)$$

   and the starting point for the iteration $X_0^{(k)}$ are

located. k is the stage index which is incremented for each new set of search directions.

3. If there is no improvement of objective function $F_t^{(k)}$ at $X_t^{(k)}$ from $F_0^{(k)}$ at $X_0^{(k)}$, set

$$X_0^{(k+1)} = X_n^{(k)} \tag{2.8}$$

$$M_i^{(k+1)} = M_i^{(k)} \qquad i = 1,2, \ldots, n \tag{2.9}$$

If $F_t^{(k)}$ is an improvement over $F_0^{(k)}$ and

$$[F_0^{(k)} - 2F_n^{(k)} + 2F_t^{(k)}][F_0^{(k)} - F_n^{(k)} - \Delta]^2 \geq \frac{\Delta [F_0^{(k)} - F_t^{(k)}]^2}{2} \tag{2.10}$$

where $$\Delta = |F_m^{(k)} - F_{m-1}^{(k)}| \tag{2.11}$$

is satisfied, the old search directions are retained and a new sequence of single variable search is started as above. If the expression (2.10) is not satisfied a single variable search is performed in the direction $Z_n^{(k)}$ given by

$$Z_n^{(k)} = X_n^{(k)} - X_0^{(k)} \tag{2.12}$$

until the best value $X_0^{(k+1)}$ is found. New search directions

$$M_i^{(k+1)} = M_i^{(k)} \qquad \text{for} \qquad i = 1,2,\ldots, m-1 \tag{2.13}$$

$$M_i^{(k+1)} = M_{i+1}^{(k)} \qquad \text{for} \qquad i = m,m+1,\ldots, n-1 \tag{2.14}$$

$$M_n^{(k+1)} = Z^{(k)} \tag{2.15}$$

are then selected and a new sequence of single variable search is started.

4. Convergence is assumed when

$$|X_i^{(k)} - X_i^{(k-1)}| < \varepsilon \quad , \quad i = 1,2,\ldots,n \tag{2.16}$$

where ε is preset limit.

The flow chart is given in Fig. 2.1

The unconstrained optimization problem as outlined in Section 2.2.1 is solved by Powell's method. Exterior penalty function formulation, along with Powell's unconstrained minimization technique is one form of sequential transformation method which is used in this thesis to obtain the optimal design of electromagnetic devices.

2.3 LP PROBLEM FORMULATION AND SOLUTION TECHNIQUE

The general LP problem is defined as follows [17,19]:

Find the design variables

$$X = (x_1, \ldots, x_n) \tag{2.17}$$

that minimizes or maximizes the objective function

$$F(X) = \sum_{j=1}^{n} c_j x_j , \tag{2.18}$$

subject to the constraints

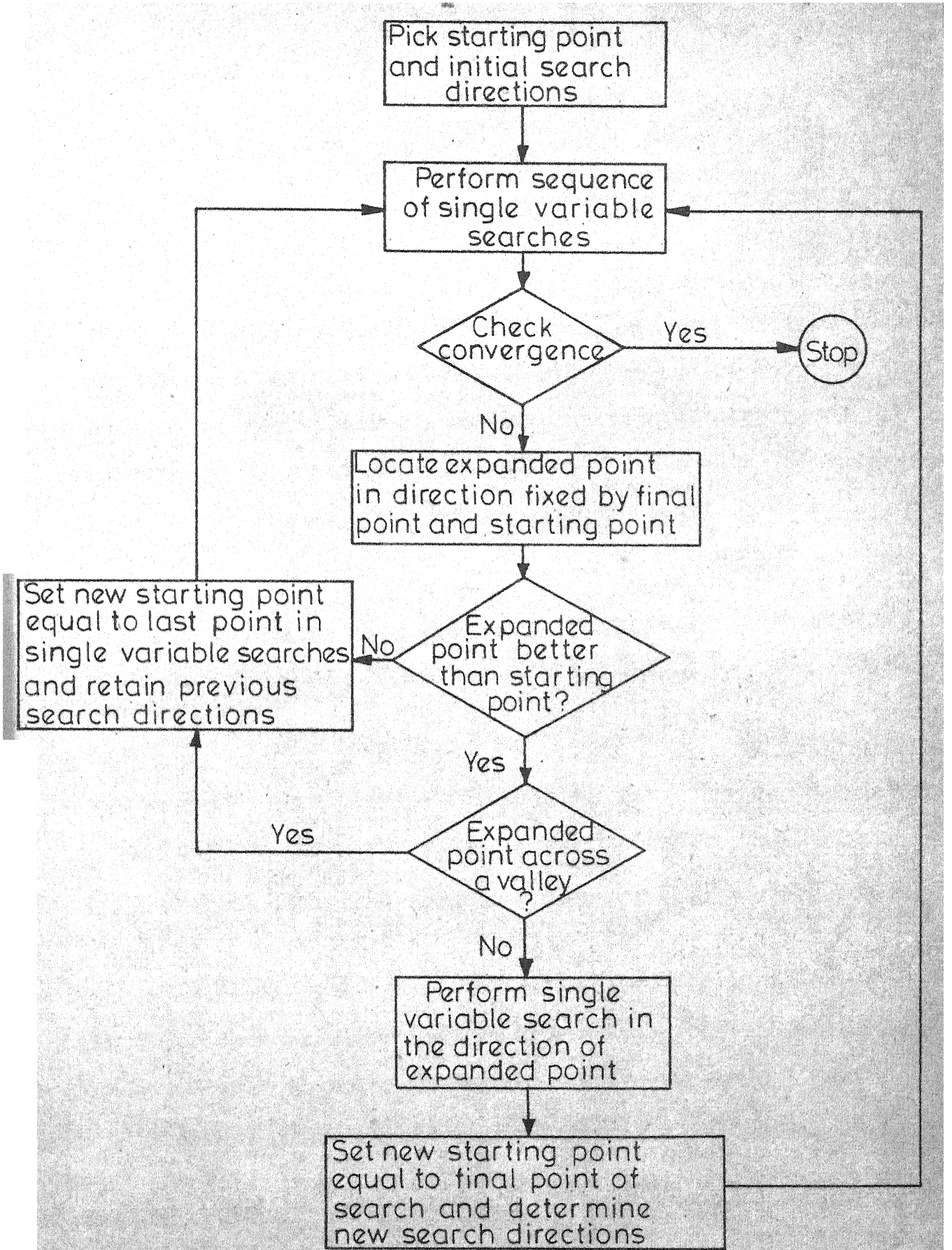

FIG. 2·1. FLOW CHART FOR POWELL'S METHOD.

$$\sum_{j=1}^{n} a_{ij} x_j \{ \leq \geq = \} b_i \quad , \; i = 1,2,\ldots,m \qquad (2.19)$$

$$x_j \geq 0 \quad , \quad j = 1,2, \ldots , n \qquad (2.20)$$

where a_{ij}, b_i, c_j are given constants and x_j are the decision variables. Slack and surplus variables are used to transform the inequalities in expression (2.19) into equalities. The variables x_j may be unrestricted i.e., the variables can be positive, negative or zero. To solve an LP problem containing unrestricted variables, first it is converted to a problem having nonnegative variables. The variable x_j unrestricted in sign, is denoted as

$$x_j = x_j' - x_j'' \quad , \quad x_j', x_j'' \geq 0 \qquad (2.21)$$

If $x_j' > x_j''$, then $x_j > 0$ and if $x_j' < x_j''$, it follows that $x_j < 0$. Also if $x_j' = x_j''$, then $x_j = 0$. Hence, depending on the magnitude of x_j' and x_j'', x_j can have any sign.

If the decision variables are permitted to vary continuously, then the LP problem is in standard form. The linear approximation of the NLP problem is similarly posed as the LP problem as discussed above and the revised simplex method is used to solve the resultant LP problem. A brief description of the revised simplex method is presented in the next sub-section.

2.3.1 Revised Simplex Method

In the revised simplex method [16,17], for any given basic feasible solution, movement from that solution to an optimal basic feasible solution is carried out by changing a single vector in the basis at a time. The same criterion as in simplex method is used to determine the vector to enter and leave the basis. An initial identity matrix is selected as a basis matrix [16] to initiate the solution on a digital computer. The objective function is treated as if it were another constraint. There are two standard forms for the revised simplex method.

Standard Form I: After adding slack and surplus variables, it is assumed that an identity matrix is present as a basis matrix. The artificial variables are not required here. The LP problem is formulated as

$$\text{Maximize} \quad z = \sum_{j=1}^{n} c_j x_j , \tag{2.22}$$

subject to the constraints

$$\sum_{j=1}^{n} a_{ij} x_j = b_i, \qquad i = 1,2,\ldots,m \tag{2.23}$$

$$x_j \geq 0, \qquad j = 1,2,\ldots,n \tag{2.24}$$

where the cost function, $z = f(x_1, x_2, \ldots, x_n)$.

Any minimization problem can be converted into a maximization problem. Equation (2.22) can be considered to

be a system of (m+1) simultaneous linear equations in (n+1) variables $z, x_1, \ldots, x_n$ and a solution is obtained such that z is as large as possible (and unrestricted in sign), subject to equation (2.24).

Standard Form II: This is used when artificial vectors must be added to obtain an identity matrix for the initial basis matrix. The artificial variables are handled by the two-phase method [17]. In phase I, the artificial variables are driven to zero, and in phase II, an optimal solution to the original problem represented by equations (2.17) to (2.20) is obtained.

In phase I, the function

$$z^* + \sum_{i=1}^{s} x_{ai} = 0 \qquad (2.25)$$

where x_{ai} are artificial variables, is maximized. If maximum $z^* = 0$, then phase II is considered. When maximum $z^* < 0$, there is no feasible solution to the problem. In phase II, the following set of equations are considered and z is maximized.

$$z - \sum_{j=1}^{n} c_j x_j = 0 \qquad (2.26)$$

$$z^* + \sum_{i=1}^{s} x_{ai} = 0 \qquad (2.27)$$

$$\sum_{i=1}^{m} a_{ik} x_k = b_i \quad , \quad k = 1,2,\ldots,p \qquad (2.28)$$

During phase II, z is the only variable which does not need to be nonnegative.

PART - I

POWER TRANSFORMERS

CHAPTER 3

OPTIMAL DESIGN OF POWER TRANSFORMER

3.1 INTRODUCTION

The power transformer is one of the most important links in a power system. The design of a power transformer involves obtaining the shape and size of the magnetic core, windings, tank and external heat exchangers while satisfying the specifications imposed by the manufacturer, customer and the national standards. The optimum design aspect arises because the values are to be chosen in such a way that the design will be one that satisfies all the limitations and restrictions placed on it and is best in some sense. Williams et al., Sharpely and Oldfield have pioneered the computer-aided design of power transformers [22,23,24]. Anderson [5] suggested a method to obtain optimized design of power transformers. The aim of this chapter is to arrive at the optimal design of a 5 MVA power transformer at minimum cost by NLP approach satisfying important constraints. First the design problem is formulated as an NLP problem, expressing the objective and constraint functions in terms of the specified independent variables. The NLP problem is then converted into a sequence of unconstrained optimization problems using Zangwill's exterior penalty function formulation and is solved by Powell's method. The performance of the optimized design of a 5 MVA, 66 kV/11 kV, three-phase, core type, delta-star connected power transformer is present

3.2 DESIGN PROBLEM FORMULATION

The formulation of the design problem as an NLP problem involves the objective and constraint functions in terms of the design or decision variables. These design variables are also called independent variables. The choice of the following five independent variables for the optimization problem out of many variables of the power transformer is based on the significant effect of these on the short-circuit reactance, weight, losses, core dimensions and finally on the cost of the transformer.

1. Maximum flux density in the core : x_1 Tesla
2. Current density in the h.v. winding : x_2 A/mm^2
3. Current density in the l.v. winding : x_3 A/mm^2
4. Height of the windings : x_4 m
5. Voltage per turn : x_5 V

All the five variables are assumed to be continuous. For an economical design of a power transformer, the objective or cost function should consist of the initial cost, capitalized cost of losses in the transformer and cost of external heat exchangers [25]. The initial cost is the material cost of stampings and copper windings. Manufacturing costs and labour costs widely vary between different shop floors of this country and so these are not included in the cost function. The degree of utilization of a power

transformer is limited by the permissible temperature rise of windings, short-circuit capability and by the magnetic properties of the active iron.

The specifications to be satisfied by the transformer and some of the performance characteristics logically form the constraints. The following constraints are imposed on the design problem:

1. Temperature rise of windings above ambient
2. Temperature rise of oil above ambient
3. Short-circuit impedance
4. Current densities in the windings
5. Flux density in the core
6. Efficiency of the transformer
7. No-load current

3.3 BRIEF DESCRIPTION OF OPTIMIZATION PROGRAM

The optimization program consists of the main program for the minimization of unconstrained optimization using Powell's algorithm and seven subroutines. The subroutines are described here and the flow diagram of the computer program is given in Fig. 3.1.

Subroutine TDATA: The purpose of this routine is to design, analyse and calculate the cost function and constraints of the transformer, given the set of independent variables, as

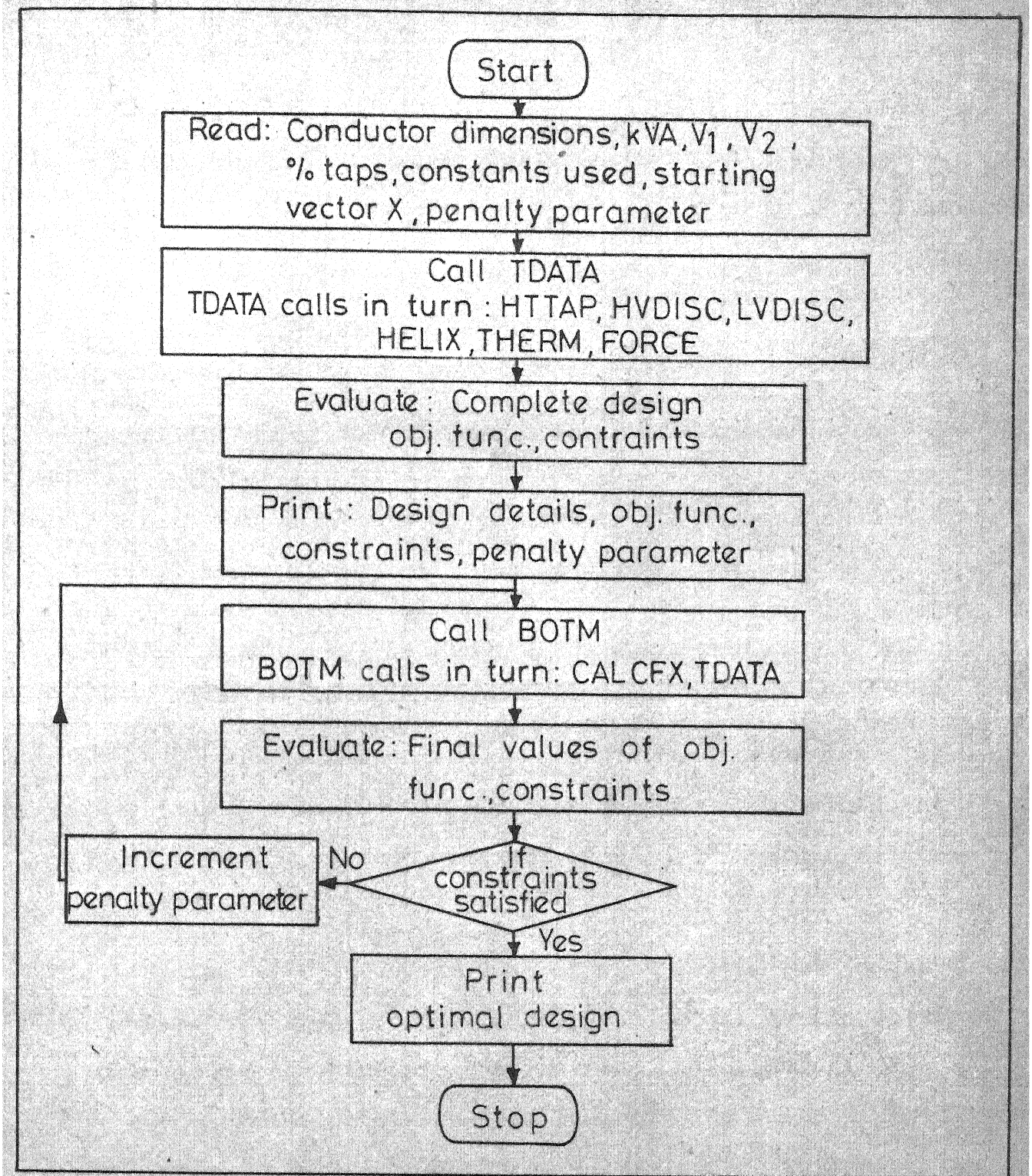

FIG. 3.1. FLOW DIAGRAM OF THE COMPUTER PROGRAM.

well as a set of constant parameters such as kVA, voltage ratings, % taps, constants used in the expressions, insulation details etc.

Subroutine HVTAP: This routine is arranged to test the following conditions in the order of sequence.

i. Turns per tap step rounded to the nearest even integer.

ii. Turns per tap step rounded to the nearest odd integer.

iii. Turns per tap step rounded to odd and even integers in alternate tap steps.

iv. Total number of turns on each step rounded to the nearest integer.

Thus the integral number of turns on each tap step is obtained without exceeding the maximum permissible ratio error of $\pm$ 0.5 percent vide ISS (Indian Standard Specifications) 2026 - 1962 for power transformers.

Subroutine HVDISC: The purpose of this routine is to design the h.v. winding with continuous disc coils. While obtaining suitable design, the program ensures the following: (i) Proper clearances between normal disc coils and increased clearances between strengthened insulation coils used at the ends. (ii) Approximately equal widths for normal coils and end coils. (iii) 1.5 to 2 times cross-section area of normal conductor for the turns used in end coils. (iv) The number of the coils is a multiple of four.

Subroutine LVDISC: This routine is similar to HVDISC except that in this case all coils are similar and smaller clearances are used between coils of l.v. winding.

Subroutine THERM: This routine calculates the average winding temperature rise above ambient, average oil temperature rise above ambient, top oil temperature rise, the number of external heat exchangers etc.

Subroutine FORCE: The purpose of this routine is to determine the mechanical strength of the transformer during a three-phase short-circuit. The coefficient for the computation of peak current, considering the aperiodical component of short-circuit current is taken as 1.8 (vide ISS). The stresses in the various windings due to axial and radial forces, and stress in spacers placed between turns of l.v. winding are calculated.

Subroutine CALCFX: This routine calculates the augmented objective or cost function using exterior penalty function formulation.

Coreloss curve, magnetization power curve for core, and joints of c.r.g.o. steel are incorporated through polynomial expressions in the computer program. Standard strap conductor dimensions are stored in the computer memory for the design of windings.

3.4 EXPRESSIONS FOR OBJECTIVE AND CONSTRAINT FUNCTIONS

3.4.1 Objective Function

As indicated in Section 3.2, the objective or cost function, FO is expressed as

FO = initial cost + capitalized cost of losses + cost of external heat exchangers.

Initial cost is the material cost of stampings and copper windings. Capitalized cost of losses depends upon (i) maximum demand charge as an additional demand caused by losses, (ii) cost of electrical energy wasted as transformer losses.

Expression for (i) is written as

$$P_c \; DM^2 \; CD + P_i \; CD \qquad (3.1)$$

where P_c = normal full-load copper loss of transformer, kW

P_i = iron loss of transformer, kW

DM = (maximum demand/CMR of transformer)

CD = maximum demand charge, Rs/kW

Expression for (ii) is written as

$$24 \times 365 \; (DR \; DM^2 \; P_c \; CE + LF_i \; P_i \; CE) \qquad (3.2)$$

where DR = (r.m.s. demand/maximum demand)^2

CE = cost of electrical energy, Rs/kWH

LF_i = iron loss load factor, assumed as unity

If i = percentage annual rate of interest

N = estimated life of the transformer in years

then the capital recovery factor, RF is given by

$$RF = i(1 + i)^N/[(1 + i)^N - 1] \quad (3.3)$$

With capital recovery factor, RF, the capitalized cost of losses is obtained by combining the expressions (3.1) and (3.2) and rewriting as

$$C1\ P_c + C2\ P_i \quad (3.4)$$

where $$C1 = (CD\ DM^2 + 24 \times 365\ DR\ DM^2\ CE)/RF \quad (3.5)$$

$$C2 = (CD + 24 \times 365\ CE)/RF \quad (3.6)$$

Denoting C1 and C2 as loss capitalization factors, the total objective function is written as

$$FO = C + C1\ P_c + C2\ P_i + C3\ NR \quad (3.7)$$

where C = initial cost

C3 = cost of each heat exchanger

NR = number of heat exchangers

$$C = CI(G_1 + G_y) + CC\ G_c \quad (3.8)$$

$$G_1 = k_1\ A_i\ (x_4 + k_2) \quad (3.9)$$

$$G_y = k_3\ A_i\ W \quad (3.10)$$

$$A_i = x_5/(4.44\ x_1\ f) \tag{3.11}$$

$$W = 2(d + 2b_2 + 2b_1 + k_4) + 0.9\ d \tag{3.12}$$

$$d = [4A_i/(\pi\ k_5)]^{\frac{1}{2}} \tag{3.13}$$

$$G_c = k_6[L_{mt1}\ m_1(T_1\ a_1 + T_s\ a_s) + L_{mt2}\ n_c\ m_2\ T_2\ a_2] \tag{3.14}$$

$$L_{mt1} = \pi(d + 2b_2 + b_1 + k_7) \tag{3.15}$$

$$L_{mt2} = \pi(d + b_2 + k_8) \tag{3.16}$$

$$b = k_9\ n_R\ BO_c + k_{10} \tag{3.17}$$

$$P_c = P_{c1} + P_{c2} + P_e + P_s \tag{3.18}$$

$$P_{c1} = 3I_1^2\ R_1/1000 \tag{3.19}$$

$$P_{c2} = 3I_2^2\ R_2/1000 \tag{3.20}$$

$$R_1 = \rho\ L_{mt1}(T_1/a_1 + T_s/a_s)/m_1 \tag{3.21}$$

$$R_2 = \rho\ L_{mt2}\ T_2/(a_2\ m_2) \tag{3.22}$$

$$I = S_1/V \tag{3.23}$$

$$S_1 = S/3 \tag{3.24}$$

$$P_e = \sum\ k_{11}\ BO^4\ n_R^2\ f^2\ \beta^2\ (3I^2R/1000) \tag{3.25}$$

$$\beta = AO\ n_A\ K_R/x_4 \tag{3.26}$$

$$K_R = 1 - [1 - e^{-(\pi\ x_4/\tau)}]/(\pi\ x_4/\tau) \tag{3.27}$$

$$\tau = b_1 + b_2 + k_{12} \tag{3.28}$$

$$P_s = \frac{k_{13}\, X_{sc}^2\, x_1^2\, A_i^2\, x_4^3\, f}{MT[x_4 + 2(KZ - 0.5\ D12)]^2} \tag{3.29}$$

$$X_{sc} = k_{14}\, f\, S_1\, K_R\, D12/(x_4\, x_5^2) \tag{3.30}$$

$$MT = 2(TKL - TKW) + \pi\ TKW \tag{3.31}$$

$$TKL = W + 2b_1 + 2b_2 + k_{15} \tag{3.32}$$

$$TKW = d + 2b_1 + 2b_2 + k_{16} \tag{3.33}$$

$$TKH = x_4 + 2(1.15\ A_i)^{\frac{1}{2}} + k_{17} \tag{3.34}$$

$$KZ = 0.5(d + 2b_1 + 2b_2 + k_{18}) \tag{3.35}$$

$$D12 = d + 2b_1 + k_{19} \tag{3.36}$$

$$P_i = [FF(x_1)\ G_1 + 1.075\ FF(B_y)\ G_y] \tag{3.37}$$

$$B_y = x_1/1.15 \tag{3.38}$$

$$NR = \frac{1}{0.75\ A_R}\left[\frac{P_i + P_c}{q_o} - MT\ TKH + 0.75\ A_L\right] \tag{3.39}$$

$$A_L = TKW(TKL - TKW) + \pi(TKW)^2/4 \tag{3.40}$$

The expressions related to the geometry of the transformer are obvious and simple to derive. For derivations of the expressions related to eddy current losses in conductors, P_e; stray load loss, P_s and short-circuit impedance, X_{sc} reference can be made to [26]. The external heat exchanger surface area, A_R for a minimum tank height is obtained from the Table 9-8 of the reference [26].

For the calculation of iron loss in the magnetic circuit, the iron loss curve is assumed to be a sixth degree polynomial of the form.

$$FF(x) = a_1 x + a_2 x^2 + a_3 x^3 + a_4 x^4 + a_5 x^5 + a_6 x^6 \qquad (3.41)$$

where FF(x) represents iron loss in Watts/kg of 0.35 mm thickness laminations of c.r.g.o. steel at 50 Hz, corresponding to the flux density x Tesla. $a_1, \ldots, a_6$ are constants. These constants are computed from expression (3.41) by substituting six sets of values of x and FF(x) from the actual iron loss curve in the usual operating range of flux density of 1.5 to 1.85 Tesla. The resultant polynomial representation is given in equation (3.42)

$$FF(x) = 172.8 x - 616.5 x^2 + 876.6 x^3 - 618.4 x^4 + 216.7 x^5 - 30.17 x^6 \qquad (3.42)$$

It is observed that the results obtained from the above procedure are sufficiently accurate, although linear interpolation of actual iron loss curve could be used to obtain specific values of iron loss.

3.4.2 Constraint Functions

Normally the specifications and performance of the transformer dictate the constraint functions. These are expressed as inequalities. The right hand side quantities of the constraints must conform to the rating of the transformer. As an example, a 5 MVA power transformer is considered here for the optimum design. The limitations on constraints are according to ISS. The expressions for constraint functions are as follows:

1. Temperature rise of winding above ambient

$$\theta_{wa} \leq 55 \tag{3.43}$$

$$\theta_{wa} = \theta_w + \theta_o \tag{3.44}$$

where

$$\theta_w = k_{20}\, q_w^{0.6} \tag{3.45}$$

$$q_w = \rho\, I\, T_c\, J\, K_e\, K_s / MC \tag{3.46}$$

$$K_e = 1 + P_e/(P_{c1} + P_{c2}) \tag{3.47}$$

$$K_s = L_{mt}/(L_{mt} - n_s\, b_s) \tag{3.48}$$

$$MC = 2[k_{21}\, n_R(B0 + k_{22}) + n_A(A0 + k_{23})]10^{-2} \tag{3.49}$$

2. Temperature rise of top oil above ambient

$$\theta_{oa} \leq 45 \tag{3.50}$$

$$\theta_{oa} = 1.2\, \theta_o + k_{24} \tag{3.51}$$

$$\theta_o = 55 - \theta_{wo} \tag{3.52}$$

$$q_o = (\theta_o/k_{25})^{1.25} \tag{3.53}$$

Specific thermal load of winding, q_w is determined from copper loss in the winding and cooling area of the coil.

$$q_w = I^2 R K_e K_s/(MC L_{mt}) \tag{3.54}$$

where K_e = eddy loss factor

K_s = space factor considering spacers in the coils

MC = perimeter of the coil, m

L_{mt} = length of mean turn of the winding, m

writing

$$I = J a \tag{3.55}$$

$$R = \rho L_{mt} T_c/a \tag{3.56}$$

and substituting in the expression (3.54)

$$q_w = \rho I T_c J K_e K_s/MC \tag{3.57}$$

Empirical formulas used for the calculation of winding temperature rise and oil temperature rise are based on the specific thermal load of 1200 to 2000 Watts/m^2 for windings and 1000 to 1500 Watts/m^2 for oil [26,27].

Here k_{20} = 0.358 for outer windings

= 0.41 for inner windings

and k_{25} = 0.262

3. Percentage short-circuit impedance

$$Z_{sc} \geq 7.15 \tag{3.58}$$

$$Z_{sc} = (R_{sc}^2 + X_{sc}^2)^{\frac{1}{2}} \tag{3.59}$$

$$R_{sc} = P_c \, 100/S \tag{3.60}$$

4. Flux density in the core

$$1.55 \leq x_1 \leq 1.65 \tag{3.61}$$

5. Current density in the windings

$$x_2 \leq 3.5 \tag{3.62}$$

$$x_3 \leq 3.5 \tag{3.63}$$

6. Percentage efficiency of the transformer

$$\eta \geq 99.0 \tag{3.64}$$

$$\eta = [1 - (P_c + P_i)/(S\ PF + P_c + P_i)]100 \tag{3.65}$$

7. Percentage no-load current

$$I_o \leq 3.0 \tag{3.66}$$

$$I_o = (I_{oa}^2 + I_{or}^2)^{\frac{1}{2}} \tag{3.67}$$

$$I_{oa} = P_i \, 100/S \tag{3.68}$$

$$I_{or} = [GG(x_1)\ G_1 + GG(B_y)\ G_y + 7\ A_i\ HH(x_1)]/(10\ S) \tag{3.69}$$

The reactive component of magnetizing current, I_{or} is obtained from similar polynomial expressions (3.41) for

the magnetizing power curve in the usual flux density range, for core and joints independently. The resultant polynomial representations are derived as

$$GG(x) = -\ 441.0\ x + 2081.0\ x^2 - 3710.0\ x^3 + 3174.0\ x^4 - 1315.0\ x^5 + 213.4\ x^6 \qquad (3.70)$$

$$HH(x) = -\ 206.0\ x + 780.1\ x^2 - 1176.0\ x^3 + 879.8\ x^4 - 326.1\ x^5 + 48.01\ x^6 \qquad (3.71)$$

In all these equations, suffixes 1 and 2 refer to h.v. and l.v windings respectively, except for x and k.

3.5 SOLUTION OF THE NLP PROBLEM

The design problem of the power transformer for minimum cost, as formulated in the earlier sections, is converted into a sequence of unconstrained optimization problems using Zangwill's exterior penalty function method. An initial vector of independent variables is selected as the starting point to initiate the iterative procedure. In the present problem, an initial penalty parameter of 7500 is used, and, after one complete unconstrained minimization cycle, it is incremented by a factor of 10. The initial value of the penalty parameter is selected such that the penalty due to the active constraints is almost equal to the value of the cost function.

Optimal solutions minimizing the cost are obtained by Powell's method for a 5 MVA, 66 kV/11 kV, three-phase, core type, delta-star connected power transformer with different starting points on IBM 7044 computer and presented in Table 3.1. Convergence to the optimal solution is achieved after 4 to 5 unconstrained minimization cycles. Table 3.1 gives optimal solutions for five starting points considered and corresponding constraint violations. The cost corresponding to the first starting point is taken as 100% for comparison. The solution which gives the lowest cost together with no constraint violations is taken as the final optimal solution. This strategy is adopted since the convexity of the function to be minimized is difficult to check [28].

In all the cases considered above, the mechanical stresses in windings and spacers for maximum short-circuit currents, obtained from standard equations (8.10) to (8.22) of reference [26] are well within the permissible values.

3.6 OPTIMIZED DESIGN OF A 5 MVA POWER TRANSFORMER

The optimized design data and performance characteristics of the specified transformer are obtained for the optimal solution corresponding to starting point 3, and are presented in Table 3.2. It is observed from Table 3.2 that the constraints on temperature rise of the windings, short-

TABLE 3.1

OPTIMAL SOLUTIONS OF A 5 MVA, 66 KV/11 KV, THREE-PHASE, CORE TYPE, DELTA-STAR CONNECTED POWER TRANSFORMER

rticulars	Starting point 1	Optimum value	Starting point 2	Optimum value	Starting point 3	Optimum* value	Starting point 4	Optimum value	Starting point 5	Optimum value
Tesla	1.50	1.646	1.50	1.648	1.50	1.643	1.50	1.648	1.65	1.644
A/mm^2	3.50	3.073	3.00	3.009	3.00	2.990	3.00	3.000	2.80	2.951
A/mm^2	2.50	2.544	2.80	2.943	2.70	3.153	2.70	2.936	2.75	2.843
m	0.85	0.842	0.90	0.896	0.85	0.888	0.90	0.896	0.95	0.933
V	33.50	33.543	31.50	31.237	31.50	31.525	31.50	31.226	30.208	30.618
st, %	100.0	95.9	99.0	96.0	99.9	95.7	99.4	96.0	97.0	96.0
of nstraint olations	1	0	1	0	1	0	1	0	0	0
of un- nstrained nimization cles		5		5		4		5		5
ecution time, conds		63		79		58		61		94

Indicates selected final optimum solution corresponding to starting point 3.

TABLE 3.2

OPTIMIZED DESIGN DATA AND PERFORMANCE OF A 5MVA, 66 KV/11 KV, THREE-PHASE, CORE TYPE, DELTA-STAR CONNECTED POWER TRANSFORMER

1.	Constraints	
	a. Temperature rise of windings above ambient, °C	54.24
	b. Temperature rise of oil above ambient, °C	40.40
	c. Percentage short-circuit impedance	7.17
	d. Percentage efficiency	99.08
	e. Percentage no-load current	1.736
2.	Design Data	
	1. Core circle diameter, m	0.370
	2. Width of core, m	1.735
	3. Height of core, m	1.038
	4. Weight of core stampings, kg	4633.67
	5. Weight of copper windings, kg	1607.77
	6. Tank dimensions, m	1.471 x 2.872 x 2.168
	7. Number of external heat exchangers	6
	8. HV winding	
	a. Number of turns on principal tap	2192
	b. Number of coils	72
	c. Width of normal coil, mm	66.84
	d. Dimensions of normal conductor, mm	5.5 x 1.56
	e. Width of coil with strengthened insulation, mm	65.58
	f. Dimensions of conductor with strengthened insulation, mm	8.0 x 1.95
	g. Resistance of winding per phase, ohm	10.4035

9. LV winding

a. Number of turns	201
b. Number of coils	43
c. Width of coil, mm	36.4
d. Dimensions of conductor, mm	6.9 x 3.05
e. Resistance of winding per phase, ohm	0.0728

3. Performance

1. Percentage magnetizing component of no-load current	1.725
2. Percentage short-circuit resistance	0.731
3. Percentage short-circuit reactance	7.135
4. Total copper loss including eddy current loss in conductors, kW	35.185
5. Stray loss, kW	1.342
6. Total core loss, kW	9.710
7. Percentage regulation @ 0.8 p.f. lagging	4.864
8. Resultant stress in copper of h.v. winding, kg/cm^2	673.17
9. Resultant stress in copper of l.v. winding, kg/cm^2	381.54
10. Stress in spacers placed between turns of l.v. winding, kg/cm^2	153.28

circuit impedance, flux density of the core and efficiency of the transformer have become active at the optimal solution and are driven to their limits.

3.7 CONCLUSIONS

NLP technique is successfully applied to the optimal design problem of a power transformer, representing the mathematical model with only five independent variables. Important constraints are imposed on the design problem to satisfy many performance requirements. The active constraints are temperature rise of the windings, short-circuit impedance, flux density in the core, and efficiency of the transformer. The results for the 5 KVA transformer compare well with normal design of the same rating transformer and a similar procedure can be adopted for a line of transformers. The execution time for obtaining each optimal solution on IBM 7044 computer is on the average one minute. Powell's method, in conjunction with Zangwill's exterior penalty function formulation, is well suited for finding optimal design of power transformers.

In Table 3.1, the last starting point and the corresponding optimal solution are not very far from each other. In view of this, the use of LP technique to the design optimization of power transformer may be contemplated when the nonlinear model is linearized around an operating point. This procedure is discussed in the next chapter.

CHAPTER 4

A LINEAR PROGRAMMING APPROACH TO THE OPTIMAL DESIGN OF POWER TRANSFORMER

4.1 INTRODUCTION

In Chapter 3, nonlinear optimization procedure to the design of power transformers is considered. As indicated in Section 2.1, one possible way of approaching nonlinear problems is linear approximation [19]. An attempt is made here for the first time to solve the optimal design problem of an electrical equipment by linear approximation. It was observed while solving the nonlinear optimization problem of a power transformer that the optimal solutions are not far from the operating points. This points to the possibility of using LP techniques for obtaining optimal design. The idea of linearizing the nonlinear objective function and nonlinear constraint functions of the power transformer around an operating point and the application of Linear Programming (LP) technique is explained in this chapter.

First the design problem is formulated as an LP problem, with linearized objective and constraint functions around an operating point by Taylor's series expansion. The LP problem is then solved by revised simplex method. The resulting optimal solution is tested with the original nonlinear mathematical model to ascertain whether all the nonlinear constraints are satisfied.

In many practical problems, it is of interest to know the change in optimal solution with a change in various parameters of the design problem. This study, known as sensitivity analysis or post-optimality, is also considered in this chapter. The effect of variation of flux density and temperature rise of windings on cost function is investigated as well. The design optimization of a 5 MVA, 66 kV/11 kV, three-phase, core type, delta-star connected power transformer is presented.

4.2 LINEARIZATION APPROACHES TO NONLINEAR PROBLEMS [19]

The original nonlinear problem of Chapter 2 is considered and stated as

$$\text{Find } X = (x_1, x_2, \ldots, x_n)$$

$$\text{such that } F(X) \text{ is minimum,}$$

$$\text{subject to } G_j(X) \leq 0 \quad , \quad j = 1,2,\ldots, m \qquad (4.1)$$

where X, $F(X)$ and $G_j(X)$ have the usual meanings.

For a given reasonable starting point X_o, which may be feasible or not, expanding (4.1) by Taylor's first order approximation,

$$F(X) \simeq F(X_o) + \nabla F(X_o)^T (X - X_o) = F^{(o)}(X) \qquad (4.2)$$

$$G_j(X) \simeq G_j(X_o) + \nabla G_j(X_o)^T (X - X_o) = G_j^{(o)}(X) \qquad (4.3)$$

The corresponding LP problem is stated as

Find X,

such that $F^{(o)}(X)$ is a minimum,

subject to $G_j^{(o)}(X) \leq 0 \quad , \quad j = 1,2,\ldots, m \qquad (4.4)$

This problem is expected to have a solution near to the actual solution of the original problem. Calling this solution point as X_1 and expanding again

$$F^{(1)}(X) \equiv F(X_1) + \nabla F(X_1)^T (X - X_1) \qquad (4.5)$$

$$G_j^{(1)}(X) \equiv G_j(X_1) + \nabla F(X_1)^T (X - X_1) \qquad (4.6)$$

The LP problem corresponding to expressions (4.5) and (4.6) is

Find X,

such that $F^{(1)}(X)$ is a minimum,

subject to $G_j^{(o)}(X) \leq 0 \quad , \quad j = 1,2,\ldots, m$

$$G_j^{(1)}(X) \leq 0 \quad , \quad j = 1,2,\ldots, m \qquad (4.7)$$

This process can be continued by adding new constraint approximations to expression (4.7) until the solution is seen to converge. Additional upper and lower bound constraints may be added to limit the movement of the solution from the point about which linearization is made [29].

4.3 DESIGN PROBLEM FORMULATION

The optimal design problem of a power transformer for minimum cost is posed as a problem of LP. The same five variables as in Section 3.2 are selected as independent variables and the corresponding change in variables Δx_1, Δx_2, Δx_3, Δx_4, Δx_5 which are unrestricted in sign are taken as decision variables for the LP problem. The same objective and constraint functions as stated in Chapter 3 for power transformer are considered here also. An initial vector of independent variables is selected as an operating point. The nonlinear objective function and nonlinear constraint functions of Section 3.4.1 and Section 3.4.2 respectively, are linearized around this operating point by first order approximation of Taylor's series expansion as indicated in expressions (4.2) and (4.3). The design problem may be posed as either a maximization or minimization problem.The right hand side quantities of the constraint equations are maintained as positive, if necessary by multiplying the equations throughout by -1. Similarly, the objective function is multiplied by -1 so that the formulation becomes a maximization problem. Revised simplex method as explained in Section 2.3.1 is applied to obtain optimal solution of the power transformer.

4.4 OPTIMIZATION PROGRAM

The optimization program includes the main program for the maximization of the objective function using revised simplex method and six subroutines. The main program generates the basis matrix, inverse of the initial basis and indicates the vectors in the basis. The input to the program consists of a number of equations, number of total variables, actual variables, artificial variables if any and the coefficients of objective and constraint functions in matrix form. The simplex algorithm operates in Standard Form I or Standard Form II, indicating end of phase I and beginning of phase II. The basis is transformed at each iteration by the usual transformation formula for the simplex method [17]. The subroutines are described in Section 3.3.

4.5 SOLUTION OF THE LP PROBLEM

The design problem of the power transformer for minimum cost, as formulated in the earlier sections with linearized equations, is solved by revised simplex method of LP. The solution of this problem is obtained in terms of the variables Δx_1, Δx_2, Δx_3, Δx_4, Δx_5 which are unrestricted in sign. The solution for the original nonlinear problem is derived from these variables and tested with the original nonlinear mathematical model to ascertain whether all the constraints are

satisfied. Otherwise, the present solution point is taken as the new operating point and new objective and constraint functions are evaluated as detailed in expressions (4.5) and (4.6). The new constraint equations are added to the old constraint equations and the process is continued until the optimal solution thus obtained is also feasible with the nonlinear model.

Optimal solutions minimizing the cost are thus obtained for a 5 MVA, 66 kV/11 kV, three-phase, core type, delta-star connected power transformer with different operating points, satisfying all the constraints in the nonlinear model after one or two cumulative iterations i.e., successive addition of old constraint equations to the new constraint equations. Table 4.1 gives optimal solutions for two initial operating points considered. The cost corresponding to the first starting point is taken as 100% for comparison. The optimal solution which gives the lowest cost and no constraint violations is taken as the final optimal solution. The mechanical stresses in windings and spacers for maximum short-circuit currents are seen to be well within permissible values in the nonlinear model as calculated from equations (8.10) to (8.22) of the reference [26].

TABLE 4.1

OPTIMAL SOLUTIONS OF A 5MVA, 66 KV/11 KV, THREE-PHASE, CORE TYPE, DELTA-STAR CONNECTED POWER TRANSFORMER

Particulars	Operating point 1	Optimum solution	Operating point 2	Optimum* solution
x_1 Tesla	1.600	1.650	1.630	1.650
x_2 A/mm^2	3.200	3.000	3.400	2.600
x_3 A/mm^2	2.800	2.800	2.800	2.600
x_4 m	0.975	0.875	0.975	0.875
x_5 V	29.500	31.181	31.000	32.750
Cost, %	100.0	99.2	99.2	99.0
No. of constraint violations	0	0	2	0
Execution time, seconds		28		43

* Indicates selected final optimum solution corresponding to operating point 2.

4.6 SENSITIVITY ANALYSIS OR POST-OPTIMALITY [30]

After obtaining optimal solution to an LP problem, it is often desirable to study the effect of discrete changes in the different parameters of the problem on the current optimal solution. The changes in the LP problem which are usually studied by sensitivity analysis include:

i. Tightness of constraints i.e., changes in the right hand side quantities of the constraint functions.

ii. Coefficients of the objective function.

iii. Addition of new constraints.

The first aspect is considered here.

With the improvement in magnetic and insulating materials, higher flux densities and higher temperature rise in windings can be allowed. Larger current densities are possible with better cooling arrangements.

For a given operating point, the effect of relaxing the maximum limit on constraints like flux density of core and temperature rise of windings above ambient keeping the other constraints same, on the overall objective function is investigated. The change in the optimal value of the cost for various flux densities is shown in Table 4.2.

A flux density of 1.82 Tesla in the core is observed to be critical value for the problem considered, satisfying all the constraints. The flux density may be increased to

TABLE 4.2

VARIATION OF COST RELAXING FLUX DENSITY IN CORE OF A 5 MVA, 66 KV/11 KV, THREE-PHASE, CORE TYPE, DELTA-STAR CONNECTED POWER TRANSFORMER

Permissible flux density in core, Tesla	1.60	1.65	1.70	1.75	1.80	1.82
Cost, %	100.0	99.2	98.7	98.0	97.3	96.8

TABLE 4.3

VARIATION OF COST RELAXING WINDING TEMPERATURE RISE OF A 5 MVA, 66 KV/11 KV, THREE-PHASE, CORE TYPE, DELTA-STAR CONNECTED POWER TRANSFORMER

Allowable winding temperature rise, °C	55.0	60.0
Cost, %	99.1	98.1
Current density in h.v. winding, A/mm^2	2.6	3.0
Current density in l.v. winding, A/mm^2	2.6	2.75

1.85 Tesla if the constraint on the magnetizing current could be relaxed slightly.

The effect of increase in the allowable winding temparature rise conforming to better insulating materials or method of cooling resulted in the reduction of cost as shown in Table 4.3.

In this example, the winding temperature could reach the upper bound only after the permissible current density in windings was raised. The corresponding values for each permissible temperature rise are given in the Table 4.3. Higher temperature rise in windings resulted in increased current densities and in an increased number of external heat exchangers at the optimal point. However, the reduction in weight of copper required for the windings resulted in the decrease of overall cost.

4.7 OPTIMIZED DESIGN OF A 5 MVA POWER TRANSFORMER

The optimized design data and performance characteristics of a 5 MVA, 66 kV/11 kV, three-phase, core type, delta-star connected power transformer are obtained for the optimal solution corresponding to operating point 2 and are presented in Table 4.4.

TABLE 4.4

OPTIMIZED DESIGN DATA AND PERFORMANCE OF A 5 MVA, 66 KV/11 KV, THREE-PHASE, CORE TYPE, DELTA-STAR CONNECTED POWER TRANSFORMER

1.	Constraints	
	a. Temperature rise of windings above ambient, °C	50.77
	b. Temperature rise of oil above ambient, °C	41.36
	c. Percentage short-circuit impedance	7.538
	d. Percentage efficiency	99.18
	e. Percentage no-load current	1.854
2.	Design Data	
	1. Core circle diameter, m	0.377
	2. Width of core, m	1.817
	3. Height of core, m	1.025
	4. Weight of core stampings, kg	4896.823
	5. Weight of copper windings, kg	1921.18
	6. Tank dimensions, m	1.51 x 2.99 x 2.17
	7. Number of external heat exchangers	5
	8. HV winding	
	a. Number of turns on principal tap	2114
	b. Number of coils	72
	c. Width of normal coil, mm	76.39
	d. Dimensions of normal conductor, mm	5.9 x 1.95
	e. Width of strengthened insulation coil, mm	75.62

f.	Dimensions of conductor of strengthened insulation coil, mm	7.4 x 2.1
g.	Resistance of winding per phase, ohm	9.05

9. LV winding

a.	Number of turns	194
b.	Number of coils	40
c.	Width of coil, mm	42.8
d.	Dimensions of conductor, mm	7.4 x 3.53
e.	Resistance of winding per phase, ohm	0.0582

3. Performance

1.	Percentage magnetizing component of no-load current	1.843
2.	Percentage short-circuit resistance	0.624
3.	Percentage short-circuit reactance	7.512
4.	Total copper loss including eddy current loss in conductors, kW	29.737
5.	Stray loss, kW	1.497
6.	Total core loss, kW	10.308
7.	Percentage regulation @ 0.8 p.f. lagging	5.005
8.	Resultant stress in copper of h.v. winding, kg/cm^2	569.4385
9.	Resultant stress in copper of l.v. winding, kg/cm^2	265.481
10.	Stress in spacers placed between turns of l.v. winding, kg/cm^2	120.78

4.8 CONCLUSIONS

The linear approximation of a nonlinear design problem of a power transformer is solved by a well developed LP technique using considerably less computational time. The execution time on IBM 7044 computer for solving each LP problem on the average is 35 seconds. The NLP problem of Chapter 3 required about one minute when the nonlinear mathematical model is defined with only five independent variables. In the linearized mathematical model of the LP problem, with decision variable unrestricted in sign, the variables are ten. Though the computational time is less in this case, the complexity of the computer program is increased. The optimized design of the 5 MVA power transformer obtained by both NLP and LP approaches does not deviate much as seen from Tables 3.2 and 4.4.

The sensitivity analysis as indicated in Section 4.5 may bring into focus the point upto which the magnetic and insulating materials could be stressed in the construction of power transformers. The effect of cost coefficients of different core materials, copper or aluminum for windings, M.S. or aluminum heat exchangers can be studied with a few modifications in the program. More exacting constraints of equality type may also be included in this study.

The complexity of the computer program with the linearized model may sometimes overweigh the advantage gained in computational time in design optimization of electrical equipment. With more number of independent variables and more constraints, the design problem becomes too unwieldy. Hence, the linear approximation method is not considered further for the other design problems. The design optimization of two special purpose power transformers which are different in construction and operation from a conventional power transformer is taken up in the next two chapters.

CHAPTER 5

OPTIMAL DESIGN OF FURNACE TRANSFORMER

5.1 INTRODUCTION

Optimal design, minimizing the cost of special purpose transformers supplying the direct arc furnace loads is the topic of this chapter. Today large furnaces for making steel, with production capabilities of 50, 75 and even 100 tons per hour and shell diameters of 22 to 24 feet, are in operation [31]. For optimum operating conditions of the furnace, the electrical design of the associated power system, in particular the furnace transformer, contributes major share. Substantial increase in the rating of these transformers supplying large furnaces and the duty cycle of furnace, prompts one to go in for an optimal design with the desired constraints. Although computer-aided design of power and distribution type transformers has been considered in references [22-24], the design procedure of special purpose transformers used for furnace loads does not figure much in published literature. The construction, electrical characteristics and various types of connections of furnace transformers are outlined in references [32-34]. Modern trends and requirements of large furnace transformers are emphasized in references [35-38].

In this chapter, the furnace transformer with its associated power system is first described. The design

problem is formulated with specified independent variables and important constraints like temperature rise, efficiency, no-load current etc., of the transformer. This problem is then posed as a problem of NLP, the objective function being minimum cost of the transformer. The NLP problem is solved satisfying the constraints and the results of optimized design are obtained.

5.2 DESCRIPTION OF FURNACE TRANSFORMERS

Transformers for steel furnaces must conform to a very special technique which results from the very particular operating conditions of the furnace itself. In a direct arc furnace, heat is generated by a powerful electric arc struck between carbon or graphite electrodes and the metal charge. In addition to the normal constructional methods, a transformer for an arc furnace must be designed to supply a very large current by its secondary winding at a very low voltage and to withstand repeated electrical and mechanical stresses. The transformer's secondary or arc voltage must be sufficiently high to deliver the desired power and the secondary current capacity must be high enough to permit operation at currents higher than the normal current at the maximum voltage [39]. Regulation of the furnace voltage over a wide range is usually required and is attained by a large tapping

range of the transformer which extends from the maximum secondary voltage down to 50-25 percent of this voltage. In developing the transformer rating, arc power, secondary circuit impedance and arc resistance are important factors. The secondary circuit consists of secondary bus, flexible cables, copper bus tubes and electrodes. For a given effective arc voltage and arc current, a wide range of circuit impedances can be applied that result in the same average arc resistance [40].

5.3 DESIGN PROBLEM FORMULATION

5.3.1 Development of Furnace Transformer Rating

In this thesis, for the design problem, a star-delta connected, three-phase transformer is presumed to supply a 22-feet shell diameter, 150 ton furnace with a secondary circuit current of 60,000 amperes. A single line connection diagram of the power system, transformer and arc furnace is shown in Fig. 5.1. A typical average arc resistance curve when the transformer is operating on highest voltage tap is shown in Fig. 5.2 [40]. The KVA rating of the transformer is calculated as indicated here with known values of average arc resistance and secondary circuit impedance. Assuming,

average arc resistance/ph, R_A : 4.8 milliohms

secondary circuit impedance/ph, Z_s : 0.5 + j 2.7 milliohms

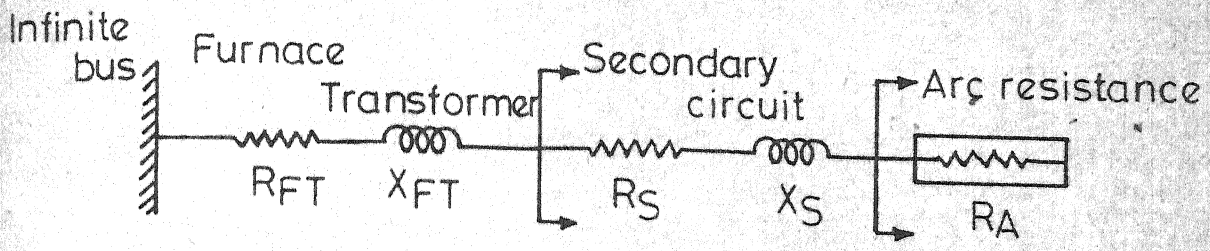

R_{FT} Resistance of furnace transformer
R_S Resistance of secondary circuit
X_{FT} Reactance of furnace transformer
X_S Reactance of secondary circuit
R_A Arc resistance

FIG. 5.1. CONNECTION DIAGRAM OF POWER SYSTEM, TRANSFORMER AND ARC RESISTANCE.

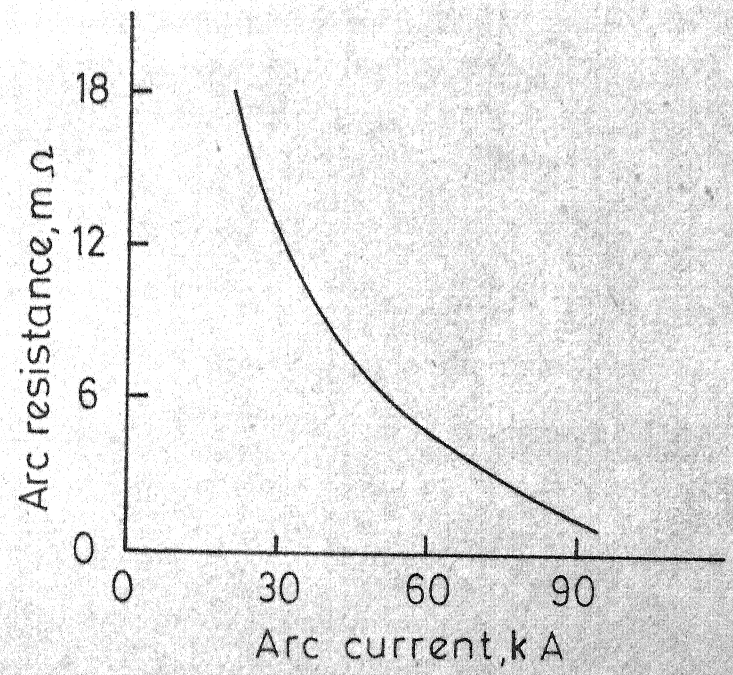

FIG. 5.2. ARC RESISTANCE CURVE.

for a 150 ton direct arc furnace, the secondary circuit current, I_c = 60 kA

The total circuit impedance, $Z_c = R_A + Z_s$

$= 5.3 + j\ 2.7$ milliohms

circuit voltage, $V_c = \sqrt{3}\ I_c\ Z_c$

= 620 volts on load

Transformer kVA rating, $S = \sqrt{3}\ V_c\ I_c$

= 64500 kVA

A supply voltage of 33 kV is assumed which is normal for transformers of this rating.

5.3.2 Structure of the Transformer

A 64.5 MVA, 33 kV/384-712 volts, star-delta connected, three-phase, core type transformer is considered here as an example for the optimal design problem. Wide secondary voltage range of 384 V to 712 V is arrived at by ± 30% taps, so that on the highest tap, the stipulated power is fed into the furnace and on the lowest tap, stable arc is maintained at low power input required for the holding of the melt. The three-legged core type construction is favoured in accordance with the present day practice. The desired secondary winding fixes the number of groups of coils, while the magnitude of current determines the arrangement of this winding.

Continuous disc type is chosen for the h.v. winding which is near the core, while for the l.v. side, two types of windings - helical and pair discs - are considered separately in the design procedure. These types of windings are normally used by the manufacturers depending upon the manufacturing practice [35,38]. Continuous disc type winding is more reliable from the point of mechanical strength. Helical winding is generally preferred when the number of turns are small but the current is large. The l.v. winding consists of a number of coils of multistrand conductor connected in parallel and arranged one above the other. The tappings provided on the h.v. winding of the transformer are arranged to give nine different voltages as per the specifications. Forced oil cooling of the transformer core and windings is considered. The above configurations of core and windings are obtained from manufacturer's pamphlets [35-38] on similar furnace transformers. The secondary winding is considered delta connected to minimize the stray loss and reactance drop caused by high secondary current, the start and finish leads of each phase winding is interleaved as far as the delta connection which is made as close to the furnace as possible.

5.3.3 Design Variables, Cost Function and Constraints

The choice of design variables is on similar lines as for ordinary power transformer mentioned in Section 3.2.

The following six design variables are selected as independent variables.

1. Flux density in the core : x_1 Tesla
2. Current density in the h.v. winding : x_2 A/mm^2
3. Current density in the l.v. winding : x_3 A/mm^2
4. Height of the windings : x_4 m
5. Voltage per turn : x_5 V
6. Distance between core-centres : x_6 m

The combined cost of stampings, copper windings and capitalized cost of losses is taken as the cost function to be minimized, satisfying the following important constraints.

1. Temperature rise of windings above ambient
2. Temperature rise of oil above ambient
3. Short-circuit impedance
4. Permissible flux density in the core
5. No-load current
6. Clearance between different phase windings
7. Maximum height of the windings
8. Efficiency
9. Maximum current densities in the windings

The constraints on temperature rise of windings and oil are necessary since they influence the life of the

transformer and hot spot temperature of the winding. The short-circuit impedance of the transformer affects the operation of the furnace and, to limit the voltage drop, an upper limit is put on this constraint. Over voltages and inrush current during the operation of circuit breakers for furnace switching, dictate the flux density in the core and no-load current of the furnace transformer. Hence two more constraints are incorporated to limit these values. Minimum clearance between phase windings is ensured to bring out heavy current secondary winding conductor leads, by another constraint.

With the specified rating of the transformer, the design problem is posed as an NLP problem to minimize the cost of the transformer, expressing the cost function and constraint functions in terms of the specified independent variables.

5.4 OPTIMIZATION PROGRAM

The optimization program consists of the main program of Powell's unconstrained minimization algorithm and eight subroutines. A brief description of seven subroutines is already given in Section 3.3. The additional subroutine HELIX is used in the program for the design of l.v. helical winding, since the l.v. winding design is approached separately with continuous disc coils and helical coils. Also the

subroutine CALCFX of Section 3.3 is modified to obtain augmented objective function with normalized constraints. The flow diagram of the computer program is similar to Fig. 3.1 of Chapter 3 but with the changes indicated in the subroutines.

5.5 EXPRESSIONS FOR OBJECTIVE AND CONSTRAINT FUNCTIONS

5.5.1 Objective Function

Since the cost of the stampings and copper windings is taken as the initial cost of the transformer in Section 3.2, the objective function, FO is expressed as

FO = Initial cost + capitalized cost of losses

$$FO = C + C1\ P_c + C2\ P_i \tag{5.1}$$

where the expressions for loss capitalization factors are already derived in Section 3.4.1.

$$C = CI\ (G_1 + G_y) + CC\ G_c \tag{5.2}$$

$$G_1 = k_1\ A_i\ (x_4 + k_2) \tag{5.3}$$

$$G_y = k_3\ A_i\ (2x_6 + 0.9\ d) \tag{5.4}$$

$$A_i = x_5/(4.44\ x_1\ f) \tag{5.5}$$

$$d = [4A_i/(\pi\ k_4)]^{\frac{1}{2}} \tag{5.6}$$

$$G_c = k_5[L_{mt1}\ m_1(T_1\ a_1 + T_s\ a_s) + L_{mt2}\ n_c\ m_2\ T_2\ a_2] \tag{5.7}$$

$$L_{mt1} = \pi(d + b_1 + k_6) \tag{5.8}$$

$$L_{mt2} = \pi(d + 2b_1 + b_2 + k_7) \tag{5.9}$$

$$b = k_8\, n_R\, BO_c + k_9 \tag{5.10}$$

$$P_c = P_{c1} + P_{c2} + P_e + P_s \tag{5.11}$$

$$P_{c1} = 3\, I_1^2\, R_1/1000 \tag{5.12}$$

$$P_{c2} = 3\, I_2^2\, R_2/1000 \tag{5.13}$$

$$R_1 = \rho\, L_{mt1}(T_1/a_1 + T_s/a_s)/m_1 \tag{5.14}$$

$$R_2 = \rho\, L_{mt2}\, T_2/(a_2\, m_2) \tag{5.15}$$

$$I = S_1/V \tag{5.16}$$

$$S_1 = S/3 \tag{5.17}$$

$$P_e = \sum k_{10}\, BO^4\, n_R^2\, f^2\, \beta^2\, (3\, I^2\, R/1000) \tag{5.18}$$

$$\beta = AO\, n_A\, K_R/x_4 \tag{5.19}$$

$$K_R = 1 - [1 - e^{-(\pi\, x_4/\tau)}]/(\pi\, x_4/\tau) \tag{5.20}$$

$$\tau = b_1 + b_2 + k_{11} \tag{5.21}$$

$$P_s = \frac{k_{12}\, X_{sc}^2\, x_1^2\, A_i^2\, x_4^3\, f}{MT[x_4 + 2(KZ - 0.5\, D12)]^2} \tag{5.22}$$

$$X_{sc} = 100\, I_1[X_2(T_1^2/T_2^2) + X_1]/V_1 \tag{5.23}$$

$$X = 2\pi\, f\, \mu_o\, T^2\, L_{mt}\, k_{13}(k_{14}/2 + b/3)/x_4 \tag{5.24}$$

$$MT = 2(TKL - TKW) + \pi\, TKW \tag{5.25}$$

$$TKL = 2x_6 + d + 2b_1 + 2b_2 + k_{15} \tag{5.26}$$

$$TKW = d + 2b_1 + 2b_2 + k_{16} \tag{5.27}$$

$$TKH = x_4 + 2(1.15\ A_i)^{\frac{1}{2}} + k_{17} \tag{5.28}$$

$$KZ = 0.5(d + 2b_1 + 2b_2 + k_{18}) \tag{5.29}$$

$$D12 = d + 2b_1 + k_{19} \tag{5.30}$$

$$P_i = [FF(x_1)\ G_1 + FF(B_y)\ G_y\ 1.075] \tag{5.31}$$

$$B_y = x_1/1.15 \tag{5.32}$$

The expressions related to the geometry of the transformer are obvious and simple to derive. Equations (5.18), (5.22) and (5.24) are derived in the references [26,41]. The expression (5.31) for iron loss, P_i is obtained by the similar procedure indicated in Section 3.4.1.

5.5.2 Constraint Functions

The expressions for constraint functions are as follows:

1. Temperature rise of winding above ambient

$$\theta_{wa} \leq 55 \tag{5.33}$$

$$\theta_{wa} = \theta_w + \theta_o \tag{5.34}$$

$$\theta_w = k_{20}\ q_w^{0.7} \tag{5.35}$$

$$q_w = \rho\ I\ T_c\ J\ K_e\ K_s/MC \tag{5.36}$$

$$K_o = 1 + P_e/(P_{c1} + P_{c2}) \tag{5.37}$$

$$K_s = L_{mt}/(L_{mt} - n_s\, b_s) \tag{5.38}$$

$$MC = 2[k_{21}\, n_R(B0 + k_{22}) + n_A(A0 + k_{23})]10^{-2} \tag{5.39}$$

2. Temperature rise of top oil above ambien

$$\theta_{oa} \leq 45 \tag{5.40}$$

$$\theta_{oa} = 1.2\, \theta_o + k_{24} \tag{5.41}$$

$$\theta_o = 55 - \theta_{wo} \tag{5.42}$$

$$q_o = (\theta_o/k_{25})^{1.25} \tag{5.43}$$

Equation (5.36) is derived in Section 3.4.2. Empirical formulas used for the equations (5.35) and (5.43) are based on the specific thermal load of 2500 to 3000 Watts/m^2 for windings and 1000 to 1500 Watts/m^2 for oil [26,27]. Here

K_{20} = 0.1 for windings

k_{25} = 0.12 for oil

3. Percentage short-circuit impedance

$$Z_{sc} \leq 10.0 \tag{5.44}$$

$$Z_{sc} = (R_{sc}^2 + X_{sc}^2)^{\frac{1}{2}} \tag{5.45}$$

$$R_{sc} = P_c\, 100/s \tag{5.46}$$

4. Permissible flux density in the core

$$1.55 \leq x_1 \leq 1.68 \tag{5.47}$$

5. Percentage no-load current

$$I_o \leq 1.5 \tag{5.48}$$

$$I_o = (I_{oa}^2 + I_{or}^2)^{\frac{1}{2}} \tag{5.49}$$

$$I_{oa} = P_i \, 100/S \tag{5.50}$$

$$I_{or} = [GG(x_1)\, G_1 + GG(B_y)\, G_y + 7\, A_i\, HH(x_1)]/(10\, S) \tag{5.51}$$

Expression (5.51) is derived on the similar lines as indicated in Section 3.4.2.

6. Clearance between different phase windings

$$0.05 \leq b_{ph} \leq 0.10 \tag{5.52}$$

$$b_{ph} = x_6 - (0.9\, d + 2b_1 + 2b_2 + k_{22}) \tag{5.53}$$

7. Maximum height of the windings

$$x_4 \leq 3.5 \tag{5.54}$$

8. Percentage efficiency

$$\eta \geq 99.0 \tag{5.55}$$

$$\eta = [1 - (P_c + P_i)/(S\, PF + P_c + P_i)]100 \tag{5.56}$$

9. Maximum current densities in the windings

$$x_2 \leq 3.65 \tag{5.57}$$

$$x_3 \leq 3.25 \tag{5.58}$$

In all those equations subscripts 1 and 2 refer to h.v. and l.v. windings respectively except for x and k.

5.6 SOLUTION OF THE NLP PROBLEM

In the design problem the insulation level of the windings and clearances are assumed to be equal to that of an ordinary power transformer for the next higher voltage range.

The optimal design problem of the specified furnace transformer, as formulated in the earlier sections, is solved by Powell's unconstrained minimization technique using exterior penalty function method. An initial penalty factor of 7500 is used with each starting vector of independent variables. Optimal solutions minimizing the cost are obtained with different starting points for a 64.5 MVA, 33 kV/384-712 V, star-delta connected, three-phase, core type furnace transformer, satisfying the imposed constraints and the results are presented in Table 5.1 and Table 5.2. Convergence to the optimal solutions is achieved after 7 to 12 unconstrained minimization cycles the penalty parameter being incremented 10 times after each unconstrained minimization cycle. The execution time to obtain each optimized design is given in Table 5.1 and Table 5.2. Optimal solutions, in the Table 5.1 refer to the design with l.v. helical winding

TABLE 5.1

OPTIMAL SOLUTIONS OF A 64.5 MVA, 33 KV/384-712 VOLTS, THREE-PHASE, CORE TYPE, STAR-DELTA CONNECTED FURNACE TRANSFORMER WITH LV HELICAL WINDING

articulars	Starting point 1	Optimal value	Starting point 2	Optimal value	Starting point 3	Optimal* value	Starting point 4	Optimal value	Starting point 5	Optimal value
1 Tesla	1.56	1.632	1.58	1.674	1.55	1.674	1.57	1.680	1.58	1.680
2 A/mm^2	2.72	3.646	2.50	3.636	2.75	3.489	2.95	3.650	2.70	3.649
3 A/mm^2	2.41	2.277	2.00	2.156	2.75	2.230	2.20	2.600	2.20	2.560
4 m	3.45	3.258	3.20	3.211	3.30	3.240	3.20	3.249	3.30	3.204
5 V	112.00	111.226	108.00	111.125	110.00	111.407	106.00	111.532	115.0	112.783
6 m	0.90	0.902	0.88	0.889	0.80	0.882	0.87	0.903	0.88	0.870
ost,%	61.9	57.2	100.00	56.5	99.60	56.4	88.4	57.0	62.5	57.4
o. of con-traint iolations	3	0	4	0	4	0	3	0	3	0
o. of un-onstrained inimization ycles		12		10		10		12		12
xecution ime, econds		204		220		170		308		264

OPTIMAL SOLUTIONS OF A 64.5 MVA, 33 KV/384-712 VOLTS, THREE-PHASE, CORE TYPE, STAR-DELTA CONNECTED FURNACE TRANSFORMER WITH LV CONTINUOUS DISC WINDING

Particulars	Starting point 1	Optimal value	Starting point 2	Optimal value	Starting point 3	Optimal* value	Starting poing 4	Optimal value
x_1 Tesla	1.58	1.651	1.58	1.678	1.56	1.676	1.53	1.604
x_2 A/mm^2	3.50	3.647	3.00	3.497	3.48	3.490	2.75	3.650
x_3 A/mm^2	4.00	3.481	3.20	2.396	2.41	2.490	2.20	2.414
x_4 m	3.75	3.144	3.75	3.369	3.45	3.163	3.30	3.157
x_5 V	111.00	111.174	111.00	111.166	112.00	112.000	112.00	111.517
x_6 m	0.9	0.877	0.95	0.898	0.9	0.9	0.87	0.911
Cost,%	85.9	56.9	85.6	56.5	61.8	56.0	61.3	57.2
No. of constraint violations	6	0	3	0	4	0	5	0
No. of unconstrained minimization cycles		12		7		11		11
Execution time, seconds		407		360		530		571

*Indicates selected final optimal solution corresponding to starting point 3.

and in the Table 5.2 to l.v. continuous disc winding. In the design of continuous disc winding, every pair of discs is connected in series. From the Tables 5.1 and 5.2, the optimal solution which gives the lowest objective function and no constraint violations is taken as the final optimal solution. The transformer impedance is referred to the furnace side and the mechanical stresses in the windings are calculated on the basis of total secondary circuit impedance. It is observed that for all the optimal solutions of the specified transformer obtained earlier, the mechanical stresses in windings and spacers for maximum short-circuit currents as calculated from equations (8.10) to (8.22) of the reference [26] are well within permissible values.

5.7 OPTIMIZED DESIGN OF A 64.5 MVA FURNACE TRANSFORMER

The optimized design and important performance characteristics of the specified furnace transformer corresponding to the selected final optimal solution of Tables 5.1 and 5.2 is presented in Table 5.3. It is seen from Tables 5.1, 5.2 and 5.3 that the constraints on temperature rise of windings, temperature rise of oil and flux density in the core have become active at the optimal solutions and are driven to their limits. The cost corresponding to the second starting point in Table 5.1 is taken as 100% for comparison with

TABLE 5.3

OPTIMIZED DESIGN AND PERFORMANCE OF A 64.5 MVA, 33 KV/384-712 VOLTS, THREE-PHASE, CORE TYPE, STAR-DELTA CONNECTED FURNACE TRANSFORMER

Particulars	l.v. helical winding	l.v. continuous disc winding
1. Temperature rise of windings above ambient, °C	55.0	55.0
2. Temperature rise of oil above ambient, °C	44.29	44.28
3. Percentage short-circuit impedance	9.268	9.51
4. Percentage no-load current	1.192	1.191
5. Percentage efficiency	99.43	99.41
6. Clearance between phases, m	0.063	0.080
7. Core circle diameter, m	0.702	0.704
8. Total width of core, m	2.395	2.433
9. Number of h.v. coils	64	64
10. Area of C.S. of h.v. normal conductor, mm^2	40.50	40.50
11. Dimensions of h.v. winding conductor, mm	11.6 x 3.53	11.6 x 3.53
12. Number of l.v. coils	12	24
13. Number of l.v. turns	4	4
14. Area of C.S. of l.v. winding conductor, mm^2	323.635	579.699
15. Dimensions of l.v. winding conductor, mm	68.13 x 4.75	127.41 x 4.55
16. Number of parallel conductors in l.v. winding	4	2

17.	Total copper loss including eddy current loss, kW	18.098	18.82
18.	Stray loss, kW	10.753	10.961
19.	Core loss, kW	8.369	8.33
20.	Weight of copper windings, kg	8401.68	7944.314
21.	Weight of stampings, kg	35967.20	35781.89
22.	Dimensions of the tank, m	1.689 x 3.452 x 5.134	1.69 x 3.49 x 5.06
23.	Specific thermal load, Watts/m^2	1144.25	1144.28
24.	Hot spot temperature rise of windings, °C	97.0	97.0
25.	Arc voltage, V	197.0	197.0
26.	Secondary voltages, V	384, 407, 435, 464, 501, 540, 586, 646, 712	384, 407, 435, 464, 501, 540, 586, 646, 712

other values in Tables 5.1 and 5.2. The percentage costs at the final optimal solution for both types of l.v. winding arrangements considered are nearly equal as seen from Tables 5.1 and 5.2.

5.8 CONCLUSIONS

The importance of power system impedance, arc resistance and arc power is well recognized while deriving the rating of a furnace transformer. The design procedure of large furnace transformer supplying a 150 ton direct arc furnace is developed. The design optimization problem of the furnace transformer is solved as an NLP problem, minimizing the cost and satisfying desired constraints. Zangwill's exterior penalty function method coupled with Powell's unconstrained minimization technique has been found to be well suited for obtaining the optimal design of furnace transformer. The execution time on IBM 7044 computer for obtaining each optimized design is 4 minutes on the average when l.v. helical winding is considered. When l.v. continuous disc winding is considered, the average execution time has been almost doubled. Computed results indicate large amount of stray loss, which can be reduced by special measures. The mechanical stresses in a furnace transformer are not very large though there are frequent short-circuits whenever the

electrodes come in contact with the metal in the furnace. This is due to a very largevalue of secondary circuit impedance which is normally about 50 to 80 % .

The design optimization of another special purpose transformer which is used for d.c. loads is considered in the next chapter.

CHAPTER 6

OPTIMAL DESIGN OF RECTIFIER POWER TRANSFORMER

6.1 INTRODUCTION

The optimal design of one special purpose transformer for furnace loads is discussed in Chapter 5. In this chapter, the problem of designing another special purpose transformer viz.,rectifier power transformer, at a minimum cost, supplying d.c loads through a six-pulse converter (three-phase diode bridge), is approached using NLP. Rectifier transformers are used in railways, mining, and electrochemical industries. The optimal design of these transformers is imperative with the growth of static converting equipment supplying high current loads. Computer-aided optimal design of rectifier transformers does not figure again in published literature but important characteristics and different configurations of these special purpose transformers have appeared in references [42-44].

The design optimization problem of a rectifier power transformer is formulated in this chapter, considering the effect of converting equipment on the transformer. The converting equipment and the connection of transformer normally influence the primary and secondary currents of the transformer. A brief description of the structure of the transformer is presented. For a star-delta connection of the transformer, the expression for secondary phase current is

derived, considering the source impedance. In the design analysis program, eddy current losses in the conductors, temperature rise of the equipment and mechanical stresses in windings are obtained on the basis of actual current waveform. The optimal design problem is solved as an NLP problem, satisfying important constraints like d.c. voltage regulation, short-circuit impedance, no-load current, efficiency of the transformer etc.

6.2 RECTIFIER TRANSFORMERS

6.2.1 Brief Description

Rectifier transformers are essentially power transformers that have been modified in some important details to make them suitable for rectifier service. In a two-winding transformer, if the primary voltage is not unduly high, the h.v. winding can be inner most, nearest to the iron, while the heavy current secondary can be on the outside and subdivided into a number of parallel coils. The windings are usually wound with rectangular conductors of large cross-section and are so arranged as to give high mechanical strength in the direction of the greatest force. Due to the nonsinusoidal nature of current in the windings and because these transformers supply large currents at low voltage, the mechanical stresses arising from short-circuit currents are

completely different. High power silicon diodes have made it possible to transfer currents in the order of tens of thousands and even hundreds of thousands of amperes. Transformer connections influence the duty of the converting equipment and hence they must be co-ordinated with the available rectifying devices. For a specific connection of the transformer, the phase current waveforms in the windings must be known before proceeding with the design analysis.

6.2.2 Analysis of Phase Current Waveform

A three-phase star-delta connected rectifier transformer supplying a d.c. load through a three-phase bridge rectifier is considered and represented in Fig. 6.1. The phase current waveform of the secondary winding, considering source impedance [45] is as shown in Fig. 6.2.

The secondary rms current, I_2 for a given d.c. load is derived by assuming

i. direct current supplied to the load is without ripple,

ii. commutation loop comprises only inductance.

The instantaneous current, i(t) is represented mathematically as a function of θ in one half-cycle, as

$$f_1(\theta) = \frac{2}{3} I_d \frac{1 - \cos(\theta - \delta)}{1 - \cos u} - \frac{1}{3} I_d$$

$$\text{for } 0 < \theta < u - \delta \qquad (6.1)$$

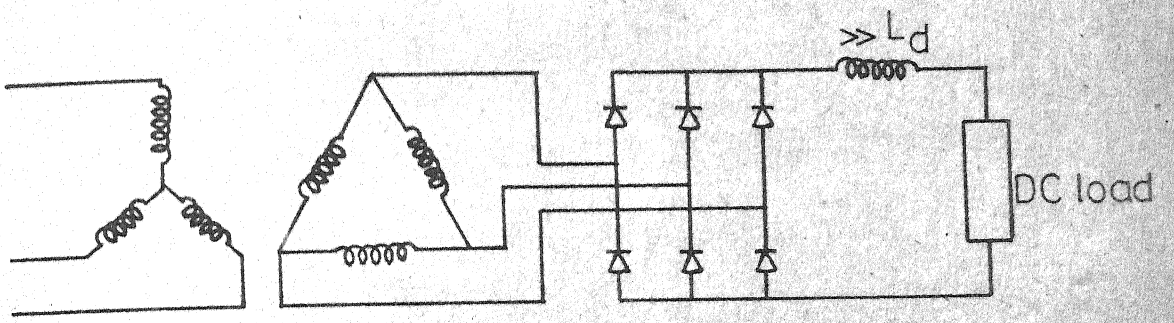

FIG. 6.1. SCHEMATIC DIAGRAM.

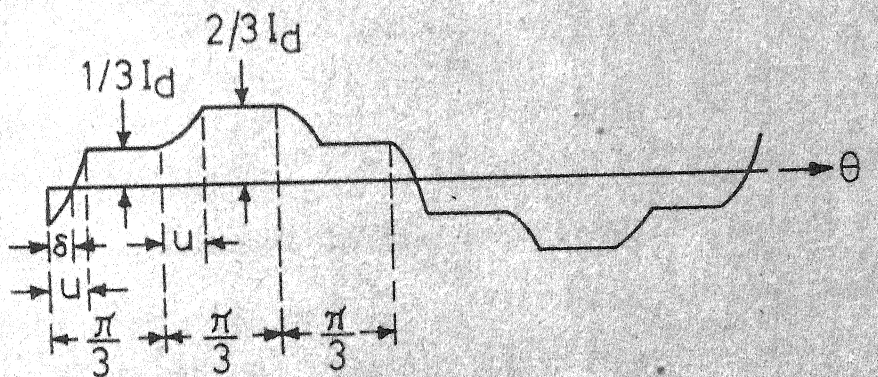

FIG. 6.2. PHASE CURRENT WAVEFORM.

$$f_2(\theta) = \frac{1}{3} I_d \qquad u - \delta < \theta < \frac{\pi}{3} - \delta \tag{6.2}$$

$$f_3(\theta) = \frac{1}{3} I_d + \frac{1}{3} I_d \frac{1 - \cos\{\theta - (\frac{\pi}{3} - \delta)\}}{1 - \cos u}$$

$$\frac{\pi}{3} - \delta < \theta < \frac{\pi}{3} - \delta + u \tag{6.3}$$

$$f_4(\theta) = \frac{2}{3} I_d \qquad \frac{\pi}{3} - \delta + u < \theta < \frac{2\pi}{3} - \delta \tag{6.4}$$

$$f_5(\theta) = \frac{2}{3} I_d - \frac{1}{3} I_d \frac{1 - \cos\{\theta - (\frac{2\pi}{3} - \delta)\}}{1 - \cos u}$$

$$\frac{2\pi}{3} - \delta < \theta < \frac{2\pi}{3} - \delta + u \tag{6.5}$$

$$f_6(\theta) = \frac{1}{3} I_d \qquad \frac{2\pi}{3} - \delta + u < \theta < \pi - \delta \tag{6.6}$$

$$f_7(\theta) = \frac{1}{3} I_d - \frac{2}{3} I_d \frac{1 - \cos\{\theta - (\pi - \delta)\}}{1 - \cos u}$$

$$\pi - \delta < \theta < \pi \tag{6.7}$$

where the functions $f_1(\theta), \ldots, f_7(\theta)$ are the values of instantaneous current in the intervals indicated. u and δ are defined in Fig. 6.2. The secondary rms current, I_2 is calculated from the following expression

$$I_2 = \sqrt{\frac{1}{\pi}} \left\{ \int_0^{u-\delta} [f_1(\theta)]^2 \, d\theta + \int_{u-\delta}^{(\frac{\pi}{3})-\delta} [f_2(\theta)]^2 \, d\theta \right.$$

$$\left. + \int_{(\frac{\pi}{3})-\delta}^{(\frac{\pi}{3})-\delta+u} [f_3(\theta)]^2 \, d\theta + \int_{(\frac{\pi}{3})-\delta+u}^{(\frac{2\pi}{3})-\delta} [f_4(\theta)]^2 \, d\theta \right.$$

$$+ \int_{(\frac{2\pi}{3})-\delta}^{(\frac{2\pi}{3})-\delta+u} [f_5(\theta)]^2 \, d\theta + \int_{(\frac{2\pi}{3})-\delta+u}^{\pi-\delta} [f_6(\theta)]^2 d\theta$$

$$+ \int_{\pi-\delta}^{\pi} [f_7(\theta)]^2 \, d\theta \Big\}^{\frac{1}{2}} \qquad (6.8)$$

where $\delta = \cos^{-1}(\frac{1 + \cos u}{2})$ (6.9)

From the d.c. load voltage, V_d the secondary rms voltage, V_2 is given by

$$V_2 = V_d \, \pi/(3\sqrt{2}) \qquad (6.10)$$

The kVA rating of the transformer is fixed from the secondary rms current and rms voltage. The kVA loading of the transformer, S is given by

$$S = 3 \, V_2 \, I_2 \, 10^{-3} \qquad (6.11)$$

while the current waveform is distorted, the voltage wave impressed on the primary, when the converter is fed from a system whose capacity is reasonably large, approximates a sinewave. Hence the iron loss calculation in the design procedure is similar to an ordinary power transformer. On the other hand, the eddy current losses in the conductors are calculated on the basis of an analysis of the actual current wave shape [46]. Eddy current losses in a transformer

winding with sinusoidal current is generally given by

$$K_{e,sin} = \frac{5m^2 - 1}{45} \varsigma^4 \qquad (6.12)$$

where
$$\varsigma = BO \left[\frac{\pi f \mu_o}{\rho} \frac{h_c}{h_w} \right]^{\frac{1}{2}} \qquad (6.13)$$

m = number of parallel conductors in radial direction

BO = radial dimension of the conductor, mm

f = frequency of the supply, Hz

μ_o = magnetic space constant, H/m

ρ = conductivity of the material, ohm-m/mm^2

h_c = height of copper in axial direction, m

h_w = height of winding, m

There are two approaches to the evaluation of eddy current loss with pulsating current,

i. finding a formula similar to equation (6.12) for a current of arbitrary wave shape,

ii. determining the losses as sum of several contributions of harmonic components of actual current.

The first approach is very simple and gives general conclusive expression as indicated below if the expression for rms current is known. Expression (6.12) is written as

$$K_{e,sin} = \left(\frac{5m^2-1}{45}\right)\left(\frac{h_c^2}{h_w^2}\right)\left(\frac{B0^4}{4}\right)(4\pi^2 f^2)\left(\frac{\mu_o^2}{\rho^2}\right) \qquad (6.14)$$

The three factors in brackets on right hand side represent, respectively

i. influence of geometric dimensions of windings where eddy current loss occurs,

ii. influence of variation of current with time,

iii. physical parameters characterizing the conductor material.

Since $i = \sqrt{2}\, I \sin \omega t$ (6.15)

and $\omega = 2\pi f$ (6.16)

$$\frac{I'}{I} = \omega \qquad (6.17)$$

where I = rms current, A

I' = time derivative of rms current, A

Hence factor (ii) signifies

$$\omega^2 = \left(\frac{I'}{I}\right)^2 = \frac{\text{mean-square value of derivative of current}}{\text{mean-square value of current}} \qquad (6.18)$$

Substituting equation (6.17) in equation (6.14), the eddy loss ratio for a current of arbitrary wave shape is

given by

$$K_{e,pul} = \frac{5m^2-1}{45} \frac{h_c^2}{h_w^2} \frac{B0^4}{4} \frac{I'^2}{I^2} \frac{\mu_o^2}{\rho^2} \qquad (6.19)$$

Therefore the first approach is used in the design calculations to evaluate eddy losses in both the windings of the transformer.

6.3 MATHEMATICAL FORMULATION OF THE PROBLEM

The formulation of the present design problem as an NLP problem is on the same lines as indicated in Chapter 5. The six variables that are selected as independent variables are the same as in Section 5.3.3. An additional constraint on d.c. voltage regulation is imposed in addition to the constraints already considered in Section 5.3.3 for furnace transformer. The drop in d.c. voltage due to source impedance, including 10% drop in leads, is accounted for while calculating d.c. voltage regulation. The objective or cost function of the transformer consists of the initial cost and capitalized cost of losses, the active material cost of stampings and windings of the transformer form the initial cost.

As an example, a 4 MVA, 33 kV/296 volts, star-delta connected, three-phase, core type rectifier power transformer with ± 10% taps on primary, supplying a d.c. load at 10,000

amperes and 400 volts is considered for the optimal design. An initial overlap angle of 15° is assumed to account for the source impedance. This value depends upon the leakage reactance of the transformer and current at commutation. Continuous disc coils for h.v. winding, and helical coils for l.v. winding, are adopted with forced oil cooling in accordance with the current practice [44]. The h.v. winding is near the core.

The cost function and constraint equations are expressed in terms of the specified independent variables and are listed as follows.

6.4 EXPRESSIONS FOR OBJECTIVE AND CONSTRAINT FUNCTIONS

6.4.1 Objective Function

FO = initial cost + capitalized cost of losses

$$FO = C + C1\ P_c + C2\ P_i \qquad (6.20)$$

where C1, C2 are loss capitalization factors.

The expressions for C1 and C2 are derived in Section 3.4.1.

C = initial cost

$$P_c = P_{c1} + P_{c2} + P_e + P_s \qquad (6.21)$$

The expressions for C, P_{c1}, P_{c2} and P_s are similar to the furnace transformer and derived in Section 5.5.1.

$$P_e = \sum K_{e,pul}(3\ I^2\ R/1000) \qquad (6.22)$$

The value of $K_{e,pul}$ is calculated separately for h.v. and l.v. windings using equation (6.18). The expression for P_i is derived in Section 5.5.1.

6.4.2 Constraint Functions

The following constraints are imposed on the design problem.

1. Temperature rise of windings above ambient

$$\theta_{wa} \leq 55 \qquad (6.23)$$

2. Temperature rise of oil above ambient

$$\theta_{oa} \leq 45 \qquad (6.24)$$

3. Percentage short-circuit impedance

$$Z_{sc} \leq 5.0 \qquad (6.25)$$

4. Permissible flux density in the core

$$1.55 \leq x_1 \leq 1.68 \qquad (6.26)$$

5. Percentage no-load current

$$I_o \leq 2.5 \qquad (6.27)$$

6. Clearance between different phase windings

$$0.03 \leq b_{ph} \leq 0.10 \qquad (6.28)$$

7. Maximum height of the windings

$$x_4 \leq 3.0 \tag{6.29}$$

8. Percentage efficiency

$$\eta \geq 99.0 \tag{6.30}$$

9. DC voltage regulation

$$DZS - (V_d - \frac{3\sqrt{2}\, V_2}{\pi} \cos u) \leq 0 \tag{6.31}$$

where $DZS = [3\, I_d\, 1.1(X_1\, T_2^2/T_1^2 + X_2)/\pi - 2\, I_d\, 1.1$

$$x\, (R_1\, T_2^2/T_1^2 + R_2)]/3 \tag{6.32}$$

Expressions (6.23) to (6.30) are already derived in Section 5.5.2. Expression (6.31) is derived in the references [45,47].

6.5 SOLUTION OF THE NLP PROBLEM

The design optimization problem of the specified rectifier power transformer is posed as an NLP problem to minimize the cost, while satisfying the desired constraints. The optimization program used is similar to the one explained in Section 5.4. Subroutine HELIX is used for l.v. helical winding design. Exterior penalty function method, along with Powell's unconstrained minimization technique is used to solve the NLP problem. An initial penalty factor of 5000 or

7500 is well suited for the optimization problem and after one complete unconstrained minimization cycle, if the constraints are not satisfied, it is incremented by a factor of 10.

Optimal solutions, minimizing the cost are obtained with different starting points for the specified rectifier power transformer, satisfying the imposed constraints. The solutions are presented in Table 6.1. Convergence to the optimal solutions is achieved after 3 to 7 unconstrained minimization cycles. The computer time for each unconstrained minimization cycle on the average is 35 seconds. From Table 6.1 the solution with the lowest cost together with no constraint violations is taken as the final optimal solution. The cost corresponding to the last starting point is considered as 100% for comparison with other values. Short-circuit current calculations are based on the transformer impedance referred to the load side. For all the optimal solutions obtained, the mechanical stresses in windings and spacers for maximum short-circuit currents are well within the permissible values as calculated from equations (8.10) to (8.22) of the reference [26].

OPTIMAL SOLUTIONS OF A 4 MVA, 33 KV/296 VOLTS, THREE-PHASE, CORE TYPE, STAR-DELTA CONNECTED RECTIFIER POWER TRANSFORMER

Particulars	Starting point 1	Optimal value	Starting point 2	Optimal value	Starting point 3	Optimal* value	Starting point 4	Optimal value	Starting point 5	Optimal value
x_1 Tesla	1.62	1.622	1.62	1.653	1.56	1.673	1.67	1.598	1.60	1.680
x_2 A/mm^2	2.40	2.699	2.50	2.320	2.80	2.766	2.58	2.722	2.80	2.759
x_3 A/mm^2	2.80	2.775	2.75	2.789	2.80	2.552	2.65	2.133	2.50	2.769
x_4 m	1.00	0.841	1.00	0.949	1.75	1.024	1.40	1.026	2.40	1.027
x_5 V	48.00	39.592	38.00	34.899	28.00	31.214	36.00	31.198	28.00	31.297
x_6 m	0.80	0.634	0.65	0.590	0.90	0.585	0.80	0.607	0.85	0.571
Cost,%	87.6	70.2	75.0	67.6	93.4	66.5	84.1	67.7	100.0	66.6
No. of constraint violations	4	0	5	0	4	0	3	0	4	0
No. of unconstrained minimization cycles		5		2		7		3		5
Execution time, seconds		182		125		271		141		180

* Indicates selected final optimal solution corresponding to starting point 3.

6.6 OPTIMIZED DESIGN OF A 4MVA RECTIFIER POWER TRANSFORMER

The optimized design and important performance characteristics of the specified rectifier transformer corresponding to the final optimal solution of Table 6.1 is presented in Table 6.2. It is seen from Table 6.2 that the constraints on temperature rise of windings, temperature rise of oil and no-load current have become active at the optimal solution and are driven to their limits.

6.7 CONCLUSIONS

The effect of the nonsinusoidal nature of the current flowing in a rectifier power transformer when supplying d.c. loads through a six-pulse converter is recognised. Actual current waveform for a specified connection of the transformer is derived and its effect on eddy current losses of conductors, temperature rise and mechanical stresses of the equipment is considered in the design procedure. The design optimization problem of the rectifier power transformer is solved as an NLP problem, minimizing the cost and satisfying the desired constraints. Exterior penalty function method, along with Powell's unconstrained minimization technique has been found to be well suited for obtaining the optimal design of the rectifier power transformer. The execution

TABLE 6.2

OPTIMIZED DESIGN AND PERFORMANCE OF A 4 MVA, 33 KV/296 VOLTS, THREE-PHASE, CORE TYPE, STAR-DELTA CONNECTED RECTIFIER POWER TRANSFORMER

1.	Temperature rise of windings above ambient, °C	55.0
2.	Temperature rise of oil above ambient, °C	44.0
3.	Percentage short-circuit impedance	2.953
4.	Percentage efficiency	99.27
5.	Percentage no-load current	2.417
6.	Clearance between phase windings, m	0.0397
7.	Core circle diameter, m	0.372
8.	Number of h.v. winding coils	80
9.	Area of c.s. of h.v. winding conductor, mm^2	14.00
10.	Dimensions of h.v. winding conductor, mm	6.40 x 2.26
11.	Average number of turns per h.v. coil	9.76
12.	Number of l.v. winding coils	18
13.	Area of c.s. l.v. winding conductor, mm^2	16.82
14.	Dimensions of l.v. winding conductor, mm	4.00 x 4.20
15.	Average turns per l.v. coil	9
16.	Number of parallel conductors in l.v. winding	6
17.	Total copper loss, kW	17.476
18.	Total eddy current loss in conductors, kW	2.533
19.	Core loss, kW	10.191
20.	Weight of copper windings, kg	1091.75
21.	Weight of stampings, kg	4562.98
22.	Percentage magnetizing component of no-load current	2.404

23.	Percentage active component of no-load current	0.247
24.	Dimensions of tank, m	1.382 x 2.552 x 2.365
25.	Permissible specific thermal load, Watts/m^2	1205.34
26.	Source reactance drop, V	10.304
27.	Source resistance drop, V	3.283
28.	Average power factor of converter	0.725
29.	Overlap angle of the converter, degrees	16.26

time for obtaining each optimized design is three minutes on the average on IBM 7044 computer.

The design optimization of a d.c. arc furnace transformer [48] may be obtained on similar lines from the design procedures developed for the two special purpose transformers.

In the next two parts of this thesis, the design optimization of d.c. and a.c. motors with unconventional power supplies are investigated.

PART - II

DC MOTORS

CHAPTER 7

OPTIMAL DESIGN OF SEPARATELY EXCITED DC MOTOR SUPPLIED THROUGH A THREE-PHASE THYRISTOR CONVERTER

7.1 INTRODUCTION

The design optimization of a separately excited d.c. motor supplied by a six-pulse thyristor converter is the topic of this chapter. Separately excited d.c. motors find wide application in industrial drives. As a mill motor, it has good speed control over a wide range, durability and fast response. A large percentage of d.c. motors manufactured today is supplied by thyristor converters. Thyristor controlled d.c. motor has become quite competitive with other more established forms of variable speed drives. Cost reduction, new production methods and redesign of motors to suit rectified power supply are some of the demands made by the manufacturers and the users. The effect of rectifier or thyristor power supply on d.c. motors is well explained in references [49-54]. Some problems in the design and construction of modern d.c. machines supplied by semiconductors is emphasized in references [55-64]. The application of nonlinear optimization procedures to obtain the optimal design of these machines does not figure in the published literature, although the optimal design of conventional electrical machines are well established [5-7, 10,11]. In this chapter, the problem of designing a separately excited d.c. motor supplied through a three-phase thyristor converter at minimum material cost is

posed as an NLP problem with the important performance characteristics as constraints.

The mathematical model of the design problem is formulated with sixteen design variables, Laminated field structure with octagonal frame, compensating winding in the pole-faces and interpole winding are considered for the motor in line with the current design practice [58,62]. The design analysis program includes calculation of armature circuit inductance, peak current through the armature winding and various harmonic components of current. The additional losses due to flux pulsations in the armature and magnetic circuit are considered. The skin-effect in armature, compensating and interpole winding conductors, due to commutation and ripple in the armature current are also considered. Important constraints like commutating ability of the machine, ratio of torque to armature moment of inertia, pulse duty factor with reference to armature current, efficiency of the machine etc., are imposed on the design optimization problem.

The NLP problem of minimizing the active material cost of the motor is solved and the optimized design is obtained. The effects of source impedance and of firing angle of the converter on the optimal solution is studied.

7.2 DESIGN PROBLEM FORMULATION

7.2.1 Design Variables and the Constraints

A d.c. motor fed from a thyristor converter is subjected to a pulsating voltage. The ripple current due to pulsating voltage causes

i. additional iron losses in the excitation circuit, interpoles and yoke

ii. increased copper losses in the armature, interpole and compensating windings

iii. deterioration of commutation

iv. appearance of large voltages between shaft and bearings.

In the present design problem, a six-pulse fully controlled thyristor bridge is considered as power source to the d.c. motor. The schematic arrangement is shown in Fig. 7.1(a). The d.c. output voltage and current waveforms are presented in Figs. 7.1(b) and 7.1(c). The effect of source impedance is neglected on the waveforms.

Before identifying the design variables and the constraints for the mathematical formulation of the design problem, some important aspects are to be considered and these are briefly summarised here.

The terminal voltage of the machine decides the commutating ability and the pulse duty factor of the armature current affects both the commutation and losses. Torque to

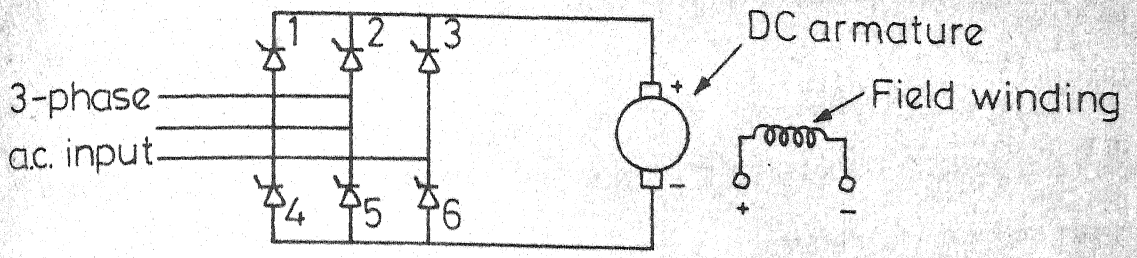

1, 2, ..., 6 SCRs

FIG. 7·1a. SCHEMATIC DIAGRAM.

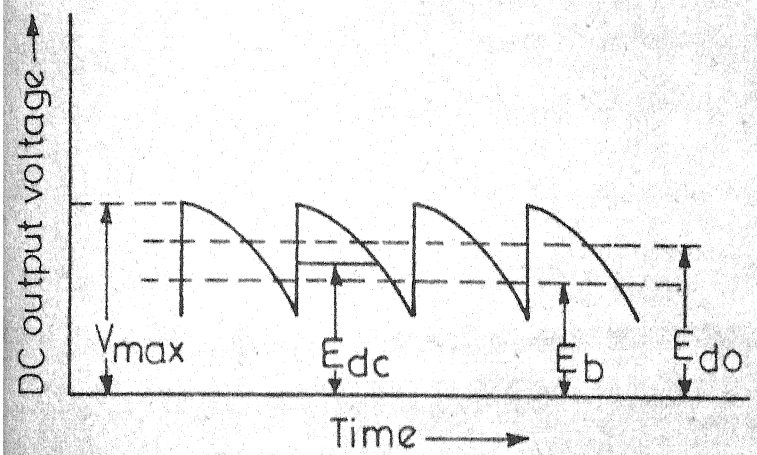

V_{max} – Maximum value of a.c. line voltage

E_{dc} – Average value of d.c. voltage

E_b – Armature counter e.m

E_{do} – Maximum value of average d.c. voltage

FIG. 7·1b. VOLTAGE WAVEFORM.

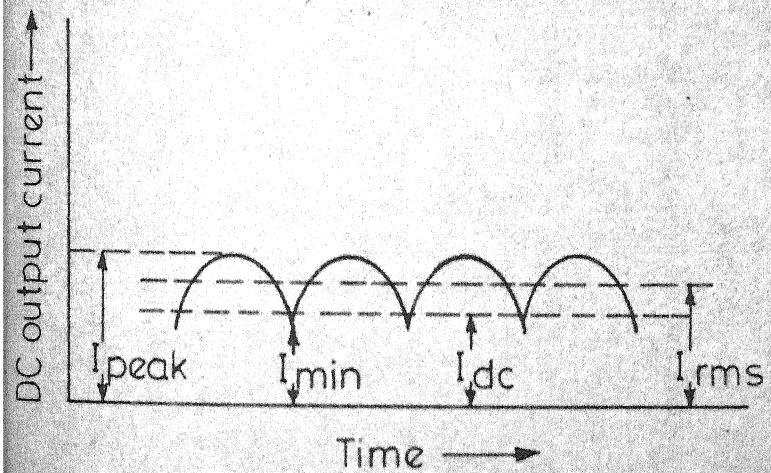

I_{peak} – Peak value of d.c. curren

I_{min} – Minimum value of d.c current

I_{dc} – Average value of d.c. current

I_{rms} – r.m.s. value of d.c. current

FIG. 7·1c. CURRENT WAVEFORM.

weight ratio and torque to armature moment of inertia ratio are the indices of overall volume and dynamic behaviour respectively of the motor. Combined axial and radial ventilation gives a more compact machine with smaller external dimensions [65]. Laminated field structure with octagonal frame construction permits a larger diameter armature in a given frame size thereby larger rating, improved commutating ability and dynamic response of the motor [54,59,63,65].

Considering all these aspects, the following sixteen variables are selected as independent variables.

1. Average flux density in the air gap, Tesla x_1
2. Width of main pole body, m x_2
3. Height of interpole winding, m x_3
4. Current density in the field winding, A/mm^2 x_4
5. Diameter of armature, m x_5
6. Length of armature core, m x_6
7. Width of armature slot, m x_7
8. Depth of armature slot, m x_8
9. Number of armature slots x_9
10. Length of air gap under main pole, m x_{10}
11. Length of air gap under interpole, m x_{11}
12. Depth of armature core, m x_{12}
13. Depth of stator yoke, m x_{13}
14. Number of axial ventilating ducts in the armature x_{14}

15. Height of main pole-shoe, m x_{15}
16. Width of main field winding on one side, m x_{16}

Since the optimization technique employed for the design problem requires the parameters to be continuously variable, the optimum design values of the number of slots (i.e., x_9) and axial ventilating ducts in armature (i.e., x_{14}) are rounded off to the nearest integer values [19,66].

The commutating ability of the motor is taken into consideration by introducing constraints like maximum reactance voltage of the commutating coil and maximum voltage between adjacent commutator segments. The minimum clearances between the main field and interpole windings are ensured by two more constraints obtained from the geometry of the magnetic circuit and position of the windings.

The following constraints are considered for the design problem.

1. Maximum flux density in the air gap.
2. Maximum flux density in the armature teeth.
3. Maximum flux density in the poles.
4. Peripheral speed of armature.
5. Ratio of armature slot depth to slot width.
6. Ratio of armature teeth width to slot width.
7. Pitch of commutator segments.
8. Pulse duty factor with reference to armature current.

9. Maximum reactance voltage of commutating coil.
10. Maximum voltage between adjacent commutator segments.
11. Ratio of torque to armature moment of inertia.
12. Efficiency of the motor.
13. Temperature rise of armature above ambient.
14. Temperature rise of commutator above ambient.
15. Minimum clearance between main field winding and tip of interpole winding.
16. Minimum clearance between tip of pole-shoe and interpole winding.

In addition, some of the design variables are constrained with upper and lower bounds.

7.2.2 Design Procedure

While designing d.c. motors for thyristor power supply, the average, r.m.s., and peak values of the d.c. current must be clearly distinguished from one another as these are responsible for producing torque, heating and commutation respectively in the motor. The instantaneous value of armature current, i(t) under the assumption of continuous conduction supplied by a six-pulse thyristor converter, with source reactance is given by [67],

$$i(t) = I_{dc} + \sqrt{2}\, I_1 \sin(6\,\omega t - \beta_1) + \sqrt{2}\, I_1' \cos(6\,\omega t - \beta_1) + \cdots$$
$$+ \sqrt{2}\, I_m \sin(6\,m\omega t - \beta_m) + \sqrt{2}\, I_m' \cos(6\,m\omega t - \beta_m) \qquad (7.1)$$

where $I_{dc} = (E_{dc} - E_b)/R_t$ (7.2)

$$I_m = \frac{E_{do}\cos(m\pi)}{2\sqrt{2}\sqrt{R_t^2 + 36\,m^2\,\omega^2\,L_t^2}} \times$$

$$\left[\frac{\sin(6m+1)(u+\alpha) + \sin(6m+1)\alpha}{6m+1} - \frac{\sin(6m-1)(u+\alpha) + \sin(6m-1)\alpha}{6m-1}\right] \quad (7.3)$$

$$I'_m = \frac{E_{do}\cos(m\pi)}{2\sqrt{2}\sqrt{R_t^2 + 36\,m^2\,\omega^2\,L_t^2}} \times$$

$$\left[\frac{\cos(6m+1)(u+\alpha) + \cos(6m+1)\alpha}{6m+1} - \frac{\cos(6m-1)(u+\alpha) + \cos(6m-1)\alpha}{6m-1}\right] \quad (7.4)$$

$$\beta_m = \mathrm{Tan}^{-1}\frac{6m\,\omega L_t}{R_t}, \quad m = 1,\ldots,p \quad (7.5)$$

$$E_{do} = 3\sqrt{2}\,V_s/\pi \quad (7.6)$$

$$\omega = 2\,\pi\,f \quad (7.7)$$

R_t = resistance of the armature circuit

L_t = inductance of the armature circuit

V_s = r.m.s. supply line voltage to the converter

f = frequency of the supply voltage

u = overlap angle

α = firing angle

For the initial design, approximate value of armature circuit inductance is obtained from the expression [68],

$$L_t = 19.1\ E_{dc}\ K_x/(P\ N\ I_{dc}) \qquad (7.8)$$

where K_x = 0.15 for machines with pole face windings

P = number of poles

N = r.p.m. of the motor

and for the final design calculations, when all the design parameters are available, expressions given in reference [68] for various components of inductance are used with suitable modifications. These expressions are given in Section 7.3.2.

7.2.3 Program Details

The design analysis program consists of eleven sub-routines which analyse and evaluate the performance of the d.c. machine, given the set of independent variables, as well as a set of constant parameters such as shaft height, h.p., voltage, number of poles, speed, standard conductor dimensions, insulation details etc., of the machine and overlap angle and firing angle of the converter. The main features

of nine important subroutines are briefly described here.

ARMW : This routine designs the lap winding with strap conductors in four layers for the armature.

CURAT: The magnetization characteristic of the low-hys steel [41] is stored here. This routine is called a number of times for the calculation of flux density and ampere turns of various parts of the magnetic circuit. The flux density and corresponding ampere turns of armature tapered teeth are calculated by using Simpson's rule.

CARTC: Carter's curves representing Carter's coefficients and ratio of opening to air gap length for slots and ducts [41,69] are incorporated in this routine. The coefficients obtained here are used for calculating the effective air gap length.

FWDRC: Integral coils with round conductors are designed for the main field winding in this subroutine, when the cross-section area of the conductor is less than a preset value.

FWSTRP: If the cross-section area of the main field winding conductor is more than a preset value, this routine operates and designs a winding with strap conductors.

CMWDG: This routine performs the design of interpole winding using single layer helical coils with parallel strap conductors.

CPWDG: In this routine, compensating winding provided in the pole-face slots is designed. Here parallel strap conductors are used in three layers.

PKCT : The expression (7.1) of armature current is analysed in this routine for peak, minimum, r.m.s. and various harmonic components.

LOSS : The hysteresis and eddy current losses in the magnetic circuit, the copper loss in the various windings are obtained for all the harmonic components of current from this routine.

Specific values from curves in these subroutines are obtained, using linear interpolation [70]. The design analysis program co-ordinates these subroutines along with some other routines to evaluate finally the cost function and the desired constraint functions. Main poles, interpoles and yoke are assumed laminated and octagonal frame is considered in line with the current practice [60,62,64,65]. The volume of the yoke is obtained from the geometry of the frame by assuming a suitable proportion between adjacent sides of the octagon. Fig. 7.2 shows the half-sectional view of a 4-pole d.c. motor.

7.2.4 Losses in the Motor

For calculating additional copper losses due to ripple current, the skin-effect factor, K_{rm} for each harmonic, is considered separately for slot and overhang portions of the armature conductor [41,71]. The eddy loss factor, K_{rm} for each harmonic is given by

$$K_{rm} = \varphi(\zeta_m) + \frac{p^2 - 1}{3} \Psi(\zeta_m) \qquad (7.9)$$

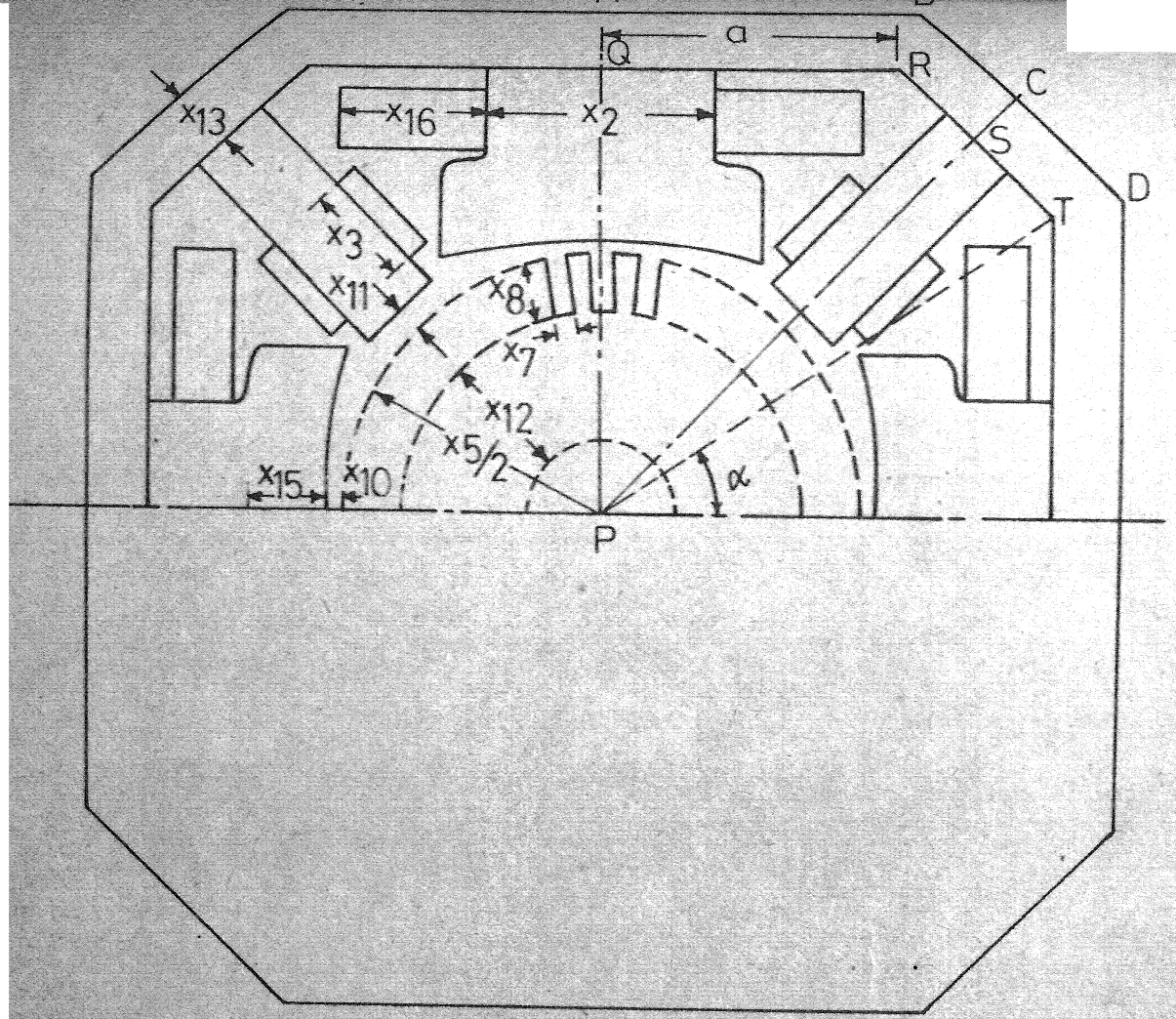

x_2 Width of pole body
x_3 Height of interpole winding
x_5 Armature diameter
x_7 Width of armature slot
x_8 Depth of armature slot
x_{10} Length of air gap under main
x_{11} Length of air gap under interp
x_{12} Depth of armature core
x_{13} Depth of field yoke
x_{15} Height of pole-shoe
x_{16} Width of field winding

FIG. 7·2. HALF SECTIONAL VIEW OF 4-POLE D C MOTOR.

where p = any arbitrary integer

$$\varphi(\zeta_m) = \zeta_m (\sinh 2\zeta_m + \sin 2\zeta_m)/(\cosh 2\zeta_m - \cos 2\zeta_m) \quad (7.10)$$

$$\psi(\zeta_m) = 2\zeta_m (\sinh \zeta_m - \sin \zeta_m)/(\cosh \zeta_m + \cos \zeta_m) \quad (7.11)$$

For slot portion of conductor,

$$\zeta_m = AO_a \left[\frac{\pi m f \mu_o (Z_s/4) BO_a}{x_7 10^3 \rho}\right]^{\frac{1}{2}} \quad (7.12)$$

For overhang portion of conductor,

$$\zeta_m = \frac{AO_a}{2} \left[\frac{\pi m f \mu_o (Z_s/4) BO_a}{(x_7 10^3 + AO_a)\rho}\right]^{\frac{1}{2}} \quad (7.13)$$

The eddy loss ratio for the complete winding is given by

$$K_{rmT} = (K_{rms} x_6 + K_{rmo} L_{oh})/(x_6 + L_{oh}) \quad (7.14)$$

where K_{rms} and K_{rmo} are eddy loss factors for slot and overhang portions of armature winding respectively.

$$L_{oh} = 0.07 + 0.535 Y \quad (7.15)$$

μ_o = magnetic space constant, $4\pi \times 10^{-7}$ H/m

ρ = specific resistance of copper, 0.021 ohm-mm^2/m

m = order of harmonic

f = frequency of supply voltage, Hz

AO_a, BO_a = armature conductor dimensions, mm

Z_s = conductors per slot

x_7 = width of the armature slot, m

Y = pole-pitch, m

The additional losses in armature conductors due to the commutation, are also calculated from the corresponding resistance coefficient [71] given by

$$K_{rcm} = \frac{1}{1+\lambda_k} \frac{8}{\pi^2} \sum_{m=1}^{\infty} \frac{1}{m^2} \times \left[\frac{\sin(m\,\beta_b)}{m\,\beta_b} \frac{m\,\alpha_c/2}{\sin(m\,\alpha_c/2)} \frac{\sin(m\,n_{cs}\,\alpha_c/2)}{m\,n_{cs}\,\alpha_c/2} \right]^2 \times \left[(\varphi(\zeta_m) - 1) + (1 + \cos\gamma)^{\frac{1}{2}} \psi(\zeta_m) \right] \quad (7.16)$$

where $\beta_6 = p\,b_b/d_c$ (7.17)

$\alpha_c = 2\pi p/N_{cs}$ (7.18)

$\lambda_k = l_{fr}/x_6$ (7.19)

$f_r = N\,p/60$ (7.20)

$p = P/2$ (7.21)

$$\zeta_m = AO_a \left[\frac{\pi m f_r\, \mu_o (Z_s/4) BO_a}{x_7\, 10^3\, \rho} \right]^{\frac{1}{2}} \quad (7.22)$$

m = order of harmonic of the tropezoid waveform assumed for ammature conductor current

p = pairs of poles

b_b = width of brush

d_c = diameter of commutator

N_{cs} = number of commutator segments

n_{cs} = commutator segments per slot

λ_k = ratio of lengths of front connections and slots

γ = phase angle displacement between currents in two layers of winding

f_r = flux reversals in the armature, Hz

$\varphi(\zeta_m)$, $\Psi(\zeta_m)$ have the same definitions of equations (7.10) and (7.11). Similarly skin-effect factors are considered for calculating additional copper losses in interpole and compensating windings, for each harmonic component of current. The skin-effect factor, K_{ipm} for interpole winding is given by

$$K_{ipm} = \varphi(\zeta_m) + \frac{(m_{ip}^2 - 1)}{3} \Psi(\zeta_m) \qquad (7.23)$$

where $\varphi(\zeta_m)$ and $\Psi(\zeta_m)$ have the same definitions of equations (7.10) and (7.11).

$$\zeta_m = BO_{ip} \left[\frac{\pi \mu_o mf \; AO_{ip} \; T_{ip}}{h_{ipw} \; 10^3 \; \rho} \right]^{\frac{1}{2}} \qquad (7.24)$$

AO_{ip}, BO_{ip} = conductor dimensions of interpole winding, mm

$h_{ip\,w}$ = height of interpole winding, m

m_{ip} = number of parallel conductors

The skin-effect factor, K_{cmm} for compensating winding is given by

$$K_{cmm} = \varphi(\zeta_m) + \frac{m_{cm}^2 - 1}{3} \psi(\zeta_m) \qquad (7.25)$$

where $$\zeta_m = AO_{cm} \left[\frac{\pi \mu_o mf}{\rho}\right]^{\frac{1}{2}} \qquad (7.26)$$

m_{cm} = number of parallel conductors

AO_{cm} = conductor dimension of compensating winding, mm

Here, the ratio copper width/slot width is assumed as unity.

The hysteresis and eddy current losses in the magnetic circuit under load are considered as follows [72]

i. in armature teeth under main poles
ii. in armature teeth under interpoles
iii. in armature core due to armature reaction flux
iv. in interpoles due to interpole flux
v. in stator yoke
vi. in teeth of pole-faces due to armature reaction flux.

All the above losses are calculated with respective flux densities for the average current and for each harmonic current separately, making use of Richter's formulas [61, 71,72].

Hysteresis loss,

$$P_h = K_h \sigma_h f_{op} B_q^2 G \qquad (7.27)$$

Eddy current loss,

$$P_e = K_e \frac{t^2}{\rho_i} f_{op}^2 B_q^2 K_E \qquad (7.28)$$

where $$K_E = 3(\sinh \zeta - \sin\zeta)/[\zeta (\cosh \zeta - \cos \zeta)] \qquad (7.29)$$

$$\zeta = 2\pi t (f_{op} \mu_r 10^{-9}/ \rho_i)^{\frac{1}{2}} \qquad (7.30)$$

K_h = hysteresis loss constant

σ_h = 3 for 0.35 mm thickness low and medium alloy steel lamination

f_{op} = operating frequency, Hz

B_q = maximum flux density, Tesla

G = weight of the material, kg

K_e = eddy current loss constant

t = lamination thickness, mm

ρ_i = specific resistance of magnetic material, ohm-cm

μ_r = relative permeability of magnetic material

7.3 EXPRESSION FOR OBJECTIVE AND CONSTRAINT FUNCTIONS

As an example for the design problem a 150 h.p., 550 volts, 4-pole, 1500 r.p.m. separately excited d.c. motor supplied from a three-phase fully controlled thyristor

bridge is considered. The a.c. supply line voltage to the converter is 440 V. The motor field supply voltage is assumed as 220 volts d.c. The objective and constraint functions are expressed in terms of the specified sixteen design variables.

7.3.1 Objective Function

FO : cost of stampings + cost of copper windings :

$$FO : \quad CI\ G_i + CC\ G_c \tag{7.31}$$

where CI and CC are defined earlier in Chapter 3.

$$\begin{aligned} G_i = k_1 \{ & x_9 L_i w_{tm} x_8 \\ & + P(N_{ps} + 1) w_{tcm}(x_{15} - k_2) L_p \\ & + [\pi x_{12}(x_5 - 2 x_8 x_{12}) - A_d] L_i \\ & + P L_p x_2 (h_{py} - x_{15}) \\ & + P L_{ip} w_{ip} h_{ip} + V_{yk} \} \end{aligned} \tag{7.32}$$

$$L_i = k_3(x_6 - n_d w_d) \tag{7.33}$$

$$n_d = x_6/0.05 \tag{7.34}$$

$$w_{tm} = \tfrac{1}{2}\left[(y_s - x_7) + \frac{\pi(x_5 - 2 x_8)}{x_9} - x_7\right] \tag{7.35}$$

$$y_s = \pi x_5/x_9 \tag{7.36}$$

$$N_{ps} = 0.7 Z/(2 P^2) \tag{7.37}$$

$$Z = k_4 \, E_{dc} \, 60 \, \varepsilon_p / (\phi \, N \, P) \tag{7.38}$$

$$\phi = x_1 \, Y \, x_6 \tag{7.39}$$

$$Y = \pi \, x_5 / P \tag{7.40}$$

$$w_{tcm} = \left(\frac{b'}{N_{ps} + 1}\right) - \frac{(k_5 + k_6 \, 3 \, BO_{cm}) 10^{-3}}{3} \tag{7.41}$$

$$b' = 0.7 \, Y \tag{7.42}$$

$$BO_{cm} = a_{cm} / (N_{ps} / m_{cm}) \tag{7.43}$$

$$a_{cm} = P \, a_a^{\,2} \tag{7.44}$$

$$a_a = AO_a \, BO_a \tag{7.45}$$

$$L_p = x_6 - k_7 \tag{7.46}$$

$$A_d = \pi (d_d \, 10^{-3})^2 \, x_{14} / 4 \tag{7.47}$$

$$h_{py} = H_s \, 10^{-3} - (k_8 + x_{13} + x_{10} + x_5/2) \tag{7.48}$$

$$L_{ip} = 0.7 \, x_6 \tag{7.49}$$

$$w_{ip} = \left(\frac{w_b}{y_c} - \frac{2a}{P} + 2 + \frac{N_{cs}}{P} - \frac{2 \, x_9}{P}\right) \frac{\pi \, x_5}{N_{cs}} \tag{7.50}$$

$$y_c = \pi \, d_c / N_{cs} \tag{7.51}$$

$$d_c = k_9 \, x_5 \tag{7.52}$$

$$N_{cs} = Z/4 \tag{7.53}$$

$$h_{ip} = PS - (x_5/2) - x_{11} \tag{7.54}$$

$$PS = (PQ + QR)/\sqrt{2} \tag{7.55}$$

$$PQ = (x_5/2) + x_{10} + h_{py} \tag{7.56}$$

$$QR = PQ/(1 + K_{yk}/\sqrt{2}) \tag{7.57}$$

$$V_{yk} = 8 \times 0.8\, L_p(ABRQ + PBC - PRS) \tag{7.58}$$

$$ABRQ = (PQ + x_{13})^2\, QR/(2\, PQ) - PQ\, QR/2 \tag{7.59}$$

$$PBC = BC(PS + x_{13})/2 \tag{7.60}$$

$$BC = (PR + x_{13})(PQ - QR)/(\sqrt{2}\, PR) \tag{7.61}$$

$$PR = (PQ^2 + QR^2)^{\frac{1}{2}} \tag{7.62}$$

$$PRS = K_{yk}\, QR\, PS/4 \tag{7.63}$$

$$\begin{aligned} G_c = k_{10}[&(x_6 + l_{fr})\, Z\, a_a \\ &+ L_{mip}\, T_{ip}\, P\, a_{ip}\, m_{ip} \\ &+ L_{mcm}\, N_b\, P\, a_{cm} \\ &+ L_{mf}\, T_f\, P\, a_f] \end{aligned} \tag{7.64}$$

$$l_{fr} = 1.15\, Y + 0.14 \tag{7.65}$$

$$L_{mip} = 2(L_{ip} + w_{ip}) + \pi\, b_{ip} \tag{7.66}$$

$$b_{ip} = (BO_{ip} + k_{11})\, m_{ip} \tag{7.67}$$

$$T_{ip} = \left(0.3\, \frac{I_{peak}}{k_{12} a_p}\, \frac{Z}{P} + k_{13}\, K_{ipg}\, \frac{B_{ipg}\, x_{11}}{\mu_o}\right)/I_{peak} \tag{7.68}$$

$$K_{ipg} = L_{ip}\, y_a/[(L_{ip} - K_d\, n_d\, w_d)(y_a - K_o\, x_7)] \tag{7.69}$$

$$y_a = \pi\, x_5/x_9 \tag{7.70}$$

$$B_{ipg} = x_6\, 2\, Z\, I_{peak}\, \lambda/(L_{ip}\, x_9\, 2\, a_p\, \beta) \tag{7.71}$$

$$\beta = [(\frac{Z}{2\ x_9} - 1)y_c + (w_{br} - k_{14})10^{-3}]x_5/d_c \quad (7.72)$$

$$\lambda = \mu_o[\frac{x_8 - k_{15}}{3\ x_7} + \frac{k_{16}}{x_7} + \frac{w_{ip}}{6\ x_{11}}] + k_{17}\frac{l_{fr}}{x_6} \times [0.23 \log \frac{l_{fr}}{b_{pc}} + 0.07] \quad (7.73)$$

$$b_{pc} = 2[2\ AO_a + Z\ BO_a/(4\ x_9) + k_{18}]10^{-3} \quad (7.74)$$

$$a_{ip} = I_{peak}/(k_{19}\ m_{ip}) \quad (7.75)$$

$$L_{mcm} = 1.8\ Y + L_p \quad (7.76)$$

$$N_b = k_{19}\ b'\ Z/(Y\ 2\ P\ a_p) \quad (7.77)$$

$$L_{mf} = 2(x_2 + L_p + k_{20}) + \pi\ x_{16} \quad (7.78)$$

$$T_f = \Delta T_f/(a_f\ x_4) \quad (7.79)$$

$$\Delta T_f = \Delta T_t + \Delta T_c + \Delta T_g + \Delta T_p + \Delta T_y \quad (7.80)$$

$$\Delta T_g = K_g\ B_{gm}\ x_{10}/\mu_o \quad (7.81)$$

$$K_g = x_6\ y_a/[(x_6 - K_d\ n_d\ w_d)(y_a - K_o\ x_7)] \quad (7.82)$$

$$B_{gm} = x_1\ Y/b' \quad (7.83)$$

$$a_f = \rho L_{mtf}\ \Delta T_f/(k_{21}\ E_f/P) \quad (7.84)$$

Equations (7.50), (7.68), (7.71), (7.80) and (7.81) are derived in reference [69]. Equations (7.54) to (7.63) are obtained from Fig. 7.2.

7.3.2 Constraint Functions

The following constraints are considered for the design problem.

1. Maximum flux density in the gap

$$B_{gm} \leq 1.1 \tag{7.85}$$

2. Maximum flux density in the armature teeth

$$1.65 \leq \frac{P\phi}{x_9 \, w_t \, L_i} \leq 2.0 \tag{7.86}$$

$$w_t = [\pi(x_5 - k_{22}\, x_8)/x_9] - x_7 \tag{7.87}$$

3. Maximum flux density in the poles

$$1.5 \leq \frac{k_{23}\,\phi}{L_p \, x_2} \leq 1.95 \tag{7.88}$$

4. Peripheral speed of armature

$$35.0 \leq u_a \leq 70.0 \tag{7.89}$$

$$u_a = \pi \, x_5 \, N/60 \tag{7.90}$$

5. Ratio of armature slot depth to slot width

$$x_8/x_7 \leq 5.0 \tag{7.91}$$

6. Ratio of armature teeth width to slot width

$$w_{tt}/x_7 \leq 1.3 \tag{7.92}$$

7. Pitch of commutator segments

$$y_c \geq 0.005 \tag{7.93}$$

8. Percentage pulse duty factor with reference to armature current

$$\frac{I_{peak} - I_{min}}{I_{peak} + I_{min}} \; 100 \leq 10.0 \tag{7.94}$$

9. Maximum reactance voltage of commutating coil

$$L_t \; \frac{T_c^2}{T_a^2} \; \frac{2\, I_{peak}}{k_{24}\, a_p} \; \frac{v_c}{w_{br}} \leq 2.0 \tag{7.95}$$

$$L_t = L_{al} + L_{bl} + L_g + L_{ipg} + L_{cl} + L_{an} + L_{sn} \tag{7.96}$$

$$L_{al} = \frac{\mu_o\, Z^2\, x_6}{k_{27}\, x_9\, a_p^2\, x_7} \left[k_{25} + \frac{(x_8 - k_{26})}{3}\right] \tag{7.97}$$

$$L_{bl} = \frac{\mu_o\, PN_b\, x_6}{k_{29}\, m_{cm}^2} \left[\frac{k_{28}\, AO_{cm}}{(BO_{cm} + k_{30})} + k_{31}\right] \tag{7.98}$$

$$L_g = L_{ag} - 2\, L_{abg} + L_{bg} \tag{7.99}$$

$$L_{ag} = \frac{\mu_o\, Z^2\, x_6}{k_{32}} \; \frac{(b' + 2\, l_g')^3}{l_g'\, P\, a_p^2\, Y^2} \tag{7.100}$$

$$l_g' = 1.5\, x_{10} \tag{7.101}$$

$$L_{abg} = \frac{\mu_o\, P\, N_b\, Z\, x_6}{k_{33}} \; \frac{(b' + 2\, l_g')^2}{l_g'\, x_5\, a_p\, m_{cm}} \tag{7.102}$$

$$L_{bg} = \frac{\mu_o\, P^2\, N_b^2\, x_6}{k_{34}} \; \frac{(b' + 2\, l_g')}{l_g'\, P\, m_{cm}^2} \tag{7.103}$$

$$L_{ipg} = \frac{\mu_o (w_{ip} + 2.5\, x_{11})\, x_6\, P}{x_{11}} \times \left[\frac{T_{ip}}{m_{ip}} + \frac{N_6}{2\, m_{cm}} - \frac{Z}{4\, a_p\, P}\right]^2 \tag{7.104}$$

$$L_{cl} = \frac{8\ \mu_o\ T_{ip}^2\ x_6\ x_{15}\ P}{[2Y-b'-x_2-(b'-x_2)-2w_{ip}]m_{ip}^2}$$

$$+ \frac{2\ \mu_o\ T_{ip}^2\ P^2\ x_6}{\pi\ m_{ip}^2} \times$$

$$[(\frac{x_3+r_{cl}}{x_3})^2 \ln\ (\frac{x_3+r_{cl}}{x_3}) - 1.5 - \frac{r_{cl}}{x_3}] \quad (7.105)$$

$$r_{cl} = \frac{x_5}{2} + x_{15} + 2\ x_{10} - \tfrac{1}{2}[\frac{w_{ip}}{\sin(\frac{\pi}{P})} + \frac{x_2}{\mathrm{Tan}(\frac{\pi}{P})}] \quad (7.106)$$

$$L_{an} = \frac{\mu_o\ Z^2\ x_5}{k_{35}\ a_p^2\ \cos(\frac{\pi}{6})}[\sin^2(\frac{\pi}{P}) + \frac{1}{9}\ \sin^2(\frac{3\pi}{P})$$

$$+ \frac{1}{25}\ \sin^2(\frac{5\pi}{P})] \quad (7.107)$$

$$L_{sn} = \frac{\mu_o\ x_5\ (P\ N_b)^2}{k_{36}\ m_{cm}^2\ P^2}\ [\ln \frac{2\ r_{sn}}{(BO_{cm}\ 10^{-3} + k_{37})} + 0.25] \quad (7.108)$$

$$r_{sn} = \tfrac{1}{2}[(2\ L_{ip} - x_6 - BO_{cm}\ 10^{-3})^2 + h_{py}^2]^{\frac{1}{2}} \quad (7.109)$$

$$T_a = Z/4 \quad (7.110)$$

$$v_c = \pi\ d_c\ N/60 \quad (7.111)$$

10. Maximum voltage between adjacent commutator segments

$$2\ T_c\ \frac{P}{a}\ B_{gm}\ L_i\ u \leq 45.0 \quad (7.112)$$

11. Ratio of torque to armature moment of inertia

$$\frac{k_{38}(P_d - P_{fw})60}{2\pi N x_5^4 x_6} \geq 4.0 \qquad (7.113)$$

$$P_d = (E_d - I_{av} R_t) I_{av} \qquad (7.114)$$

$$R_t = R_a + R_{ip} + R_{cm} \qquad (7.115)$$

$$R_a = \rho(x_6 + l_{fr})Z/(k_{39} a_p^2 a_a) \qquad (7.116)$$

$$R_{ip} = \rho T_{ip} P L_{mip}/(k_{40} a_{ip}) \qquad (7.117)$$

$$R_{cm} = \rho N_b P L_{mcm}/(k_{41} a_{cm}) \qquad (7.118)$$

$$P_{fw} = k_{42} n_{br}^2 a_{br} v_c + k_{43}(d_{sh} - k_{44})^2 \times [\pi(d_{sh} - k_{44})\frac{N}{60}]^{1.5} + k_{45} x_5(x_6 + 2 l_o)u_a^2 \qquad (7.119)$$

$$d_{sh} = k_{46}(P_d/N)^{1/3} \qquad (7.120)$$

$$l_o = 0.07 + 0.3 Y \qquad (7.121)$$

12. Percentage efficiency of the motor

$$\frac{E_{dc} I_{rms} - (P_{fw} + P_a + P_{ip} + P_{cm} + P_y + P_f + P_{bc})}{E_{dc} I_{rms}} \geq 90.0 \qquad (7.122)$$

$$P_a = P_{ahc} + P_{acd} + P_{acc} \qquad (7.123)$$

where P_{ahc} = hysteresis and eddy current loss in armature teeth and core

P_{aed} = eddy current loss in armature conductors

P_{acc} = copper loss in armature conductors due to average current including eddy current loss due to commutation

$$P_{ip} = P_{ipc} + P_{ipe} + P_{iphe} \qquad (7.124)$$

where P_{ipc} = copper loss in interpole winding due to average current

P_{ipe} = eddy current loss in interpole winding

P_{iphc} = hysteresis and eddy current loss in interpoles

$$P_{cm} = P_{cmc} + P_{cme} + P_{cmhc} \qquad (7.125)$$

where P_{cmc} = copper loss in compensating winding due to average current

P_{cme} = eddy current loss in compensating winding

P_{cmhc} = hysteresis and eddy current loss in teeth of pole-face slots

$$P_{y} = P_{yhc} \qquad (7.126)$$

where P_{yhc} = hysteresis and eddy current loss in yoke

$$P_{f} = P_{fc} \qquad (7.127)$$

where P_{fc} = copper loss in field winding

$$P_{bc} = 2\ I_{rms} \tag{7.128}$$

13. Temperature rise of armature above ambient

$$P_{ar}\left\{\frac{C_{cex}}{\pi\ x_5(x_6+4l_o)} + \frac{C_{cin}}{(\pi\ d_{in}\ x_6 - A_d)} + \frac{C_{cd}}{\frac{\pi}{4}[x_5^2 - (d_{in}-x_{12})^2](n_d+2)}\right\} \leq 115.0 \tag{7.129}$$

$$C_{cex} = 0.03/(1 + 0.1\ u_a) \tag{7.130}$$

$$C_{cin} = 0.03/[1 + 0.1\ u_a(d_{in}/x_5)] \tag{7.131}$$

$$d_{in} = x_5 - 2\ x_8 \tag{7.132}$$

$$C_{cd} = 0.08/(0.1\ u_a) \tag{7.133}$$

14. Temperature rise of commutator above ambient

$$\left\{\frac{(P_{bc} + k_{42}\ n_{br}^2 a_{br}\ v_c)C_{cc}}{\pi\ d_c\ l_{cm} + \frac{\pi}{4}[(d_c+0.1)^2 - d_c^2] + 0.05\ w_{bb}}\right\} \leq 80.0 \tag{7.134}$$

$$C_{cc} = 0.03/(1 + 0.1\ v_c) \tag{7.135}$$

$$l_{cm} = \frac{k_{47}}{k_{48}\ t_{br}\ w_{br}}(w_{br} + k_{49}) + k_{50} \tag{7.136}$$

15. Minimum clearance between main field winding and tip of the interpole winding

$$0.015 \leq [PQ - (h_{py} - x_{15}) - KN] \leq 0.05 \tag{7.137}$$

$$KN = [(x_5/2) + x_{11} + x_3 + b_{ip} + (w_{ip}/2)] \times [\mathrm{Tan}(\tfrac{\pi}{4})]/\sqrt{2} \qquad (7.138)$$

16. Minimum clearance between tip of pole-shoe and interpole winding

$$\frac{1}{\sqrt{2}}(x_5 + x_{11}) - [\tfrac{1}{2} w_{sh} + \frac{1}{\sqrt{2}}(\frac{w_{ip}}{2} + \frac{b_{ip}}{2})] \geq 0.015 \qquad (7.139)$$

$$w_{sh} = 2(\frac{x_5}{2} + 2\, x_{10}) \sin(\frac{b'}{2(\frac{x_5}{2} + x_{10})}) \qquad (7.140)$$

Expressions (7.97) to (7.111) are derived in the reference [68]. Equations (7.95), (7.112) and (7.119) are taken from the references [69,73,74]. Equation (7.113) is derived in the reference [75]. The empirical formulas used for the cooling coefficients are given in the reference [41].

7.4 SOLUTION OF THE NLP PROBLEM

The mathematical model of the design problem of the specified d.c. motor is formulated in terms of the cost and constraint functions of earlier sections. The problem is converted into a sequence of unconstrained minimization problems with normalized constraints using Zangwill's exterior penalty function method. The iterative procedure is initiated with a starting vector of independent variables and the objective function is evaluated. An initial

penalty parameter of 1500 is used in the augmented cost function and Powell's minimization technique is adopted to obtain the minimum active material cost of the unconstrained problem. The penalty parameter is incremented ten times at the end of each unconstrained minimization cycle, if the constraints are not satisfied.

Optimal solutions minimizing the active material cost of a 150 h.p., 550 volts, 4-pole, 1500 r.p.m. separately excited d.c. motor supplied through a six-pulse thyristor converter are obtained. Two different starting points are tried for this problem. Two sets of firing angles, α and overlap angles, u are assumed for each starting point and the corresponding optimal solutions are presented in Table 7.1.

7.5 OPTIMIZED DESIGN OF A 150 HP MOTOR

The optimized design data and performance characteristics of the specified motor are obtained at the optimal solution corresponding to first starting point when $\alpha = 60°$, $u = 15°$ of Table 7.1. The active material cost corresponding to the second starting point is taken as 100% for comparison. Table 7.2 lists the specified constraints and the constraints at the optimal solution selected. The constraints on flux densities in the air gap, armature teeth and poles have become active at the optimal solution. It is observed from

OPTIMAL SOLUTIONS OF A 150 HP, 550 VOLTS, 4-POLE,
1500 RPM DC SEPARATELY EXCITED MOTOR

Particulars	Starting point 1	$\alpha=0°$, $u=0°$ Optimal value	$\alpha=30°$, $u=15°$ Optimal value	$\alpha=60°$, $u=15°$ Optimal value*	Starting point 2	$\alpha=0°$, $u=0°$ Optimal value	$\alpha=60°$ $u=15°$ Optimal value
Diameter of armature, $m(x_5)$	0.55	0.4915	0.4915	0.4774	0.54	0.4706	0.4706
Length of armature core, $m(x_6)$	0.35	0.2507	0.2695	0.2985	0.26	0.2996	0.2996
Width of armature slot, $m(x_7)$	0.016	0.0111	0.0111	0.0121	0.016	0.0116	0.0116
Depth of armature slot, $m(x_8)$	0.045	0.0505	0.0505	0.0576	0.07	0.0525	0.0526
Depth of armature core, $m(x_{12})$	0.15	0.1469	0.1469	0.1469	0.15	0.1500	0.1500
Number of armature slots (x_9)	80	70	70	62	81	66	66
Number of axial ventilating ducts in armature (x_{14})	12	48	48	48	14	18	16
Width of main pole body, $m(x_2)$	0.12	0.2203	0.2203	0.1832	0.15	0.1066	0.1066
Height of main pole-shoe, $m(x_{15})$	0.03	0.0463	0.0488	0.0502	0.025	0.0329	0.0329
Width of main field winding on one side, $m(x_{16})$	0.10	0.0955	0.0955	0.1002	0.08	0.1037	0.1038
Depth of stator yoke, $m(x_{13})$	0.15	0.0524	0.0524	0.0629	0.12	0.0853	0.0854
Height of interpole winding, $m(x_3)$	0.09	0.0738	0.0738	0.0756	0.04	0.0582	0.0582
Length of air gap under main pole, m (x_{10})	0.003	0.008	0.008	0.0096	0.003	0.0177	0.0177

Particulars	Starting point 1	$\alpha=0°$, $u=0°$ Optimal value	$\alpha=30°$, $u=15°$ Optimal value	$\alpha=60°$, $u=15°$ Optimal* value	Starting point 2	$\alpha=0°$, $u=0°$ Optimal value	$\alpha=60°$ $u=15°$ Optimal value
Length of air gap under interpole, m (x_{11})	0.0075	0.0148	0.0148	0.0176	0.01	0.0231	0.0231
Average flux density in the air gap, Tesla (x_1)	0.68	0.8536	0.8536	0.7177	0.69	0.5387	0.5240
Current density in the field winding, A/mm^2 (x_4)	4.0	2.9915	2.9915	2.7277	6.0	2.7066	2.7066
Cost, %	99.7	58.7	61.9	70.5	100.0	80.5	80.8
No. of unconstrained minimization cycles		5	5	8		12	12

α = firing angle of the converter

u = overlap angle

* indicates selected final optimal solution

TABLE 7.2

CONSTRAINTS ON A 150 HP, 550 VOLTS, 4-POLE, 1500 RPM DC SEPARATELY EXCITED MOTOR

CONSTRAINTS	SPECIFIED	At the optimum point for $\alpha=60°$, $u=15°$
1. Maximum flux density in the air gap, Tesla	1.1	1.0253
2. Maximum flux density in the armature teeth, Tesla	1.65-2.0	1.6565
3. Maximum flux density in the poles, Tesla	1.50-1.95	1.5027
4. Peripheral speed of armature, m/sec.	35.00-70.0	37.5
5. Ratio of armature slot depth to slot width	5.0	4.76
6. Ratio of armature teeth width to slot width	1.3	1.00
7. Pitch of commutator segments, m	0.005	0.0086
8. Pulse-duty factor with reference to armature current, %	10.00	10.72
9. Maximum reactance voltage of commutating coil, V	2.0	0.002
10. Maximum voltage between adjacent commutator segments, V	45.0	17.20
11. Ratio of torque to moment of inertia of armature	4.0	5.09
12. Efficiency of the motor,	90.0	91.30
13. Temperature rise of armature above ambient, °C	115.0	109.9
14. Temperature rise of commutator above ambient, °C	80.0	75.55
15. Clearance between main field winding and tip of the interpole winding, m	0.015-0.05	0.0308
16. Minimum clearance between tip of pole shoe and interpole winding, m	0.015	0.02

α = firing angle of the converter

u = overlap angle

Table 7.2 that the constraint on percentage pulse-duty factor with reference to armature current is deviated by a little margin from the specified value. This constraint is satisfied when the firing angle of the converter is less then 60° . The performance and other design data of the motor is presented in Table 7.3.

7.6 CONCLUSIONS

A design procedure is developed for a medium h.p separately excited d.c. motor supplied through a thyristor converter. The mathematical model of the design problem represented with sixteen design variables is solved by NLP technique satisfying many desired constraints. The modifications in the motor design proposed by manufacturers to suit the rectified power supply are considered. The design optimization of a 150 h.p. motor is obtained on IBM 7044 computer for minimum material cost. The convergence to the optimal solution is observed to be slow as the number of design variables are large and the optimization routine has to perform about 180 function evaluations in every unconstrained minimization cycle. Another reason for slow convergence is the presence of two integer variables viz., number of slots and number of axial ventilating ducts in armature. The execution time to obtain each optimal solution is about 3 hours.

TABLE 7.3

PERFORMANCE AND DESIGN DATA OF A 150 HP, 550 VOLTS, 4-POLE, 1500 RPM DC SEPARATELY EXCITED MOTOR

	At $\alpha=60°, u=15°$
1. Average current in armature, A	226.0
2. Peak current in armature, A	249.6344
3. Minimum current in armature, A	201.2692
4. Inductance of total armature circuit, H	0.0030
5. Resistance of total armature circuit, ohm	0.0274
6. Dimensions of armature conductor, mm	11.6 x 4.1
7. Copper space factor of armature slot	0.63
8. Number of armature conductors	496
9. Number of commutator segments	124
10. Diameter of commutator, m	0.3387
11. Number of field winding turns per pole	550
12. Height of field winding, m	0.1136
13. Width of pole shoe, m	0.2513
14. Number of interpole winding turns	5
15. Dimensions of interpole winding conductor, mm	10.84 x 3.05
16. Number of parallel conductors in interpole winding	4
17. Width of interpole winding, m	0.0242
18. Height of interpole, m	0.2369
19. Number of slots in each pole-face	10
20. Number of conductors in each pole-face	90
21. Number of parallel conductors in each pole-face slot	9

TABLE 7.3 (continued)

	At $\alpha=60°; u=15°$
22. Dimensions of conductor of compensating winding, mm	13.41 x 3.10
23. Total weight of stampings, kg	877.6659
24. Total weight of windings, kg	400.3249
25. Hysteresis and eddy current losses in the magnetic circuit, W	1888.6971
26. Losses in armature winding, W	409.2597
27. Losses in interpole winding, W	125.9245
28. Losses in compensating winding, W	991.7303
29. Losses in field winding, W	1328.999
30. Brush contact losses, W	452.1212
31. Friction and winding losses, W	3569.7402

α = firing angle of the converter

u = overlap angle

The increase in cost with an increase in firing angle indicated, the requirement of a generously dimensioned motor. The length of the armature core is increased by about 8%. If the excitation voltage to the field winding is through a thyristor or diode bridge, very little modification, is required in the computer program. Standard shaft heights according to IEC recommendations can be adopted in the design procedure for different ratings of motors. The computer program developed is general and can be used for a line of motors.

The design optimization of series motor is considered in the next chapter.

CHAPTER 8

OPTIMAL DESIGN OF DC SERIES MOTOR SUPPLIED THROUGH A THREE-PHASE THYRISTOR CONVERTER

8.1 INTRODUCTION

The application of d.c. series motors as traction and rolling mill motors is well known. Reference [61] highlights the efficient use of power pulse controlled d.c. series motors for such applications. The desire to increase the output and to reduce the manufacturing costs for a given size of machine calls for an optimal design. An attempt is made here for the first time to obtain the optimized design of a d.c. series motor when supplied through a six-pulse thyristor bridge, minimizing the active material cost by NLP approach.

The mathematical model is represented by the same sixteen design variables as are given in Chapter 7. Similar considerations as indicated in Chapter 7 for a separately excited d.c. motor hold good for the series motor as well. However, appropriate modifications are to be made in the design analysis program to include the nonlinearity of the magnetic circuit. A linear approximation of the magnetization curve is considered in the design analysis to account for the nonlinearity of the magnetic circuit. The design problem is posed as an NLP problem with the same constraints as detailed in Chapter 7 and optimized design of the

specified motor is obtained, minimizing the active material cost of the motor.

The effects of source impedance and of firing angle of the converter on the optimal solution is studied. The torque pulsation and the associated speed variation of the series motor is derived at the optimal solution.

8.2 PROBLEM FORMULATION

The d.c. series motor, when supplied through a six-pulse thyristor converter, has the same design problems as a separately excited motor discussed in Chapter 7. Also, additional iron and copper losses in the magnetic and electric circuit of the main field are to be considered. The same sixteen variables as listed in Section 7.2.1 for a separately excited motor are considered as independent variables for this problem as well. Similarly, the same constraints listed as in Section 7.2.1 are considered while arriving at a feasible optimal solution. The cost of the active materials of stampings and windings form the objective function. The magnetic field structure is assumed to be completely laminated and an octagonal frame is considered for the yoke. Interpole and compensating windings are considered for the specified 150 h.p. d.c. motor in accordance with the current practice. The armature winding is arranged in four layers. Strap conductors are considered for all the windings.

8.3 DESIGN PROCEDURE

The ripple content of the armature current in a series motor is small due to the large inductance of the field winding. The armature current, i(t) of the series motor supplied from a six-pulse thyristor converter is given by the equation (7.1) of Section 7.2.2. The total resistance of the armature circuit in this expression includes the main field winding resistance in addition to the resistance of the interpole and compensating windings. Similarly the total circuit inductance includes the main field winding inductance in addition to the armature circuit inductance.

The main field circuit inductance, L_f is the flux linkages per ampere of the field coils times the number of such coils in series. Saturation will change the effective value of L_f and a correction must be made. Reference [61] gives the representation of nonlinear magnetization curve with its linear approximation based on equivalence of stored magnetic energy. The slope of the curve is determined from the magnetization characteristic drawn over the operating range by assuming suitable terminal voltages of the motor. Fig. 8.1 represents a typical approximation of magnetization curve. The slope, c_m of the curve is used in the calculations of inductance, flux, the power developed and the losses in the motor.

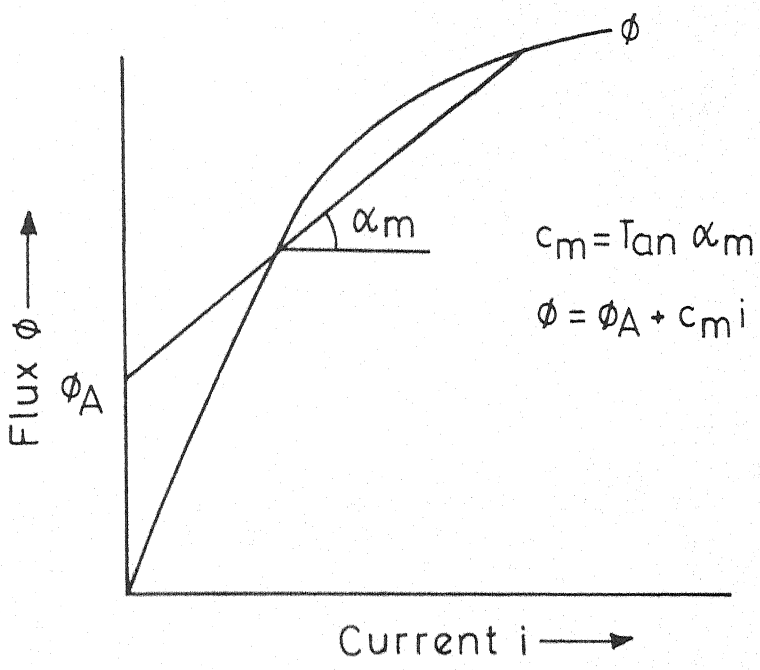

FIG. 8·1. APPROXIMATION OF MAGNETIZATION CURVE.

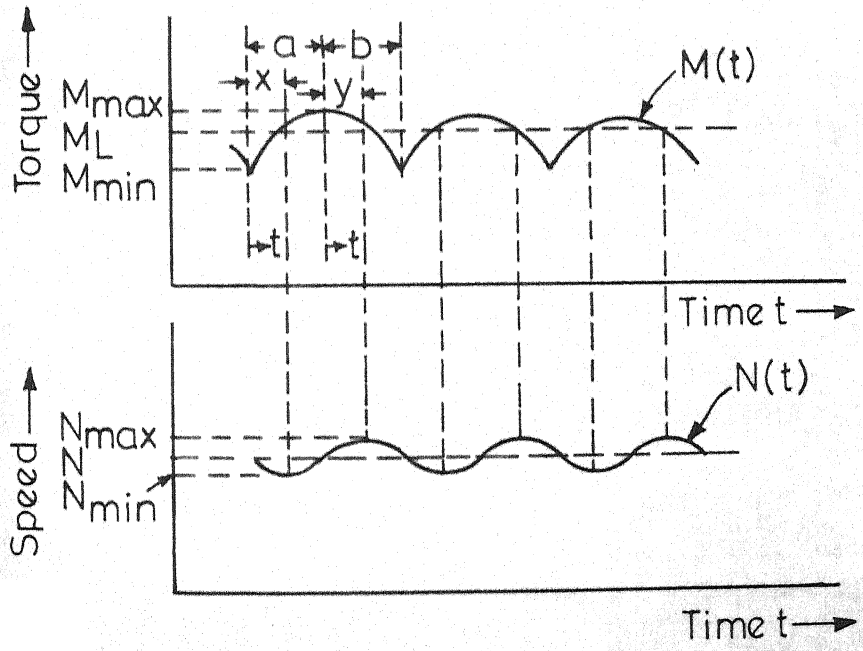

FIG. 8·2. TORQUE AND SPEED VARIATIONS.

The total circuit inductance, L_{to} is given by

$$L_{to} = L_t + L_f + c_m T_f P \qquad (8.1)$$

where L_t = armature circuit inductance

T_f = series turns of field winding per pole

P = number of poles

The flux, ϕ is represented as

$$\phi = \phi_A + c_m i \qquad (8.2)$$

where ϕ_A is defined in Fig. 8.1

i = field or armature current

The power developed, P_d in the motor is derived as [61].

Power developed = $E_b i$

$$= \phi Z N P i/(60 a_p K_m)$$

$$= K_{pd}(\phi_A + c_m i)i$$

Average power developed,

$$P_d = K_{pd}(\phi_A I_{av} + c_m I^2_{rms}) \qquad (8.3)$$

where $K_{pd} = Z N P/(60 a_p K_m)$

E_b = armature counter e.m.f.

Z = total number of armature conductors

N = speed of the motor, r.p.m.

a_p = number of parallel paths in armature

K_m = constant to account for number of parallel conductors in slots

I_{av} = average value of d.c. current

I_{rms} = r.m.s. value of d.c. current

Expression (7.8) of Section 7.2.2 is used for the armature circuit inductance in the initial design and for the final design, expressions given in reference [68] are used with some modifications as indicated in Section 7.3.2.

The design analysis program consists of twelve subroutines. Eleven of these subroutines are already described in Section 7.2.2. The other subroutine MAGCH develops the magnetization characteristic. The flux level is calculated assuming terminal voltages over the operating range of the motor. Leakage factor is considered [69] while calculating flux density in the poles and yoke. The constant, c_m and flux, ϕ_A are determined from this routine.

The losses in various magnetic parts are calculated on similar lines as indicated in Section 7.2.2. The effect of field flux is considered in the calculation of loss in teeth under main poles, in core and in pole-face teeth. The iron loss in main poles is calculated for the average current and as well as for the harmonic components of field current.

The pulsation amplitude of the magnetic density, B_q is given by [61]

$$B_q = B_o \frac{c_m I_h}{\phi_A + c_m I_{av}} \qquad (8.4)$$

where B_o = average flux density of the magnetic circuit at a particular location

I_h = harmonic amplitude of current

The hysteresis and eddy current losses in the magnetic circuit are obtained from expressions (7.27) and (7.28) of Section 7.2.2.

The copper losses in various windings are obtained taking skin-effect factors into account for armature, interpole and compensating windings given by expressions (7.9), (7.23) and (7.25) of Section 7.2.2. The additional losses in armature conductors due to commutation of current is calculated from expression (7.16). The eddy current losses in main field winding are also similarly calculated for each harmonic component of current from the skin-effect factor, K_{fd} given by

$$K_{fd} = \varphi(\zeta_m) + \frac{(T_{fw}^2 - 1)}{3} \psi(\zeta_m) \qquad (8.5)$$

where $$\zeta_m = BO_f \left[\frac{\pi \mu_o \, nf \, AO_f \, T_{fv}}{h_{fd} \, 10^3 \, \rho} \right]^{\frac{1}{2}} \qquad (8.6)$$

AO_f, BO_f = conductor dimensions of field winding, mm

T_{fw} = number of field winding turns on each pole width-wise

T_{fv} = number of field winding turns on each pole depth-wise

h_{fd} = height of exciting coil, m

The input to the design analysis program is a set of independent variables and constant parameters such as shaft height, h.p., voltage, number of poles, speed, standard conductor dimensions, insulation details etc., of the machine. The overlap and firing angles of the converter are also specified.

8.4 EXPRESSION FOR OBJECTIVE AND CONSTRAINT FUNCTIONS

A 150 h.p., 550 volts, 4-pole, 1500 r.p.m. d.c. series motor supplied from a three-phase fully controlled thyristor bridge is considered for the design problem as an example. The a.c. supply line voltage to the converter is 440 volts. The objective and constraint functions are expressed in terms of the specified sixteen design variables.

8.4.1 Objective Function

Equations (7.31) to (7.78) of Section 7.3.1 are applicable for series motor also. The following equations are added to the above equations to express the objective function of the design problem.

$$T_f = AT_f / I_{peak} \tag{8.7}$$

$$AT_{fl} = E_{do}\, a_f / (P \rho\, L_{mf}) \tag{8.8}$$

$$E_{do} = 3\sqrt{2}\, V_s / \pi \tag{8.9}$$

$$a_f = I_{peak}/x_4 \tag{8.10}$$

8.4.2 Constraint Functions

The constraints given in Section 7.3.2 for separately excited motor are applicable to the series motor with some modifications. These changes are outlined here. The constraints 1-9 given by the expressions (7.85) to (7.111) are the same for the design problem of series motor. The total circuit inductance is modified by adding main field winding inductance to the other components of inductance in equation (7.96). The modified equation for L_t is

$$L_t = L_{al}+L_{bl}+L_g+L_{ipg}+L_{cl}+L_{an}+L_{sn}+L_f+c_m T_f P \tag{8.11}$$

where the components L_{al}, L_{bl}, L_g, L_{ipg}, L_{cl}, L_{an}, L_{sn} are defined by equations (7.97) to (7.111)

$$L_f = \frac{T_f^2 P^2 \mu_o \mu_{rp} A_p}{h_{py}} \tag{8.12}$$

$$A_p = L_p x_2 \tag{8.13}$$

The constraint 10 represented by equation (7.112) is applicable without any modification. Equations (7.114) and (7.115) representing P_d and R_t of constraint 11 are modified as

$$P_d = K_t(\phi_A I_{av} + c_m I_{rms}^2) \tag{8.14}$$

$$R_t = R_a + R_{ip} + R_{cm} + R_f \quad (8.15)$$

$$R_f = \rho L_{mf} T_f P/a_f \quad (8.16)$$

and other equations of this constraint are used without any modification. In constraint 12, the percentage efficiency of the motor is modified in equation (7.127) representing the main field loss.

Here $P_f = P_{fc} + P_{fcd} + P_{fhc}$ (8.17)

Equations (7.129) to (7.140) representing the constraints 13, 14, 15, 16 are the same.

8.5 SOLUTION OF THE NLP PROBLEM

The mathematical model of the specified d.c. series motor, representing the cost and constraint functions in terms of the specified design variables is posed as an NLP problem. The problem is converted into a sequence of unconstrained minimization problems with normalized constraints using Zangwill's exterior penalty function method. The iterative process is initiated with a starting vector of independent variables and a penalty parameter of 1500. Powell's minimization technique is adopted and optimal solution is obtained for minimum active material cost of the unconstrained problem.

Optimal solutions minimizing the active material cost of a 150 h.p., 550 volts, 4-pole, 1500 r.p.m. d.c. series motor supplied through a six-pulse thyristor converter are presented in Table 8.1. Initially, the overlap angle and firing angle of the converter are assumed to be equal to zeros. At the optimal solution, the change in cost function and the optimized design is investigated for different overlap and firing angles of the converter.

8.6 OPTIMIZED DESIGN OF A 150 HP DC SERIES MOTOR

The optimized design data and performance characteristics of the specified d.c. series motor are obtained at the optimal solution corresponding to the second starting point when $\alpha = 30°$, $u = 15°$ of Table 8.1. The active material cost corresponding to the second starting point is taken as 100 % for comparison. Table 8.2 lists the specified constraints and the constraints at the selected optimal solution. The constraints on temperature rise of the armature, flux density in the poles and number of axial ventilating ducts in armature have become active at the optimal solution.

8.7 CALCULATION OF TORQUE AND SPEED FLUCTUATIONS

Normally, in the design equations, the speed is assumed to be constant. But when the motor is operated with

TABLE 8.1

OPTIMAL SOLUTIONS OF A 150 HP, 550 VOLTS, 4-POLE, 1500 RPM DC SERIES MOTOR

Particulars		Starting point 1	$\alpha=0°$; $u=0°$ Optimal value	Starting point 2	$\alpha=30°$; $u=15°$ Optimal* value
Diameter of armature, m	(x_5)	0.497	0.4761	0.48	0.4780
Length of armature core, m	(x_6)	0.256	0.2571	0.257	0.2456
Width of armature slot, m	(x_7)	0.012	0.0107	0.012	0.0107
Depth of armature slot, m	(x_8)	0.059	0.0548	0.061	0.0582
Depth of armature core, m	(x_{12})	0.147	0.1469	0.146	0.1447
Number of armature slots	(x_9)	68.[illegible]	70	69	70.[illegible]
Number of axial ventilating ducts in armature	(x_{14})	54.[illegible]	66	50	50 [illegible]
Width of main pole body, m	(x_2)	0.318	0.1256	0.173	0.1384
Height of main pole, m	(x_{15})	0.079	0.1045	0.079	0.0803
Width of main field winding on one side, m	(x_{16})	0.099	0.0708	0.089	0.0764
Depth of stator yoke, m	(x_{13})	0.126	0.2188	0.136	0.1813
Height of interpole winding, m	(x_3)	0.057	0.0854	0.076	0.0842
Length of air gap under main pole, m	(x_{10})	0.012	0.0135	0.031	0.0173
Length of air gap under interpole, m	(x_{11})	0.010	0.0351	0.023	0.0102
Average flux density in the air gap, Tesla	(x_1)	0.609	0.7057	0.712	0.7208
Current density in the field winding, A/mm^2	(x_4)	2.97	2.5509	2.748	2.5415

TABLE 8.1 (continued)

Particulars	Starting point 1	$\alpha=0°$; $u=0°$ Optimal value	Starting point 2	$\alpha=30°$, $u=15°$ Optimal* value
Cost, %	98.0	94.2	100.0	95.0
No. of unconstrained minimization cycles		12		3

α = firing angle of the converter

u = overlap angle

* indicates selected final optimal solution

TABLE 8.2

CONSTRAINTS ON A 150 HP, 550 VOLTS, 4-POLE, 1500 RPM DC SERIES MOTOR

CONSTRAINTS	SPECIFIED	At the optimum point for $\alpha=30°, u=15$
1. Maximum flux density in the air gap, Tesla	1.1	1.03
2. Maximum flux density in the armature teeth, Tesla	1.65-2.0	1.6506
3. Maximum flux density in the poles, Tesla	1.5 -2.0	2.054
4. Peripheral speed of armature, m/sec.	35.00-70.0	37.6
5. Ratio of armature slot depth to slot width	5.0	5.44
6. Ratio of armature teeth width to slot width	1.3	1.01
7. Pitch of commutator segments, m	0.005	0.0051
8. Pulse-duty factor with reference to armature current, %	10.0	0.0558
9. Maximum reactance voltage of commutating coil, V	2.0	0.2179
10. Maximum voltage between adjacent commutator segments, V	45.0	14.31
11. Ratio of torque to moment of inertia of the armature	4.0	5.8546
12. Efficiency of the motor	80.0	81.49
13. Temperature rise of armature above ambient, °C	125.0	126.0
14. Temperature rise of commutator above ambient, °C	80.0	75.5517
15. Clearance between main field winding and tip of the interpole winding, m	0.015-0.03	0.0192
16. Minimum clearance between tip of pole shoe and interpole winding, m	0.015	0.0248

α = firing angle of the converter

u = overlap angle

thyristor power supply, the torque and corresponding speed pulsations are inherent. The speed variation of the optimally designed motor is investigated here. The overlap and firing angles of the converter supplying the motor are assumed to be equal to zeros. The instantaneous torque of the motor is given by

$$M(t) = \frac{E_b\, i}{2\pi n} \tag{8.18}$$

$$= \frac{1}{2\pi n} \frac{\phi Z N}{60} \frac{P}{a_p k_m} i \quad \text{Nm} \tag{8.19}$$

where n = r.p.s. of the motor

Substituting for $\phi = \phi_A + c_m i$

$$M(t) = K_t(\phi_A + c_m i)i \tag{8.20}$$

where $K_t = Z P/(2\pi a_p K_m)$ (8.21)

For a given load torque, M_1 the relation between motor speed, N(t) and the instantaneous torque of the motor is shown in Fig. 8.2 and given by

$$\frac{2\pi}{60} J \frac{dN}{dt} = M(t) - M_1 \tag{8.22}$$

$$\frac{dN}{dt} = \frac{60}{2\pi J} [M(t) - M_1] \tag{8.23}$$

where J = moment of inertia, kg-m^2

Integrating between the limits for maximum and minimum speed with reference to Fig. 8.2

$$N_{max} - N_{min} = \frac{60}{2\pi J} \left\{ \int_{x}^{a} M(t)_a \, dt + \int_{0}^{y} M(t)_b \, dt - M_1(a - x + y) \right\} \quad (8.24)$$

where $$M(t)_a = K_t(\phi_A + c_m I_{peak}) I_{peak} \quad (8.25)$$

$$M(t)_b = K_t(\phi_A + c_m I_{min}) I_{min} \quad (8.26)$$

$$N_{max} - N_{min} = \frac{60}{2\pi J} [M(t)_a (a-x) + M(t)_b y - M_1(a - x + y)] \quad (8.27)$$

The maximum and minimum torques corresponding to peak and minimum currents respectively can be calculated. The values of a,x and y in seconds can be obtained from the plot of waveform of instantaneous torque. The load torque, M_1 is assumed to be equal to full-load torque corresponding to 150 h.p.

The coefficient of speed variation is given by

$$Q_N = \frac{N_{max} - N_{min}}{N}$$

The instantaneous torque is observed to be fairly constant with very little variation from maximum to minimum values, for the optimal solutions of Table 8.1. Hence the speed fluctuation is also negligible thus validating the assumption made in the optimum design.

8.8 CONCLUSIONS

The optimized design of a medium h.p. d.c. series motor supplied through a three-phase thyristor converter is obtained minimizing the active material cost and satisfying many important performance requirements as constraints by NLP technique. The mathematical model of the design problem is formulated with sixteen important design variables. Design modifications necessary to suit the thyristor power supply are incorporated by considering laminated magnetic structure with an octagonal frame for yoke. The nonlinearity of the magnetic circuit in a d.c. series motor is recognised and accounted for in the design procedure. The execution time to obtain each optimal solution is about 3 hours on IBM 7044 computer. The convergence process to the optimal solution is also slow as in the case of design optimization of d.c. separately excited motor. Table 8.3 lists the performance and design data of the specified series motor.

TABLE 8.3

PERFORMANCE AND DESIGN DATA OF A 150 HP, 550 VOLTS, 4-POLE, 1500 RPM DC SERIES MOTOR

		At $\alpha=30°, u=15°$
1.	Average current in armature, A	226.0
2.	Peak current in armature, A	226.216
3.	Minimum current in armature, A	225.899
4.	Inductance of total circuit, H	0.0464
5.	Resistance of total circuit, ohm	0.1141
6.	Dimensions of armature conductor, mm	12.5 x 3.28
7.	Copper space factor of armature slot	0.79
8.	Number of armature conductors	840
9.	Number of commutator segments	210
10.	Diameter of commutator, m	0.3387
11.	Number of field winding turns per pole	56
12.	Height of field winding, m	0.0853
13.	Width of pole-shoe, m	0.2528
14.	Number of interpole winding turns	7
15.	Dimensions of interpole winding conductor, mm	8.67 x 3.05
16.	Number of parallel conductors in interpole winding	5
17.	Width of interpole winding, m	0.0302
18.	Height of interpole, m	0.2227
19.	Number of slots in each pole-face	18
20.	Number of conductors in each pole-face	162
21.	Number of parallel conductors in each pole-face slot	9

(Table 8.3 (continued)

22.	Dimensions of conductor of compensating winding, mm	23.44 x 1.54
23.	Total weight of stampings, kg	1391.961
24.	Total weight of copper windings, kg	697.4293
25.	Hysteresis and eddy current losses in the magnetic circuit, W	12010.1398
26.	Losses in armature winding, W	880.7587
27.	Losses in interpole winding, W	177.1805
28.	Losses in compensating winding, W	1945.5863
29.	Losses in field winding, W	2629.4340
30.	Brush contact losses, W	452.1212
31.	Friction and windage losses, W	3569.7402

α = firing angle of the converter

u = overlap angle

PART - III

AC MOTOR

CHAPTER 9

OPTIMAL DESIGN OF A VARIABLE SPEED SQUIRREL-CAGE INDUCTION MOTOR WITH NONSINUSOIDAL VOLTAGE SUPPLY

9.1 INTRODUCTION

The squirrel-cage induction motor has special mechanical and electrical features which make it an economic proposition for variable speed drives. In the previous two chapters, the optimal design of two types of d.c. motors supplied with rectified voltage are studied. Using variable frequency and variable voltage supplies, the induction motor operates with the same torque characteristics as d.c. machines. Some important applications of these motors are in electric traction, steel and grinding industries, machine tool and textile industries. Variable speed operation of induction motors using thyristor power supplies require modifications in the design procedure. Static inverter fed induction motor drive is an important competitor in the field of variable speed drives. The need for the optimum design aspect of a variable speed squirrel-cage induction motor arises due to cost considerations and many engineering constraints the drive is required to satisfy. The optimal design of conventional induction motors has been dealt with by many authors in the past [4,6,7,10,76,77]. The general aspects of operating an induction motor with variable frequency and variable voltage are outlined in references [78-86]. In this chapter, the optimal design of a variable speed

squirrel-cage induction motor supplied with nonsinusoidal voltage is investigated as an NLP problem with many exacting constraints.

The squirrel-cage induction motor is considered here with a variable frequency, six-stepped, three-phase voltage supply. The mathematical model of the design problem is formulated with eleven design variables and posed as an NLP problem. Only steady state operation of the motor is considered here. In the design analysis program, the effect of variable frequency, six-stepped voltage on electric and magnetic circuits is investigated. The motor currents, losses and torques are predicted over a frequency range for the nonsinusoidal voltage supply on the basis of steady state equivalent circuits [83]. The torque pulsations produced by the harmonic voltages are determined at different input frequencies and taken as constraints on the design problem. Many important constraints like no-load power factor at minimum frequency, efficiency, temperature rise of stator, locked rotor current at minimum frequency, ratio of starting to full-load torque, pull-out torque at minimum frequency, full-load slip, full-load power factor etc., are imposed on the design optimization problem.

The NLP problem of minimizing the costs of stator copper, rotor bar copper, end rings and electrical steel of

the motor is solved over a frequency range, satisfying the desired constraints. The optimal design of the specified motor is presented.

9.2 OPERATION WITH VARIABLE FREQUENCY AND NONSINUSOIDAL SUPPLY

A three-phase, delta connected squirrel-cage induction motor is considered for the design problem. The motor is connected to a six-stepped three-phase inverter supply. Fig. 9.1 shows a six-step line-to-line output voltage waveform from a three-phase full-wave inverter with 120° conduction. The output frequency of the inverter is controlled by controlling the inverter frequency. Variation in a.c. voltage is obtained by controlling the magnitude of 120° voltage waveform. The Fourier series of the waveform of Fig. 9.1 is

$$v(t) = \sqrt{2}\, V_1 \sin \omega t + \sqrt{2}\, V_5 \sin 5\omega t + \sqrt{2}\, V_7 \sin 7\omega t + \ldots + \sqrt{2}\, V_m \sin m\omega t + \ldots \quad (9.1)$$

where $V_m = 3\, E_{dc}/(\sqrt{2}\, \pi\, m)$ (9.2)

$\omega = 2\, \pi\, f_{op}$ (9.3)

V_m = r.m.s. value of m-th harmonic voltage

E_{dc} = d.c. link voltage of the inverter

m = order of harmonic 1,5,7,11,...

f_{op} = operating frequency of the inverter, Hz

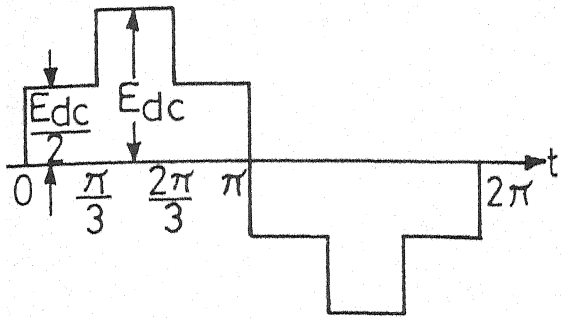

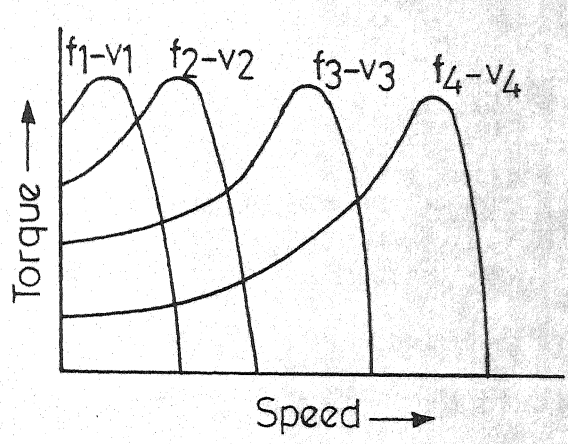

FIG. 9.1. SIX-STEP VOLTAGE WAVEFORM.

FIG. 9.2. TORQUE SPEED CURVES.

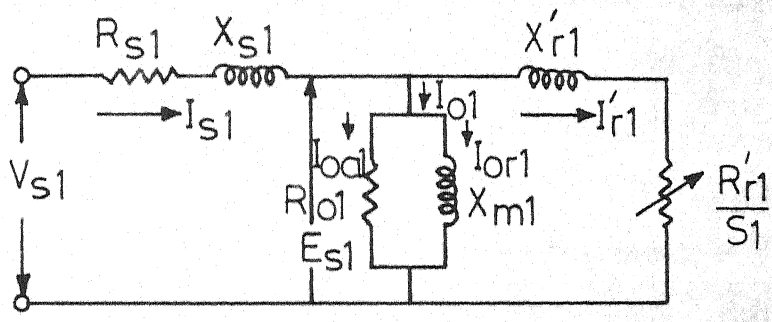

FIG. 9.3. EQUIVALENT CIRCUIT FOR FUNDAMENTAL COMPONENT.

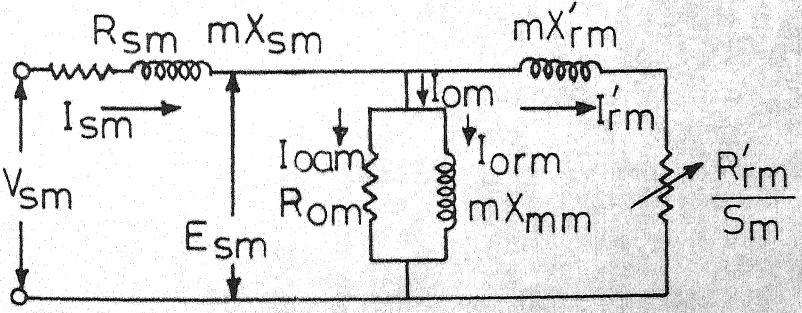

9.4. EQUIVALENT CIRCUIT FOR HARMONIC COMPONENTS.

The waveform does not contain any even harmonics or triplen harmonics. During normal balanced operation, the input voltage to the A phase of the motor is represented by equation (9.1). The motor is presumed to supply a constant torque load and the ratio of voltage per Hz over the frequency range is maintained constant to ensure proper air gap flux of the motor. The torque-speed characteristics of a constant flux, variable frequency induction motor is shown in Fig. 9.2. The operation of the motor under steady-state with nonsinusoidal voltage supply is realised by considering the equivalent circuits for fundamental and harmonic components of voltage [83,87,88]. The respective equivalent circuits are represented in Figs. 9.3 and 9.4. The principle of superposition is assumed, neglecting magnetic saturation. The net motor current or torque is obtained with the help of equivalent circuits of Figs. 9.3 and 9.4 from the resultant sum of current or torque contributions of each voltage component in supply voltage waveform.

The effects of voltage harmonics on the motor are to cause:

1. current harmonics and flux harmonics, resulting in additional copper and iron losses
2. driving or braking torque at the motor depending on the order of harmonic
3. torque pulsations due to interaction between various harmonics

The m-th time harmonic currents produces a m.m.f. rotating forwards or backwards at a speed m N_s, N_s being the speed of the fundamental m.m.f. The harmonic slip, s_m is expressed in terms of full-load slip, as

$$s_m = [(m \mp 1) \pm s_{fl}]/m \qquad (9.4)$$

The harmonic currents of the order (6p + 1) where p = 1,2,... .., k have the same phase sequence as the fundamental with positive phase rotation and harmonic currents of order (6p - 1) have the opposite phase rotation to the fundamental. The harmonic torques due to time harmonic m.m.f. waves are divided into

1. steady state harmonic torques and
2. pulsating harmonic torques.

The steady state harmonic torques are developed by the reaction of harmonic air gap flux with harmonic rotor current of same order. This is the useful or the braking torque in induction motor. The total average torque of an induction motor is the algebraic sum of the fundamental and harmonic torques. The pulsating harmonic torques are developed by interaction of harmonic flux of some order with harmonic currents of a different order [87]. The mean value of such pulsating torques is zero. With inverter power supply to the motor, such torque pulsations cannot be eliminated unless special means are adopted.

9.3 TORQUE PULSATIONS

References [89-91] highlight the phenomenon of torque pulsations in induction motors with inverter drives. The presence of torque pulsations causes the angular velocity of the rotor to vary during a revolution. For a six-stepped voltage waveform, pulsating torques at sixth and twelfth harmonic frequency are important. The magnitude of the torque pulsations are derived here from the phasor diagrams of induction motor, using single-phase equivalent circuit model of the machine, on similar lines as of reference [91]. Fig. 9.5 represents the phasor diagram for the induction motor for the fundamental of the applied voltage. When harmonic voltages are considered, Figs. 9.6 and 9.7 represent the phasor diagrams for forward and backward rotating harmonic fluxes.

The magnitude of harmonic torque at any instant is given by [91]

$$K_t \quad \phi_{mm} \; I'_{rm} \sin \quad \psi'_{rm} \tag{9.5}$$

where K_t = constant

ϕ_{mm} = m-th harmonic flux

I'_{rm} = referred m-th harmonic rotor current

ψ'_{rm} = angle between ϕ_{mm} and I'_{rm} as shown in Fig. 9.7

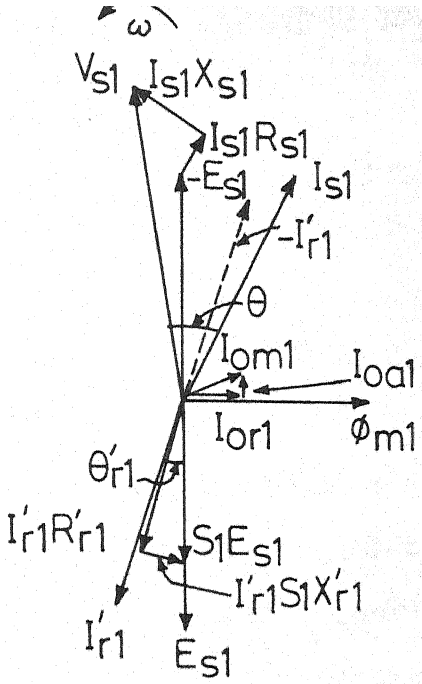

FIG. 9·5. PHASOR DIAGRAM FOR FUNDAMENTAL COMPONENT.

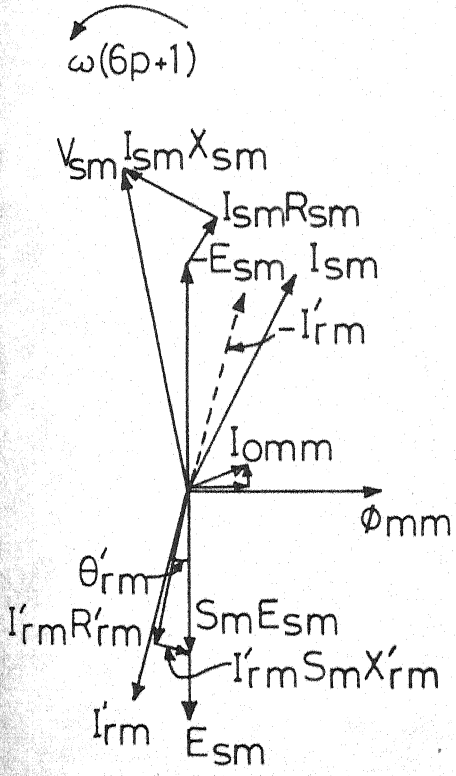

FIG. 9·6. PHASOR DIAGRAM FOR FORWARD ROTATING HARMONIC FLUX.

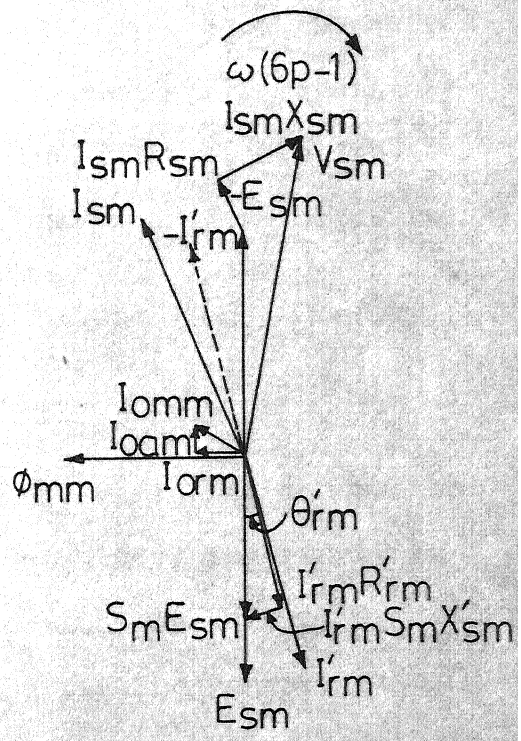

FIG. 9·7. PHASOR DIAGRAM FOR BACKWARD ROTATING HARMONIC FLUX.

Considering upto 19-th harmonic in the voltage waveform, the component fluxes and rotor currents are superimposed and shown in single phasor diagram. Fig. 9.8 represents the resultant phasor diagram. Here the fundamental components of flux and rotor current rotate with synchronous speed ω and the harmonic components of flux and rotor current with their respective harmonic speeds in the directions indicated in Fig. 9.8. The magnitude of net torque pulsations at the sixth harmonic frequency is obtained from Fig. 9.8 by assuming the fundamental components of flux and rotor current to be stationary. The method of deriving torque pulsations from vector diagram is indicated in reference [91]. Similarly the net torque pulsations at the twelfth harmonic frequency is derived from Fig. 9.8. The expressions for torque pulsations are given in Section 9.6.2.

9.4 DESIGN VARIABLES AND CONSTRAINTS

The choice of the independent variables depends on the design problem. In the present study, importance is given to the optimization of electrical aspects of induction motor when it is operating between two frequencies with nonsinusoidal voltage. Shaft height, insulation details, radial ventilating ducts etc., are treated as constant parameters. The following eleven independent variables are

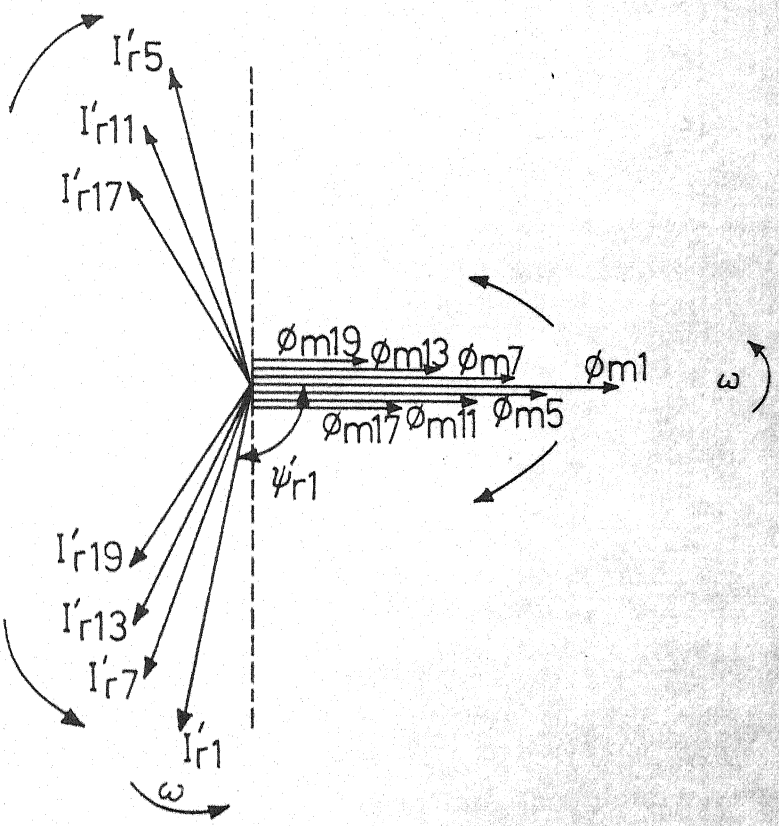

FIG. 9·8. SUPERIMPOSED PHASOR-VECTOR DIAGRAM.

chosen as design variables for the squirrel-cage motor.

1. Diameter of stator bore, m x_1
2. Length of stator core, m x_2
3. Width of stator slot, m x_3
4. Depth of stator slot, m x_4
5. Depth of stator core, m x_5
6. Length of air gap, m x_6
7. Width of rotor slot, m x_7
8. Depth of rotor slot, m x_8
9. Depth of rotor core, m x_9
10. Average flux density in air gap, Tesla x_{10}
11. Area of c.s. of end ring, mm^2. x_{11}

The design factors that influence the operation of induction motor at the two extreme frequencies of excitation are rotor loss, starting torque, starting current, pull-out torque and power factor. At the maximum frequency, the pull-out torque is a limiting factor. Under constant torque operation, the friction, windage and iron losses will increase with higher frequencies. At minimum frequency, the limiting factors are the magnetizing current and locked rotor current which greatly affect motor heating and performance. The fundamental component of locked rotor current may be 6 to 10 times full-load current [84]. The efficiency of the motor at rated load is practically constant over the

frequency range. The p.u. full-load slip remains constant over the frequency range [84,92]. The torque pulsations can be minimized by designing the motor for a minimum locked rotor current. Additional losses show up predominantly in rotor bars. A low resistance rotor bar is mandatory from the point of view of heating.

Since the no-load current, full-load current, full-load slip, full-load power factor, efficiency and air gap flux density are found to be nearly independent of operating frequency for the constant torque operation, constraints on these variables are computed at normal operating frequency of 50 Hz.

In view of all the factors mentioned earlier, the following constraints are imposed on the design problem.

1. Average torque over the frequency range
2. Per unit torque pulsation over the frequency range
3. No-load power factor at minimum frequency
4. Efficiency at full-load and full-load power factor
5. Temperature rise of stator winding above ambient at maximum frequency
6. Locked rotor current at minimum frequency
7. Ratio of starting torque to full-load torque
8. Pull-out torque at maximum frequency
9. No-load current

10. Full-load slip
11. Full-load power factor
12. Minimum width of stator teeth
13. Ratio of minimum width of stator tooth to width of stator slot
14. Maximum flux density in stator teeth
15. Minimum width of rotor teeth
16. Ratio of minimum width of rotor tooth to width of rotor slot
17. Maximum flux density in rotor teeth
18. Diameter of shaft
19. Current density in the end ring
20. Current density in the rotor bar
21. Stator current density

In addition to the above constraints, some design variables are constrained with upper and lower bounds for mechanical reasons.

9.5 DESIGN PROCEDURE

The variable frequency, six-stepped voltage waveform is divided into a series of harmonics as shown in Section 9.2. The single-phase equivalent circuits shown in Figs. 9.3 and 9.4 are used to predict the motor currents, torques and losses for various harmonic voltages in the design analysis program. Initially the frequency range of motor

operation is fixed and the ratio volts/Hz is maintained constant.

9.5.1 Program Details

The design analysis program consists of fifteen subroutines, which analyse and evaluate the performance, cost and constraint functions of the squirrel-cage motor. The input to the program is a set of independent variables and a set of constant parameters such as shaft height, h.p., number of poles, slots per pole per phase, voltage at normal frequency, frequency range, standard conductor dimensions, insulation details etc., of the motor. This is a major program in the main optimization program.

The main features of ten subroutines are briefly described here.

STWD : A double-layer lap winding is designed for the stator with standard strap conductors.

RTWD : The rotor bars and end rings are designed in this routine. Proper slots combination of stator and rotor is selected so that the parasitic torques are minimized [41,92-95]. Rotor slot skew is assumed by one stator slot pitch.

EQCT : The purpose of this routine is to obtain the equivalent circuit parameters, harmonic components of voltage and current, harmonic slip etc., over the frequency range. The direction of rotation of the

harmonics is taken care of in the program. The order of the harmonic is limited upto the 19-th avoiding even and triplen harmonics.

EDDY : The purpose of this routine is to determine the eddy current loss in conductors of stator and rotor. The skin-effect factor for each harmonic current is calculated in this routine using standard formulas.

HYST : Richter's formulas are used in this routine to calculate the hysteresis and eddy current loss in the magnetic circuit for each harmonic component. Steel laminations of 0.35 mm thickness are assumed.

STRL : Various components of stray load losses are obtained from this routine for all harmonic frequencies.

PERF : This routine calculates the performance at full-load, locked rotor and pull-out condition over the frequency range based on the equivalent circuits of Figs. 9.3 and 9.4.

TQPL : The sixth and twelfth harmonic frequency torque pulsations are evaluated in this routine from Fig. 9.8. The peak and minimum values of the net torque pulsations are noted from the instantaneous value of torque pulsations.

Two more subroutines CURAT and CARTC used in the calculations of magnetic circuit and Carter's coefficients are described in Section 7.2.3.

The design analysis program co-ordinates these subroutines along with some other routines to evaluate finally

the cost function and the desired constraint functions over the frequency range of the motor. The magnetic circuit of the motor is assumed to be laminated. Semi-closed parallel sided slots are considered for stator and rotor.

9.5.2 Losses in the Motor

The additional losses that occur in the cage induction motor due to harmonics in the motor input current when it is operating over a frequency range are

1. stator copper loss
2. rotor copper loss
3. core loss and
4. stray loss.

The formulas for each of the harmonic currents that are used in the design analysis program are briefly summarised here. The resistance skin-effect factor for the slot portion of stator conductor, K_{rsm} is given by

$$K_{rsm} = \varphi(\zeta_m) + \frac{(N_{ad}^2 - 1)}{3} \Psi(\zeta_m) \qquad (9.6)$$

where $\varphi(\zeta_m)$ and $\Psi(\zeta_m)$ have the same definitions as of Section 7.2.4.

$$\zeta_m = AO_s \left[\frac{\pi \, m \, f_{op} \, \mu_o \, BO_s \, N_{aw}}{x_3 \, 10^3 \, \rho} \right]^{\frac{1}{2}} \qquad (9.7)$$

AO_s, BO_s = conductor dimensions of stator winding, mm

N_{ad}, N_{aw} = number of stator slot conductors depth-wise and width-wise respectively

The reduction in leakage reactance in the slot portion of stator conductor is calculated from the skin-effect factor, K_{xsm} given by [27]

$$K_{xsm} = \frac{3}{2\zeta_m} \frac{\sinh 2\zeta_m - \sin 2\zeta_m}{\cosh 2\zeta_m - \cos 2\zeta_m} \tag{9.8}$$

The skin-effect factors K_{rrm} and K_{xrm} for the slot portion of rotor conductor for resistance and leakage reactance respectively are given by similar formulas.

Here $$\zeta_m = AO_r \left[\frac{\pi\, m\, s_m\, f_{op}\, \mu_o\, BO_r}{x_7\, 10^3\, \rho} \right]^{\frac{1}{2}} \tag{9.9}$$

where AO_r, BO_r = conductor dimensions of rotor conductor, mm

It is assumed in the copper loss calculations that the stator and rotor overhangs, the space harmonic (zig-zag) leakage and the leakage due to slot skewing are not affected by the skin-effect.

The core losses are calculated from well-known Richter's formulas [71]. Equations (7.27) and (7.28) of Section 7.2.4 are used in the calculation of stator and rotor core loss, with nonsinusoidal excitation.

References [83,96] broadly outline the components of stray loss of an induction motor and the equations for calculation. These components which are used in the design analysis program for each harmonic current are indicated here.

1. Stator surface loss due to zig-zag leakage flux, P_{ssz}
2. Rotor surface loss due to zig-zag leakage flux, P_{rsz}
3. Rotor surface loss due to load current, P_{rsc}
4. Rotor pulsation and I^2R loss due to zig-zag leakage flux, P_{rzz}
5. Stator end loss due to zig-zag leakage flux, P_{sez}
6. Rotor end loss due to zig-zag leakage flux, P_{rez}
7. Stator teeth pulsation loss, P_{stp}
8. Loss due to belt leakage flux, P_{bll}
9. Loss due to skew leakage flux, P_{skl}

The costs of the stator copper, rotor bar copper, end rings and laminations form the objective function for the design problem. The cost and constraint functions are expressed in terms of the eleven independent variables referred to earlier.

9.6 EXPRESSIONS FOR OBJECTIVE AND CONSTRAINT FUNCTIONS

As an example for the design problem a 5 h.p., 400 volts, 4-pole, three-phase delta connected squirrel-cage

induction motor supplied from a three-phase bridge inverter with six-stepped voltage is considered. The frequency of operation of the motor is allowed from 30 Hz to 60 Hz in steps of 5 Hz.

9.6.1 Objective Function

FO = cost of stampings + cost of copper windings + cost of end rings

$$FO = CI\ G_i + CC\ G_c + CB\ G_b \tag{9.10}$$

$$G_i = k_1[S_s\ L_{is}\ w_{ts}\ x_4 + \pi(x_1 + 2x_4 + x_5)x_5\ L_{is} + S_r\ L_2\ w_{tr}\ x_8 + \pi(d_2 - 2x_8 - x_9)x_9\ L_2] \tag{9.11}$$

$$S_s = 3\ g_s'\ 2\ p \tag{9.12}$$

$$p = P/2 \tag{9.13}$$

$$L_{is} = k_2(x_2 - n_d\ w_d) \tag{9.14}$$

$$n_d = x_2/k_3 \tag{9.15}$$

$$w_{ts} = \tfrac{1}{2}\ \{(y_s - x_3) + [\frac{\pi(x_1 + 2x_4)}{S_s} - x_3]\} \tag{9.16}$$

$$y_s = \pi\ x_1/S_1 \tag{9.17}$$

$$S_r = S_s + p \tag{9.18}$$

$$L_2 = (x_2^2 + y_s^2)^{\frac{1}{2}} \tag{9.19}$$

$$w_{tr} = \tfrac{1}{2}\ \{(y_r - x_7) + [\frac{\pi(d_2 - 2x_8)}{S_r} - x_7]\} \tag{9.20}$$

$$y_r = \pi\, d_2/S_r \tag{9.21}$$

$$d_2 = x_1 - 2x_6 \tag{9.22}$$

$$G_c = k_3[(x_2 + L_e)6\, T_{ph}\, a_s + L_2\, S_r\, a_r] \tag{9.23}$$

$$L_e = 1.15\, Y + 0.12 \tag{9.24}$$

$$Y = \pi\, x_1/P \tag{9.25}$$

$$T_{ph} = E_{sl}/(4.44\, K_{wsl}\, f_{op}\, \phi_{ml}) \tag{9.26}$$

$$E_{sl} = V_{sl}/1.05 \tag{9.27}$$

$$V_{sl} = K_f\, f_{op} \tag{9.28}$$

$$\phi_{ml} = x_{10}\, Y\, x_2 \tag{9.29}$$

$$Z_s = T_{ph}/(p\, g'_s) = N_{cw}\, N_{cd} \tag{9.30}$$

$$a_s = AO_s\, BO_s \tag{9.31}$$

$$a_r = AO_r\, BO_r \tag{9.32}$$

$$G_b = k_4\, 2\, \pi\, d_{er}\, x_{11} \tag{9.33}$$

$$d_{er} = d_2 - 1.5\, h_{er}\, 10^{-3} \tag{9.34}$$

$$h_{er} = AO_r + k_5 \tag{9.35}$$

9.6.2 Constraint Functions

1. Average torque over the frequency range

$$\sum_{m=1}^{19} \frac{3\, p\, I'^2_{rm}\, R'_{rm}}{2\, \pi\, m\, f_{op}\, s_m} \geq M_{sp} \tag{9.36}$$

$$I'_{rm} = (I^2_{sm} - I^2_{om})^{\frac{1}{2}} \tag{9.37}$$

$$R'_{rm} = \frac{12\ K^2_{wsm}\ T^2_{ph}}{S_r\ K^2_{wrm}} \left(K_{rrm}\ R_{cr} + R_{be} + \frac{R_{er}\ g_r}{\pi^2\ p}\right) \tag{9.38}$$

$$K_{wsm} = \sin(m\ g'_s\ \frac{\pi}{g_s{}^2})/[g'_s\ \sin(\frac{m\pi}{g_s{}^2})] \tag{9.39}$$

$$g_s = S_s/P \tag{9.40}$$

$$K_{wrm} = \sin(m\ g'_r\ \frac{\pi}{g_r{}^2})/[g'_r\ \sin(\frac{m\pi}{g_r{}^2})] \tag{9.41}$$

$$g_r = S_r/P \tag{9.42}$$

$$g'_r = g_r/3 \tag{9.43}$$

$$R_{cr} = \rho\ L_2/a_r \tag{9.44}$$

$$R_{bc} = \rho\ (2\ w_{cr} + k_6)10^{-3}/a_r \tag{9.45}$$

$$w_{cr} = x_{11}/h_{cr} \tag{9.46}$$

$$R_{cr} = \rho_b\ \pi\ dcr/x_{11} \tag{9.47}$$

$$s_m = [(m \mp 1) \pm s_{fl}]/m \tag{9.48}$$

$$s_{fl} = P_{cr}/(HP\ 746 + P_{cr} + P_{fw}) \tag{9.49}$$

$$P_{cr} = \sum_{m=1}^{19} 3\ I'^2_{rm}\ R'_{rm} \tag{9.50}$$

$$P_{fw} = k_7(d_{sh} - k_8)^2[\pi(d_{sh} - k_8)\ \frac{N}{60}]^{1.5} + k_9\ x_1(x_2 + 2\ L_o)u_a^2 \tag{9.51}$$

$$d_{sh} = d_2 - 2x_8 - 2x_9 \tag{9.52}$$

$$L_o = 0.07 + 0.3\,Y \tag{9.53}$$

$$u_a = \pi d_2 N/60 \tag{9.54}$$

Equations (9.36), (9.38) and (9.51) are derived in reference [41]. This constraint set is obtained for all the operating frequencies.

2. Per unit torque pulsation over the frequency range

$$M_{pul} \leq 0.15 \tag{9.55}$$

$$M_{pul} = (M_{pmx} + M_{pmn})/M_{av} \tag{9.56}$$

The maximum and minimum values of torque pulsation are obtained from resultant torque pulsation, M_{hm} where

$$M_{hm} = k_{10} \frac{60}{2\pi N} (M_{6s} + M_{6c} + M_{12s} + M_{12c}) \tag{9.57}$$

$$\begin{aligned} M_{6s} = [& \phi_{m1}(-I'_{r5} \sin \psi'_{r5} + I'_{r7} \sin \psi'_{r7}) \\ & + \phi_{m5}(I'_{r1} \sin \psi'_{r1} - I'_{r11} \sin \psi'_{r11}) \\ & + \phi_{m7}(-I'_{r1} \sin \psi'_{r1} + I'_{r13} \sin \psi'_{r13}) \\ & + \phi_{m11}(I'_{r5} \sin \psi'_{r5} - I'_{r17} \sin \psi'_{r17}) \\ & + \phi_{m13}(-I'_{r7} \sin \psi'_{r7} + I'_{r19} \sin \psi'_{r19}) \\ & + \phi_{m17} I'_{r11} \sin \psi'_{r11} - \phi_{m19} I'_{r13} \sin \psi'_{r13}] \times \\ & \sin 6\omega t \end{aligned} \tag{9.58}$$

$$M_{6c} = [\phi_{m1}(I'_{r7}\cos\psi'_{r7} - I'_{r5}\cos\psi'_{r5}) + \phi_{m5}(I'_{r1}\cos\psi'_{r1} - I'_{r11}\cos\psi'_{r11}) + \phi_{m7}(I'_{r1}\cos\psi'_{r1} + I'_{r13}\cos\psi'_{r13}) - \phi_{m11}(I'_{r5}\cos\psi'_{r5} + I'_{r17}\cos\psi'_{r17}) + \phi_{m13}(I'_{r7}\cos\psi'_{r7} + I'_{r19}\cos\psi'_{r19}) - \phi_{m17}I'_{r11}\cos\psi'_{r11} + \phi_{m19}I'_{r13}\cos\psi'_{r13}]\times \cos 6\omega t \qquad (9.59)$$

$$M_{12s} = [\phi_{m1}(-I'_{r11}\sin\psi'_{r11} + I'_{r13}\sin\psi'_{r13}) + \phi_{m5}(I'_{r7}\sin\psi'_{r7} - I'_{r17}\sin\psi'_{r17}) + \phi_{m7}(-I'_{r5}\sin\psi'_{r5} + I'_{r19}\sin\psi'_{r19}) + (\phi_{m11} - \phi_{m13})I'_{r1}\sin\psi'_{r1} - \phi_{m19}I'_{r7}\sin\psi'_{r7}]\sin 12\omega t \qquad (9.60)$$

$$M_{12c} = [\phi_{m1}(I'_{r11}\cos\psi'_{r11} + I'_{r13}\cos\psi'_{r13}) + \phi_{m5}(I'_{r7}\cos\psi'_{r7} - I'_{r17}\cos\psi'_{r17}) + \phi_{m7}(-I'_{r5}\cos\psi'_{r5} + I'_{r19}\cos\psi'_{r19}) + (\phi_{m11} - \phi_{m13})I'_{r1}\cos\psi'_{r1}$$

$$- \phi_{ml7} I'_{r5} \cos \psi'_{r5} + \phi_{ml9} I'_{r7} \cos \psi'_{r7}] x$$

$$\cos 12 \omega t \qquad (9.61)$$

$$\omega = 2 \pi f_{op} \qquad (9.62)$$

The harmonic components of flux and current are defined in Fig. 9.8. This constraint set is obtained for all the operating frequencies.

3. No-load power factor at minimum frequency

$$\frac{I_{oam}}{I_{on}} \leq 0.2 \qquad (9.63)$$

$$I_{oam} = E_{sm}/R_{sm} \qquad (9.64)$$

$$\dot{E}_{sm} = \dot{V}_{sm} - \dot{V}_{sm} Z_{sm}/Z_{Tm} \qquad (9.65)$$

$$\dot{V}_{sm} = V_m + j\, o \qquad (9.66)$$

$$V_m = 3 E_{dc}/(\sqrt{2}\, \pi\, m) \qquad (9.67)$$

$$Z_{Tm} = Z_{sm} + Z_{mm} Z'_{rm}/(Z_{mm} + Z'_{rm}) \qquad (9.68)$$

$$Z_{sm} = R_{sm} + j\, m\, X_{sm} \qquad (9.69)$$

$$R_{sm} = K_{rsm} R_{cs} + R_{es} \qquad (9.70)$$

$$R_{cs} = \rho\, x_2\, 2\, T_{ph}/a_s \qquad (9.71)$$

$$R_{es} = \rho\, L_e\, 2\, T_{ph}/a_s \qquad (9.72)$$

$$X_{sm} = K_{xsm} X_{sl} + X_{Ol} + X_{zl} \qquad (9.73)$$

$$X_{sl} = 15.8 \times 10^{-6} f_{op} T^2_{ph} g'_s x_2 \lambda_{sl}/p \qquad (9.74)$$

$$\lambda_{sl} = \lambda_{ts} + \lambda_{bs} + 2\ \lambda_{tbs} \tag{9.75}$$

$$\lambda_{ts} = \left(\frac{N_{cd}}{2}\ \frac{AO_s}{3x_3} + \frac{k_{11} + N_{cd}\ AO_s/2}{x_3}\right.$$

$$\left. + \frac{2\ k_{12}}{x_3+k_{13}} + \frac{k_{14}}{k_{13}}\right)10^{-3} \tag{9.76}$$

$$\lambda_{bs} = \left(\frac{N_{cd}}{2}\ \frac{AO_s}{3x_3} + \frac{2\ k_{12}}{x_3+k_{13}} + \frac{k_{14}}{k_{13}}\right)10^{-3} \tag{9.77}$$

$$\lambda_{tbs} = \left(\frac{N_{cd}}{2}\ \frac{AO_s}{2x_3} + \frac{2\ k_{12}}{x_3+k_{13}} + \frac{k_{14}}{k_{13}}\right)10^{-3} \tag{9.78}$$

$$X_{0l} = 15.8 \times 10^{-6}\ f_{op}\ T_{ph}^2\ g_s'[0.7\ L_e$$

$$- 0.4\ \pi(x_1 + x_4)/P]/p \tag{9.79}$$

$$X_{zl} = 5\ X_m/(6\ g_s^2) \tag{9.80}$$

$$X_m = E_{sl}/I_{orl} \tag{9.81}$$

$$I_{orl} = AT_a\ p/(T_{ph}\ 1.17\ K_{wsl}) \tag{9.82}$$

$$AT_a = AT_{ts} + AT_{cs} + AT_{tr} + AT_{cr} + AT_g \tag{9.83}$$

$$AT_g = \frac{1}{\mu_o}\ x_6\ K_g\ 1.28\ \frac{\phi_{ml}}{g_s\ L_{is}\ w_{ts}} \tag{9.84}$$

$$K_g = y_s\ y_r/[(y_s - K_{ol}\ k_{13})(y_r - K_{o2}\ k_{15})] \tag{9.85}$$

The expressions for ampere-turns for teeth and core of the magnetic circuit and the equations (9.73) to (9.85) are derived in the references [41,93].

$$Z_{mm} = R_{om} + j\ m\ X_{mm} \tag{9.86}$$

$$R_{om} = 3\ E_{sm}^2/(P_{fw} + P_{tsm} + P_{crsm} + P_{trm} + P_{crrm}) \tag{9.87}$$

where for each component of harmonic frequency P_{tsm}, P_{crsm}, P_{trm} and P_{crrm} represent hysteresis and eddy current loss in stator teeth, stator core, rotor teeth and rotor core respectively. These components of iron loss are obtained from equations (7.27) and (7.28) of Section 7.2.4.

$$X_{mm} = X_m \tag{9.88}$$

$$Z'_{rm} = R'_{rm} + j\ m\ X'_{rm} \tag{9.89}$$

$$X'_{rm} = K_{xrm}\ X_{s2}\ \frac{K_{wsm}^2\ S_s}{K_{wrm}^2\ S_r} + X_{o2} + X_{z2} \tag{9.90}$$

$$X_{s2} = 15.8 \times 10^{-6}\ f_{op}\ T_{ph}^2\ g_s^2\ x_2\ \lambda_{s2}/p \tag{9.91}$$

$$\lambda_{s2} = \left(\frac{AO_r}{3\ x_7} + \frac{k_{16}}{x_7} + \frac{2\ k_{17}}{x_7 + k_{15}} + \frac{k_{18}}{k_{15}}\right)10^{-3} \tag{9.92}$$

$$X_{o2} = 2\ \pi\ f_{op}\ \mu_o\ \frac{S_r^2}{3\ P}\ \frac{2}{3}\left(L_2 + k_{19} - x_2 + 0.18\ \frac{\pi\ d_{er}}{P}\right) \tag{9.93}$$

$$X_{z2} = 5\ X_m/(6\ g_r^2) \tag{9.94}$$

Equations (9.90) to (9.94) are derived in the references [41,93].

4. Percentage efficiency at full-load and full- load power factor

$$\frac{\sum_{i=1}^{19} 3\, V_{sm}\, I_{sm} \cos\theta_m - (P_{fw} + P_1 + P_2)}{\sum_{i=1}^{19} 3\, V_{sm}\, I_{sm} \cos\theta_m} 100 \geq 80.0 \qquad (9.95)$$

$$P_1 = P_{cs} + \sum_{m=1}^{19} P_{tsm} + \sum_{m=1}^{19} P_{crsm} + P_{ssz} + P_{scz} + P_{stp} \qquad (9.96)$$

$$P_2 = P_{cr} + \sum_{m=1}^{19} P_{trm} + \sum_{m=1}^{19} P_{crrm} + P_{rsz} + P_{rsc} + P_{rzz} + P_{rez} + P_{bll} + P_{skl} \qquad (9.97)$$

$$P_{cs} = \sum_{m=1}^{19} 3\, I_{sm}^2\, R_{sm} \qquad (9.98)$$

$$P_{ssz} = \sum_{m=1}^{19} k_{20}\, x_1\, x_2 \left(\frac{I_{sm}}{g_r\, I_{om}}\right)^2 B_{gm}^2\, c_{sl}\, y_r \qquad (9.99)$$

$$I_{om} = (I_{oam}^2 + I_{orm}^2)^{\frac{1}{2}} \qquad (9.100)$$

$$I_{orm} = E_{sm}/(m\, X_{mm}) \qquad (9.101)$$

$$B_{gm} = \pi\, \phi_{mm}\, m/(2\, Y\, x_2) \qquad (9.102)$$

c_{sl} = constant depending on the effect of frequency on the depth of penetration obtained from graph of reference [96].

$$P_{soz} = 0.3\, K_{cm}\, 3 \sum_{m=1}^{19} I_{sm}^2\, m\, f_{op} \tag{9.103}$$

$$K_{cm} = [k_{21}\, 3\, T_{ph}^2\, x_1 \log(1 + K_A/(K_B\, K_C)]/P^2 \tag{9.104}$$

$$K_A = [(K_B - K_C)^2 + K_D^2]^{\frac{1}{2}} \tag{9.105}$$

$$K_B = 0.07 + 0.23\, Y \tag{9.106}$$

$$K_C = k_{22} + 0.5\, w_{cr}\, 10^{-3} \tag{9.107}$$

$$K_D = 0.5\, d_{cr}\, 10^{-3} + x_6 + k_{23}(x_4 - k_{14})/2 \tag{9.108}$$

$$P_{stp} = \sum_{m=1}^{19} [B_{(2r-1)m}^2 + B_{(2r+1)m}^2](2\, g_r)^{1.5}\, P_{ts} \tag{9.109}$$

$$B_{(2r-1)m} = \frac{g_s}{(2\, g_r+1)^2} \sin \frac{\pi(2\, g_r+1)}{2\, g_s}\, B_{tsm} \tag{9.110}$$

$$B_{tsm} = \phi_{mm}/(w_{ts}\, g_s\, L_{is}) \tag{9.111}$$

$$B_{(2r+1)m} = \frac{g_s}{(2\, g_r-1)^2} \sin \frac{\pi(2\, g_r-1)}{2\, g_s}\, B_{tsm} \tag{9.112}$$

$$P_{rsz} = \sum_{m=1}^{19} k_{24}\, x_1\, x_2\, B_{gm}^2\, K_{pf}\, c_{s2}\, y_s \tag{9.113}$$

K_{pf} = pole face loss coefficient for stator slot openings obtained from graph of reference [96].

c_{s2} = rotor iron loss coefficient obtained from graph of reference [96].

$$P_{rsc} = \sum_{m=1}^{19} k_{25}\, x_1\, x_2 \left(\frac{I_{sm}}{g_s\, I_{om}}\right)^2 B_{gm}^2\, c_{s2}\, y_s \qquad (9.114)$$

$$P_{rzz} = \sum_{m=1}^{19} 3\, R'_{rm}(K_{co}\, I_{om}^2 + K_{cl}\, I_{sm}^2) \qquad (9.115)$$

K_{co}, K_{cl} = loss factors obtained from graphs of reference [96].

$$P_{roz} = P_{soz} \qquad (9.116)$$

$$P_{bll} = \sum_{m=1}^{19} 3\, I_{sm}^2\, K_{rbm}\, R'_{rm}(K_{5m}^2 + K_{7m}^2)/K_{wrm} \qquad (9.117)$$

where K_{rbm} is skin-effect factor for rotor bars at the phase belt frequency, $6f_{op}$.

$$K_{rbm} = \zeta_m(\sinh 2\zeta_m + \sin 2\zeta_m)/(\cosh 2\zeta_m - \cos 2\zeta_m) \qquad (9.118)$$

$$\zeta_m = AO_r \left[\frac{\pi\, 6f_{op}\, \mu_o\, BO_r}{x_7\, 10^3\, \rho}\right]^{\frac{1}{2}} \qquad (9.119)$$

$$K_{5m} = \sin(g'_r\, 5\, m\, \frac{\pi}{g_r 2})/[g'_r \sin(\frac{5\, m\, \pi}{g_r\, 2})] \qquad (9.120)$$

$$K_{7m} = \sin(g'_r\, 7\, m\, \frac{\pi}{g_r 2})/[g'_r \sin(\frac{7\, m\, \pi}{g_r\, 2})] \qquad (9.121)$$

$$P_{skl} = \sum_{m=1}^{19} \frac{\pi^2}{12}\left(k_{26}\, \frac{I'_{rm}}{g_s\, I_{om}}\right)(P_{tsm} + P_{crsn} + P_{rsz}) \qquad (9.122)$$

Equations (9.99) to (9.122) are derived in the references [90,96].

5. Temperature rise of stator winding above ambient

$$k_{27} \frac{P_1}{A_s} \leq 115.0 \tag{9.123}$$

$$A_s = [\pi x_1(x_2 + 2 L_o) + 2\pi(x_1 + 2x_4) \times (d_o - x_1 - 2x_4)](1 + 0.1 u_a) + \pi d_o x_2 \tag{9.124}$$

$$d_o = x_1 + 2x_4 + 2x_5 \tag{9.125}$$

6. Locked rotor current

$$I_1 \leq 6 I_s \tag{9.126}$$

$$I_1 = (I_{11}^2 + I_{15}^2 + ... + I_{1m}^2)^{\frac{1}{2}} \tag{9.127}$$

The harmonic components of locked rotor current are obtained from the equivalent circuit when slip is unity.

7. Ratio of starting torque to full-load torque

$$\frac{M_{st}}{M_{fl}} \geq 1.5 \tag{9.128}$$

The starting torque is calculated from the equivalent circuit when slip is unity.

$$M_{fl} = M_{av} \tag{9.129}$$

8. Pull-out torque

$$M_{po} \geq 1.5\ M_{av} \tag{9.130}$$

$$M_{po} = 3\ E_{sl}^2\ 60/(2\ X'_{rl}\ 2\ \pi\ N) \tag{9.131}$$

Equation (9.133) is derived in the reference [41].

9. No-load current

$$I_o \leq 0.6\ I_{sl} \tag{9.132}$$

$$I_o = (I_{cl}^2 + I_{o5}^2 + \ldots + I_{om}^2)^{\frac{1}{2}} \tag{9.133}$$

10. Full-load slip

$$s_{fl} \leq 0.10 \tag{9.134}$$

11. Full-load factor

$$PF \geq 0.80 \tag{9.135}$$

Power factor is obtained from Z_{Tm}

12. Minimum width of stator teeth

$$w_{ts} \geq 0.004 \tag{9.136}$$

13. Ratio of minimum width of stator tooth to width of stator slot

$$\frac{w_{ts}}{x_3} \leq 1.3 \tag{9.137}$$

14. Maximum flux density in stator teeth

$$\frac{\phi_{ml}}{g_s\ L_{is}\ w_{ts}} \leq 2.2 \tag{9.138}$$

15. Minimum width of rotor tooth

$$w_{tr} \geq 0.004 \tag{9.139}$$

16. Ratio of minimum width of rotor tooth to width of rotor slot

$$\frac{w_{tr}}{x_7} \leq 1.3 \tag{9.140}$$

17. Maximum flux density in rotor teeth

$$\frac{\phi_{ml}}{g_r L_2 w_{tr}} \leq 2.2 \tag{9.141}$$

18. Diameter of shaft

$$d_{sh} \leq k_{28}\left(\frac{HP\ 746}{N}\right)^{1/3} \tag{9.142}$$

Expression (9.142) is an empirical formula for shaft diameter [93].

19. Current density in the end ring

$$\frac{I_{er}}{x_{11}} \leq 7.5 \tag{9.143}$$

$$I_{er} = I_b\, g_r/\pi \tag{9.144}$$

$$I_b = K_{wsl}\, g_s\, Z_s\, I'_{rl}/g_r \tag{9.145}$$

Equations (9.144,145) are derived in reference [41].

20. Current density in the rotor bar

$$\frac{I_b}{a_r} \leq 10.0 \tag{9.146}$$

21. Stator current density

$$\frac{I_s}{a_s} \leq 3.5 \qquad (9.147)$$

9.7 SOLUTION OF THE NLP PROBLEM

The NLP problem is formulated with the cost and constraint functions of Section 9.6 and the augmented objective function is obtained with normalized constraints by exterior penalty function formulation. With a starting vector of independent variables and penalty parameter, the minimization process is carried out using Powell's method.

Optimal solution of a 5 h.p., 400 volts, 4-pole, three-phase delta connected squirrel-cage induction motor operating from 30 to 60 Hz with six-stepped inverter voltage is obtained, minimizing the active material cost of the motor and satisfying the desired constraints. The results are presented in Table 9.1. The constraints at the optimal solution are compared with the specified values in Table 9.2. It is observed from Table 9.2 that the constraints on no-load power factor at minimum frequency, ratio of starting torque to full-load torque, minimum width of stator teeth, minimum width of rotor teeth and current density in the rotor bar are violated by a little margin. Three other constraints i.e., the per unit torque pulsation, the efficiency

TABLE 9.1

OPTIMAL SOLUTION OF A 5 HP, 400 VOLTS, 4-POLE, 30-60 Hz, THREE-PHASE DELTA CONNECTED SQUIRREL-CAGE INDUCTION MOTOR

Particulars		Starting point	Optimal solution
x_1	Diameter of stator bore, m	0.1368	0.1046
x_2	Length of stator core, m	0.0878	0.1171
x_3	Width of stator slot, m	0.0079	0.0067
x_4	Depth of stator slot, m	0.0675	0.0392
x_5	Depth of stator core, m	0.0864	0.0500
x_6	Length of air gap, m	0.0006	0.0003
x_7	Width of rotor slot, m	0.0158	0.0042
x_8	Depth of rotor slot, m	0.0231	0.0050
x_9	Depth of rotor core, m	0.0777	0.0330
x_{10}	Average flux density in air gap, Tesla	0.4050	0.3915
x_{11}	Area of c.s. of end ring, mm^2	120.0	125.1460
	Cost, %	100.0	48.8

TABLE 9.2

CONSTRAINTS ON A 5 HP, 400 VOLTS, 4-POLE, 30-60 Hz, THREE-PHASE DELTA CONNECTED SQUIRREL-CAGE INDUCTION MOTOR

	Specified	At optimal solution
1. Average torque, Nm	23.8	26.3815
2. Per unit torque pulsation	0.15	0.1445
3. No-load power factor at minimum frequency	0.2	0.3169
4. Efficiency at full-load and full-load p.f.	0.8	0.8004
5. Temperature rise of stator winding above ambient, °C	115.0	31.2
6. Locked rotor current per phase at minimum frequency, A	25.5	7.8428
7. Ratio of starting torque to full-load torque	1.5	1.4302
8. Pull-out torque at maximum frequency, Nm	35.6	30.6595
9. No-load current per phase, A	2.55	1.403
10. Full-load slip	0.10	0.0772
11. Full-load power factor	0.8	0.80
12. Minimum width of stator teeth, m	0.004	0.0024
13. Ratio of width of stator tooth to width of stator slot	1.3	0.625
14. Maximum flux density in stator teeth, Tesla	2.2	0.9669
15. Minimum width of rotor teeth, m	0.004	0.0037
16. Ratio of width of rotor tooth to width of rotor slot	1.3	1.02

TABLE 9.2 (continued)

	Specified	At optimal solution
17. Maximum flux density in rotor teeth, Tesla	2.2	0.8230
18. Diameter of shaft, m	0.03	0.0285
19. Current density in end ring, A/mm^2	7.5	5.655
20. Current density in the rotor bar, A/mm^2	10.0	12.0865
21. Stator current density, A/mm^2	3.5	1.2975

of the motor and the full-load power factor are driven to their limits at the optimal solution.

9.8 OPTIMIZED DESIGN OF A 5 HP SQUIRREL-CAGE INDUCTION MOTOR

The design data and performance of the 5 h.p. motor corresponding to the optimal solution is presented in Table 9.3. All these values are obtained at the maximum frequency of 60 Hz.

9.9 CONCLUSIONS

The design optimization of a 5 h.p. squirrel-cage induction motor operating over a frequency range of 30-60 Hz with six-step inverter supply is obtained by NLP technique. The approximate execution time for obtaining the optimized design on IBM 7044 computer is about 4 hours. The computer program developed here based on the steady-state equivalent circuits of the induction motor is applicable to a line of motors operating over a large speed range. It is evident from Table 9.3 that the additional losses due to nonsinusoidal voltage wave shape is a considerable percentage of the total losses. The major part of the additional losses are generated in the rotor bars. It is also observed that smaller conductor dimensions are required in the stator and

TABLE 9.3

DESIGN DATA AND PERFORMANCE OF A 5 HP, 400 VOLTS, 4-POLE, 30-60 Hz, THREE-PHASE DELTA CONNECTED SQUIRREL-CAGE INDUCTION MOTOR

1. STOTOR	
Number of slots	36
Turns per phase	432
Conductor dimensions, mm	3.28 x 1.00
Resistance per phase, ohm	1.9595
Reactance per phase, ohm	64.6928
Copper loss, W	204.15
Iron loss, W	89.0851
Stray loss, W	8.2876
Copper space factor of stator slot	0.9
2. ROTOR	
Number of slots	38
Conductor dimensions, mm	4.80 x 4.00
Resistance per phase referred to stator, ohm	9.8682
Reactance per phase referred to stator, ohm	29.0635
Copper loss, W	314.3078
Iron loss, W	19.8105
Stray loss, W	247.3755
3. END RINGS	
Diameter of end ring, m	0.0748
Width of end ring, mm	6.3150

TABLE 9.3 (continued)

Depth of end ring, mm	19.8173
4. OTHER DETAILS	
DC link voltage	651.6228
Weight of copper windings, kg	24.3324
Weight of stampings, kg	34.8257
Weight of brass rings, kg	0.5114
Total losses, W	909.741

rotor. A deep bar rotor is not essential for a motor operating with inverter supply. The leakage reactance of the motor is also very large. The limit on the per unit torque pulsation has become a critical factor in the convergence process towards the optimal solution. The convergence process is slow as the optimization routine has to perform about 140 function evaluations in every unconstrained minimization cycle. About 4% decrement in the efficiency of the motor is observed when compared to a conventional induction motor of the same rating operating with sinusoidal voltage. The permissible current density in the rotor bar may be attained by choosing a different number of slots in the rotor.

CHAPTER 10

C O N C L U S I O N S

10.1 GENERAL

Mathematical programming techniques are used effectively in this thesis for the computer aided design of electromagnetic devices. Nonlinear optimization procedures are applied to specific examples of power transformers viz., conventional, furnace and rectifier power transformers, d.c. separately excited and series motors and variable speed squirrel-cage induction motor. The rotating machines are considered with rectified and nonsinusoidal voltage supplies. The feasibility of optimum design of above mentioned electromagnetic devices is demonstrated over a large number of constraints. The summary of the investigations and the contributions made in this thesis are reviewed in this chapter. The scope for further work in this area is also outlined.

10.2 REVIEW OF THE WORK DONE

Two solution techniques as applied to the design problems of this thesis, namely, (1) Powell's unconstrained minimization procedure in conjunction with Zangwill's exterior penalty function formulation (2) revised simplex method of LP to linear approximation of NLP problem are introduced in Chapter 2.

Optimal design of a 5 MVA conventional power transformer is solved as an NLP problem with five independent variables satisfying given specifications and performance figures as constraints. The first solution technique described in this thesis is adopted to obtain the minimum cost of the transformer.

The same problem of the power transformer is solved in the next chapter as an LP problem with an approximate linear model represented in terms of unrestricted variables. The optimal design, minimizing the cost of the transformer obtained by the revised simplex method of LP, is tested with the original nonlinear model. It is demonstrated that the optimal solution is very close to the operating point and the computational time as compared to the method in Chapter 3 is considerably less. Sensitivity analysis is carried out on the optimal solution. The effect of relaxing the maximum limit on constraints like flux density of core and temperature rise of windings, keeping the other constraints same on the overall cost function is investigated.

The design procedure of a special purpose transformer supplying a direct arc furnace is developed in Chapter 5. The mathematical model of the design problem of the furnace transformer is formulated with six independent variables. The power system impedance, arc resistance and arc power

of the furnace circuit are considered in this model. Important constraints are imposed on the design problem. Powell's minimization technique is adopted and optimal design of a 64.5 MVA furnace transformer is obtained, minimizing the cost.

Another special purpose transformer viz., the rectifier power transformer supplying a d.c. load through a three-phase semiconductor diode bridge is considered in Chapter 6. An equation for nonsinusoidal secondary current waveform is derived considering the effect of source impedance. The mathematical model of the NLP problem is formulated with six independent variables on similar lines of Chapter 5 and is solved by Powell's minimization technique. The optimized design of a 4 MVA rectifier transformer is obtained, minimizing the material cost and satisfying the desired constraints. The design procedure developed here is also applicable to the optimal design of a d.c. arc furnace transformer.

Redesign of d.c. motors to suit the thyristor controlled power supplies for the present day requirement of industry is considered in the next two chapters. The mathematical model of the design problem of a 150 h.p., 550 V separately excited d.c. motor supplied from a three-phase thyristor converter is formulated with sixteen independent

variables, taking into consideration the effect of rectified voltage on the performance of the motor. A general procedure is developed to design the motor when the converter supplying the motor is operated with different firing angles. Laminated field structure with octagonal frame, compensating winding in the pole-faces and interpole winding are considered in line with the current manufacturing practice. In the design analysis program, the calculation of armature circuit inductance, additional losses in the electric and magnetic circuits are considered. Commutating ability of the motor, pulse duty factor of armature current, ratio of torque to armature moment of inertia, efficiency of motor etc., are adopted as constraints on the design problem. The optimal design of a 150 h.p. motor is obtained for minimum active material cost of the motor. It is observed from the optimized design that the operation of the motor with different firing angles of the converter, requires a generously dimensioned motor.

The optimal design problem of a 150 h.p., 550 V d.c. series motor supplied through a three-phase thyristor converter is formulated with the same sixteen independent variables as considered for the separately excited d.c. motor. Nonlinearity of the magnetic circuit is considered by a suitable approximation of magnetization curve in the mathematical

model. Similar constraints as considered for the separately excited motor are imposed on the design problem. The minimum active material cost and the optimized design of the specified d.c. motor are obtained satisfying the desired constraints. An increase in the number of axial ventilating ducts in the armature and the reduction in efficiency is observed as the firing angle of the converter is increased. The procedure to calculate the torque and the associated speed fluctuations is indicated.

The optimal design of a 5 h.p. variable speed squirrel-cage induction motor supplied with nonsinusoidal voltage from a static frequency inverter is considered as the last topic of this thesis. The mathematical model of the design problem is defined with eleven independent variables over a range of frequency. The additional losses and torque pulsations in the cage motor due to a six-stepped inverter supply voltage are investigated over the frequency range based on single-phase equivalent circuit. The two extreme values of frequency decide the constraints on the design problem. Important constraints like average torque, no-load power factor, no-load current, p.u. torque pulsation, pull-out torque, starting current etc., are imposed on the design problem. The optimized design of a 5 h.p. squirrel-cage induction motor is obtained satisfying the desired constraints for minimum active material cost.

10.3 SCOPE FOR FURTHER RESEARCH

The suitability of Powell's method together with Zangwill's exterior penalty function formulation to the optimal design of power transformers, d.c. motors with thyristor power supplies and a.c. variable speed squirrel-cage induction motor for inverter power supply is well established. The same technique of NLP may be extended to the optimal design of other electromagnetic devices like alternators, synchronous motors, linear motors, variable speed reluctance motors etc.

1. A.D. Warren, L.S. Ladson and D.F. Suchnan, 'Optimization in Engineering Design,' Proc. IEEE, Vol. 55, pp. 1885-1897, 1967.

2. R.J. Duffin and C. Zener, 'Optimization of Engineering Problems,' Westinghouse Engineer, Vol. 24, pp. 154-160, 1964.

3. C. Zener, 'A Mathematical Aid in Optimizing Engineering Designs,' Proc. Natl. Acad. Sci., Vol. 47, pp. 537-539, 1961.

4. J. Appelbaum and M.S. Erlicki, 'Optimized Parameter Analysis of an Induction Motor,' IEEE Transaction on Power Apparatus and Systems, Vol. PAS-84, p. 1017, 1965.

5. O.W. Anderson, 'Optimum Design of Electrical Machines,' IEEE Transaction on Power Apparatus and Systems, Vol. PAS-86, pp. 707-711, 1967.

6. R. Ramaratnam and B.G. Desai, 'Optimization of Polyphase Induction Motor Design: A Nonlinear Programming Approach,' IEEE Transaction on Power Apparatus and Systems, Vol. PAS-90, pp. 570-579, 1971.

7. R. Ramaratnam, B.G. Desai and V. Subba Rao, 'A Comparative Study of Minimization Techniques for Optimization of Induction Motor Design,' IEEE Transaction on Power Apparatus and Systems, Vol. PAS-92, pp. 1448-1454, 1973.

8. A.V. Fiacco and G.P. McCormick, 'The Sequential Unconstrained Minimization Technique for Nonlinear Programming - A Primal Dual Method,' Management Science, Vol. 10, pp. 360-364, 1964.

9. A.V. Fiacco and G.P. McCormick, 'Computational Algorithm for the Sequential Unconstrained Minimization Technique for Nonlinear Programming,' Management Science, Vol. 10, pp. 601-617, 1964.

10. R.W. Menzies and G.W. Neal, 'Optimization Program for Large Induction Motor Design,' Proc. IEE, Vol. 122, No. 6, pp. 643-646, 1975.

11. M. Ramamoorty and P.J. Rao, 'Comparative Study of Optimization Methods for the Design of Polyphase Reluctance Motors,' Engineering Optimization, Vol. 3, pp. 51-60, 1977.

12. G. Sridhara Rao, V.V. Sastry and P. Venkata Rao, 'Comparison of Nonlinear Programming Techniques for the Optimal Design of Transformers,' Proc. IEE, Vol. 124, No. 12, pp. 1225-1226, 1977.

13. G. Stephanopoulous, 'A note on the Optimization of Constrained Design Problems,' Journal of Optimization Theory and Applications, Vol. 17, pp. 337-342, 1975.

14. W.I. Zangwill, 'Nonlinear Programming Via Penalty Functions,' Management Science, Vol. 13, pp. 344-358, 1967.

15. M.J.D. Powell, 'An Efficient Method for Finding the Minimum of a Function of Several Variables without Calculating Derivatives,' Computer Journal, Vol. 7, pp. 155-162, 1964.

16. G. Dantzig, 'Linear Programming and Extensions,' Princeton University Press, Princeton, 1963.

17. G. Hadley, 'Linear Programming,' Addison-Wesley, Reading, Massachusetts, 1974.

18. D.M. Himmelblau, 'Optimal Design Via Structural Parameters and Nonlinear Programming,' Engineering Optimization, Vol. 2, pp. 17-27, 1975.

19. R.L. Fox, 'Optimization Methods for Engineering Design,' Addison-Wesley, Reading, Mass., 1974.

20. A.V. Fiacco and G.P. McCormick, 'Nonlinear Programming: Sequential Unconstrained Minimization Techniques,' Wiley, New York, 1969.

21. J.L. Kuster and J.H. Mize, 'Optimization Techniques with Fortran,' McGraw-Hill, New York, 1973.

22. S.B. Williams, P.A. Abetti and E.F. Magnusson, 'Application of Digital Computers to Transformer Design,' AIEE Transactions, Vol. 75, Part III, pp. 728-735, 1956.

23. S.B. Williams, P.A. Abetti and H.J. Mason, 'Complete Design of Power Transformers with a Large Size Digital Computer,' AIEE Transactions, Vol. 77, Part III, pp. 1282-1291, 1959.

24. W.A. Sharpely and J.V. Oldfield, 'The Digital Computer Applied to the Design of Large Power Transformers,' Proc. IEE, Vol. 105, Part A, pp. 112-125, 1958.

25. T.H. Putman, 'Economics and Power Transformer Design,' IEEE Transaction on Power Apparatus and Systems, Vol. PAS-82, pp. 1018-1023, 1963.

26. S.B. Vasutinsky, 'Principles, Operation and Design of Power Transformer,' P.S.G. College of Technology, Coimbatore, 1962.

27. M. Kostenko and L. Piotrovsky, 'Electrical Machines, Vol. I & II,' Peace Publishers, Mascow.

28. O.L. Mangasrian, 'Techniques of Optimization,' Journal of Engineering for Industry, ASME Transactions, pp. 365-372, May 1972.

29. R.E. Griffith and R.A. Steward, 'A Nonlinear Programming Technique for the Optimization of Continuous Processing Systems,' Management Science, No. 7, pp. 379-392, 1961.

30. H.A. Taha, 'Operations Research - An Introduction,' The McMillan Company, New York, 1971.

31. J.A. Ciotti and C.G. Robinson, '400 Ton Arc Furnace,' Journal of Metals, AIME, p.17, Aug. 1973.

32. J.L. Thompson, 'Transformers for Electric Furnaces,' JIEE, Vol. 58, No. 289, pp. 201-273, Mar. 1920.

33. H.O. Stephens and L.S. Schell, 'Transformers for Electric Furnaces,' AIEE Transactions, Vol. 53, pp. 1695-1699, 1934.

34. C.R. Hatch, 'Arc Furnace Transformers - Modern Design Developments,' Electrical Review, Vol. 166, pp.52-56, Jan. 1960.

35. 'Transformers with Off-load Tap Changing for Direct Arc Melting Furnaces,' AEI Publication 1563-1, GEC Ltd., UK.

36. 'Transformers with On-load Tap Changing for Direct Arc Melting Furnaces,' AEI Publication 1563-1a, GEC Ltd., UK.

37. P. Bonis and F. Coppadoro, 'Transformers for Arc Furnace,' Brown Boveri Review, Vol. 60, pp. 456-457, Oct./Nov. 1973.

38. B. Grundmark, 'Large Furnace Transformers,' ASEA Journal, No. 6, pp. 151-156, 1972.

39. W.H. Gorga, 'Design Considerations for the Installation of Modern High Power Electric Arc Furnaces,' Iron and Steel Engineer, Vol. 49, pp. 35-41, Feb. 1972.

40. E.J. Borrebach, 'Maximum Power Operation of Arc Furnaces,' Iron and Steel Engineer, pp. 74-83, May 1969.

41. M.G. Say, 'The Performance and Design of Alternating Current Machines,' Sir Issac Pitman & Sons Ltd., London, 1970.

42. AIEE Committee Report, 'Rectifier Transformer Characteristics,' AIEE Transactions, Vol. 68, Part II, pp. 1305-1311, 1949.

43. E. Pelikan and J. Isler, 'Rectifier Transformers for Heavy Currents,' Brown Boveri Review, Vol. 48, pp. 215-218, Mar./Apr. 1961.

44. F. Coppadoro, 'Voltage Regulation of Transformers for Silicon Rectifiers,' Brown Boveri Review, Vol. 59, pp. 416-421, Aug. 1972.

45. J. Schaefer, 'Rectifier Circuits: Theory and Design,' Wiley, New York, 1965.

46. S. Crepaz, 'Eddy Current Loss in Rectifier Transformer,' IEEE Transaction on Power Apparatus and Systems, Vol. PAS-89, pp. 1651-1656, Sep./Oct. 1970.

47. M. Ramamoorty, 'An Introduction to Thyristors and Their Applications,' Affiliated East-west Press Pvt. Ltd., New Delhi, 1977.

48. K.J. Irvine, 'Arc-Furnace Research and Development,' Ironmaking and Steelmaking, Vol. 4, No. 2, pp. 110-115, 1977.

49. A. Schmidt and W.P. Smith, 'Operation of Large DC Motors from Controlled Rectifiers,' AIEE Transactions, Vol. 67, Part I, pp. 679-683, 1948.

50. E.E. Kubler, 'The Armature Current Form-Factor of a DC Motor Connected to a Controlled Rectifier,' AIEE Transactions, Vol. 78, Part II, pp. 746-770, 1959.

51. R.M. Dunaski, 'The Effect of Rectifier Power Supply on Large DC Motors,' AIEE Transactions, Vol. 79, Part III, pp. 253-259, June 1960.

52. N. Kaufman, 'An Application Guide for use of DC Motors on Rectifier Power,' IEEE Transaction on Power Apparatus and Systems, Vol. 83, pp. 1006-1008, 1964.

53. V.E. Vrana, 'The DC Motor and the Thyristor Power Supply,' Westinghouse Engineer, pp. 98-104, July 1967.

54. C.E. Robinson, 'Redesign of DC Motors for Applications with Thyristor Power Supplies,' IEEE Transaction on Industry General Applications, Vol. IGA-4, pp. 508-514, Sept./Oct. 1968.

55. P.J. Trivitse and A.N. Schiff, 'Static Power Sources for DC Motors,' Iron and Steel Engineer, pp. 67-76, Feb. 1969.

56. U.M. Elder and C.J. Photiadis, 'DC Mill Motors Rerated and Redesigned,' Westinghouse Engineer, pp. 104-108, July 1969.

57. R.L. White and R.H. Hartely, 'Optimum Design and Performance Calculations of Highly Magnetically Saturated DC Machines for Large-Scale Production,' Proc. IEE, Vol. 16, No. 11, pp. 1891-1899, Nov. 1969.

58. H.R. Bill, W. Heil and P. Stark, 'Problems in the Construction of Modern DC Machines for Industrial Applications,' Brown Boveri Review, Vol. 55, No. 10/11, pp. 599-610, Oct./Nov. 1968.

59. J. Meister and M. Renold, 'Electrical Design of the New Series of DC Machines,' Brown Boveri Review, Vol. 58, No. 10/11, pp. 611-617, Oct./Nov. 1968.

60. H. Koch, 'A New Range of DC Machines for 12 to 550 KW and 1500 rev/min,' Brown Boveri Review, Vol. 59, pp. 597-601, Dec. 1972.

61. P.W. Franklin, 'Theory of the DC Motor Controlled by Power Pulses - Part I Motor Operation, Part II Braking Methods and Additional Losses,' IEEE Transaction on Power Apparatus and Systems, Vol. PAS-91, pp. 249-262, 1972.

62. P. Mattheis and Walter Schuler, 'A New Range of DC Mill Motors,' Siemens Review, No. 2, pp. 85-89, 1972.

63. J. Le Prince, 'Some Problems in the Design of DC Machines Supplied by Semi-conductors,' ACEC Review, No. 3-4, 1974.

64. K. Keenan, P. Schramm-Neilsen and A.J. Larsen, 'A New Series of DC Motors for 0.2-600 KW,' ASEA Journal, pp. 117-123, 1975.

65. H. Prenner and W. Heil, 'Compensated DC Machines of Compact Design for Rated Torques of 2 to 125 kNm,' Brown Boveri Review, Vol. 63, pp. 477-482, Aug. 1976.

66. S.S. Rao, 'Optimization Theory and Applications,' Wiley Eastern Limited, New Delhi, 1978.

67. N.A.O. Demerdash and H.B. Hamilton, 'Effect of Complex Forms on Copper Losses in Large DC Motors,' IEEE Conference Record of Fifth Annual Meeting of Industry and General Applications Group, pp. 77-81, 1970.

68. W.D. Snively and P.B. Robinson, 'Measurement and Calculation of DC Machine Armature Circuit Inductance,' AIEE Transaction on Power Apparatus and Systems, Vol. 69, Part II, pp. 1228-1237, 1950.

69. A.E. Clayton and N.N. Hancock, 'The Performance and Design of Direct Current Machines,' Pitman, 1961.

70. F.C. Trutt, E.A. Erdelyi and R.E. Hopkins, 'Representation of the Magnetization Characteristic of DC Machines for Computer use,' IEEE Transaction on Power Apparatus and Systems, Vol. PAS-87, pp. 665-669, Mar. 1968.

71. J. Lammeraner and M. Stafl, 'Eddy Currents,' Iliffe Books Ltd., London, 1966.

72. E. Erdelyi, 'Calculation of Stray Load Losses in DC Machinery,' AIEE Transactions, Vol. 79, Part III, pp. 129-138, June 1960.

73. A.S. Langsdorf,'Principles of Direct-Current Machines,' McGraw Hill, New York, 1959.

74. R.A. Van Eck, 'Separately Excited DC Motor (Traction) Applied to DC and Single-Phase AC Rapid Transit Systems And Electrified Rail Roads - Parts I & II,' IEEE Transactions, Vol. IGA-7, No. 5, pp. 643-657, Sept./ Oct. 1971.

75. Pr Lebenbaum Jr., 'The Design of DC Motors for Use in Automatic Control Systems,' AIEE Transactions, Vol. 68, pp. 1089-1094, 1949.

76. B.J. Chalmers and B.J. Bennigton, 'Digital Computer Program for Design Synthesis of Large Squirrel-Cage Induction Motors,' Proc. IEE, Vol. 114, No. 2, pp. 261-268, 1967.

77. C.E. Tindall and P.A.J. Calvert, 'Computer Aided Synthesis and Optimization of Induction Motor Design,' IEEE Transaction on Manufacturing Technology, Vol. MFT-6, No. 2, pp. 31-37, June 1977.

78. L.A. Doggett and E.R. Queer, 'Induction Motor Operation with Nonsinusoidal Impressed Voltages,' AIEE Transactions, Vol. 48, No. 4, pp. 1217-1220, Oct. 1929.

79. G.C. Jain, 'The Effect of Voltage Waveshape on the Performance of a 3-phase Induction Motor,' IEEE Transaction on Power Apparatus and Systems, Vol. PAS-83, pp. 561-566, 1964.

80. P.J. Lawrenson and J.M. Stephenson, 'Note on Induction Machine Performance with a Variable Frequency Supply,' Proc. IEE, Vol. 113, pp. 1617-1623, 1966.

81. C.G. Helmick, 'How to Specify Adjustable Frequency Drives - Part I,' Control Engineering, Vol. 14, pp. 69-71, April 1967.

82. C.G. Helmick, 'How to Specify Adjustable Frequency Drives -- Part II,' Control Engineering, Vol. 4, pp. 83-84, May 1967.

83. E.A. Klingshirn and H.E. Jordan, 'Polyphase Induction Motor Performance and Losses on Nonsinusoidal Voltage Sources,' IEEE Transaction on Power Apparatus and Systems, Vol. PAS-87, pp. 624-631, Mar. 1968.

84. C.D. Beck and E.F. Chandler, 'Motor Drive Inverter Ratings,' IEEE Transaction on Industry and General Applications, Vol. IGA-4, pp. 589-595, Nov./Dec. 1968.

85. B.J. Chalmers and B.R. Sarkar, 'Induction Motor Losses Due to Nonsinusoidal Supply Waveforms,' Proc. IEE, Vol. 115, pp. 1777-1782, 1968.

86. G.W. McLean, G.F. Nix and S.R. Alwash, 'Performance and Design of Induction Motors with Square-wave Excitation,' Proc. IEE, Vol. 116, 1405-1411, 1969.

87. J.M.D. Murphy, 'Thyristor Control of AC Motors,' Oxford, 1973.

88. L.J. Jacovides, 'Analysis of Induction Motors with a Nonsinusoidal Supply Voltage using Fourier Analysis,' IEEE Transaction on Industry Applications, Vol. IA-9, pp. 741-747, Nov./Dec. 1973.

89. T.A. Lipo, P.C. Krause and H.E. Jordan, 'Harmonic Torque and Speed Pulsations in a Rectifier Inverter Induction Motor Drive,' IEEE Transaction on Power Apparatus and Systems, Vol. PAS-88, pp. 579-587, May 1969.

90. H. Largiader,'Design Aspects of Induction Motors for Traction Applications with Supply Through Static Frequency Changers,' Brown Boveri Review, Vol. 57, pp. 152-167, April 1970.

91. S.D.T. Robertson and K.M. Hebbar, 'Torque Pulsations in Induction Motors with Inverter Drives,' IEEE Transaction on Industry and General Applications, Vol. IGA-7, pp. 318-323, Mar./Apr. 1971.

92. A.C. Botke, J.F. Billings and K.P. Phillips, 'Special Purpose AC Converter Systems for Constant Horsepower Applications,' IEEE Conference Record of Fifth Annual Meeting of Industry and General Applications Group, pp. 695-705, 1970.

93. H. Vickers, 'The Induction Motor,' Sir Isaac Pitman & Sons, Ltd., London, 1953.

94. A. Still and C.S. Siskind, 'Elements of Electrical Machine Design,' McGraw-Hill, New York, 1954.

95. J.H. Kuhlmann, 'Design of Electrical Apparatus,' John Wiley & Sons, Inc, New York, 1959.

96. P.A. Alger, G. Angst and E.J. Davies, 'Stray Load Loss in Polyphase Induction Motors,' AIEE Transaction on Power Apparatus and Systems, Part III-A, pp. 349-357, June 1959.

97. P.J. Rao, 'Application of Mathematical Programming Methods to Optimal Design of Polyphase Reluctance Motor,' Ph.D. Thesis, I.I.T. Kanpur, July 1977.

98. B.R. Pelly, 'Thyristor Phase-controlled Converters and Cycloconverters,' Wiley-Interscience, 1971.

99. R. Fletcher, 'Function Minimization without Evaluating Derivatives - A Review,' Computer Journal, Vol. 8, pp. 33-41, 1965.

100. P.E. Gill and W. Murray, 'Numerical Methods for Constrained Optimization,' Academic Press, London, 1974.

CURRICULUM VITAE

a. Name : K.S. RAMA RAO

b. Academic Background :

Degree	Specialization	University	Year
B.E.(Hons.)	Electrical Engineering	Andhra	1962
M.Sc.(Engg.)	Electrical Engineering	Madras	1963

c. Publications :

1. 'Optimal Design of Power Transformers,' (with Dr. M. Ramamoorty and Sri P.J. Rao), Paper presented at the All India Symposium on Power Transformers and Reactors (Institution of Engineers, India), October 1976.

2. 'A Linear Programming Approach to the Optimal Design of Power Transformers,' (with Dr. M. Ramamoorty), paper presented at the All India Seminar on Design, Development and Standardization of Electrical Equipment (Institution of Engineers, India), September 1977.

3. 'Optimal Design of Rectifier Power Transformer,' (with Dr. M. Ramamoorty), a paper accepted for publication in the Journal of IE (India).